rf design

engineering principles and practices

April 1990

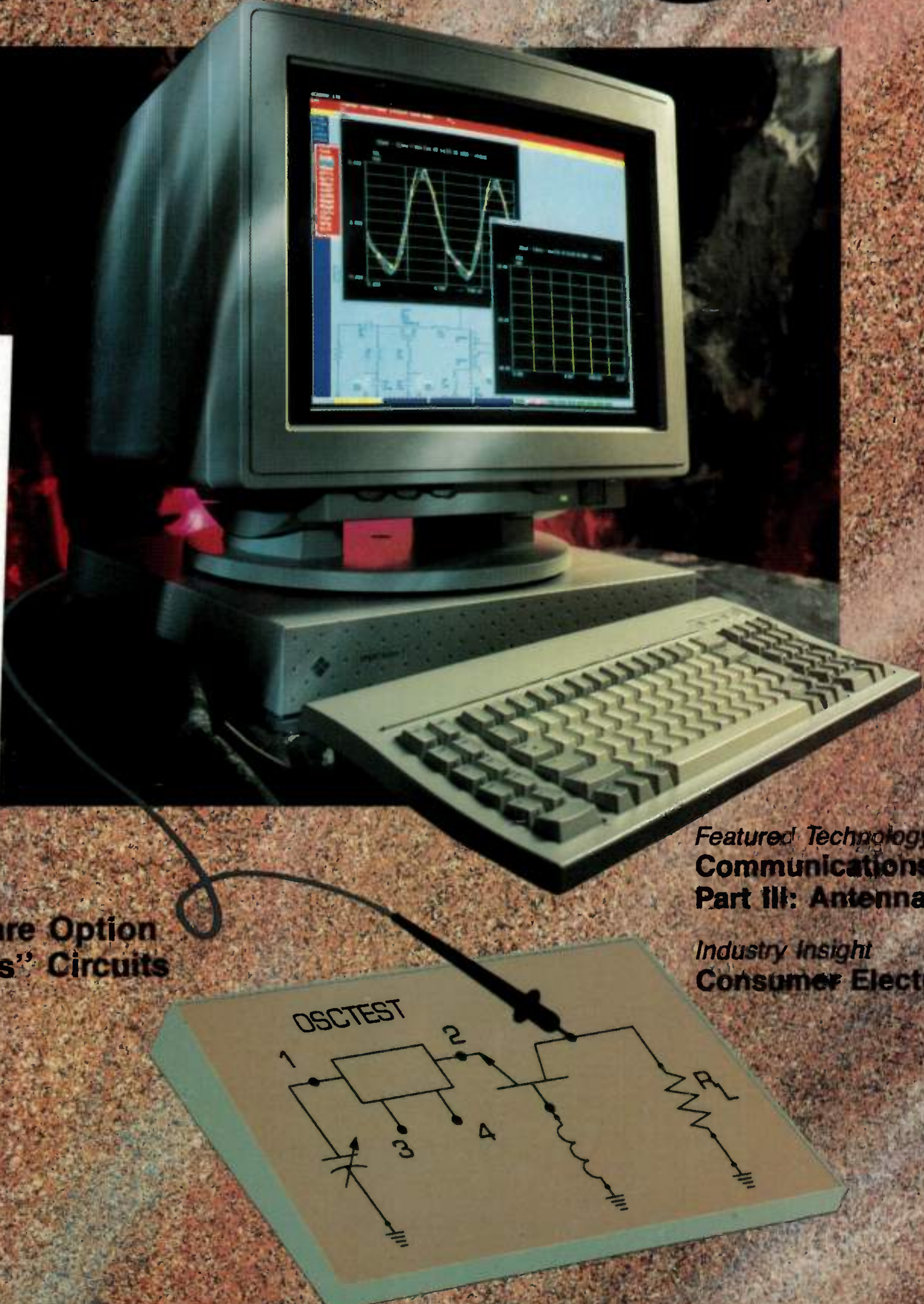

Software Option "Probes" Circuits

Featured Technology
Communications Design Part III: Antennas

Industry Insight
Consumer Electronics

Analog CAE Solutions— from picoseconds to GHz

EEsof has the high-frequency analog CAE tools you need today— to build the advanced hardware of tomorrow!

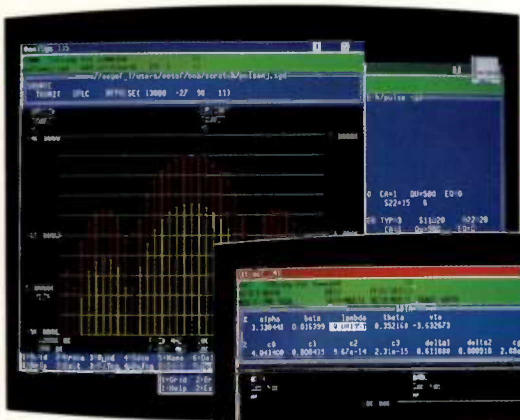

System Simulation

Device Characterization

Time-Domain Simulation

Nonlinear Simulation

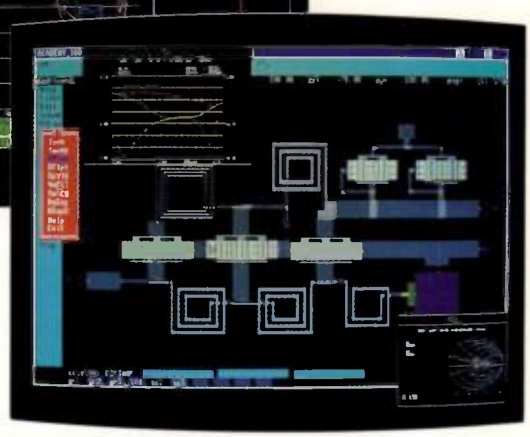

Design Environment and Circuit Layout

Call us today for details on the wide range of high-frequency analog tools manufactured by EEsof. Our software is supported on most popular CAE computers and workstations, including those from Apollo, SUN, HP, and DEC and also IBM DOS and OS/2 compatibles.

Contact us at EEsof, Inc., 5795 Lindero Canyon Rd., Westlake Village, CA 91362.

Phone: 1-800-624-8999, ext. 155
FAX: 818-991-7109

EEsof

INFO/CARD 1

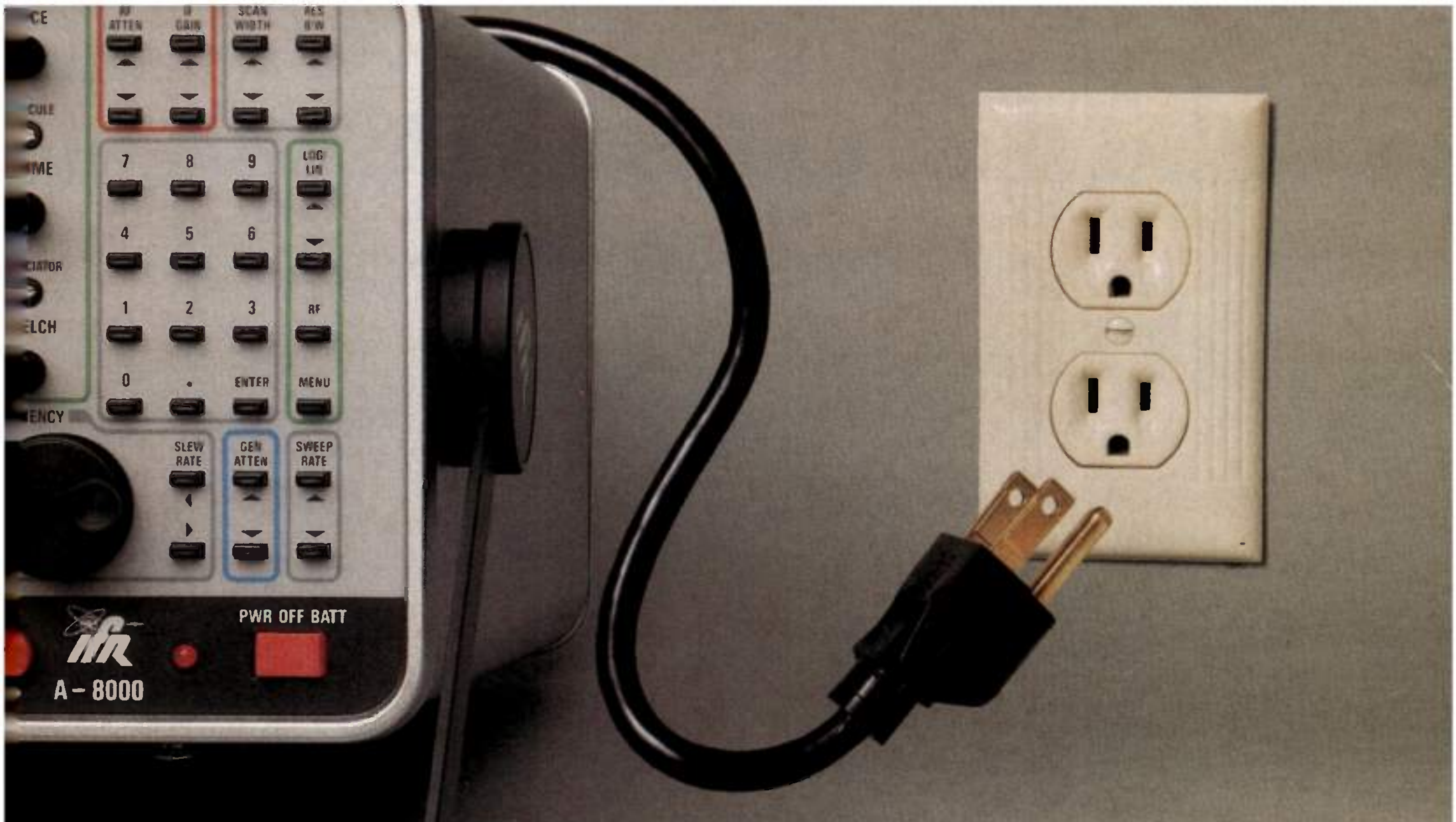

A-7550 10 kHz to 1 GHz

A-8000 10 kHz to 2.6 GHz

GaAs FET SWITCHES

- ULTRA LOW POWER CONSUMPTION
- CUSTOMIZATION AVAILABLE
- HI-REL OPTIONS AVAILABLE
- FAST SWITCHING SPEED
- INTEGRAL TTL DRIVER CIRCUITRY
- AVAILABLE FROM STOCK

GaAs FET SP2T SWITCH LOW COST

- Operating frequency: 10MHz-1GHz
- Transition time: 50ns
- Switching speed: 70ns
- Isolation: 50dB 10 - 100MHz
  40dB 100 - 300MHz
  25dB 300 - 1000MHz
- Power Requirements: 0.5mA at +5V
- Built-in 50ohm Terminations
- Built-in TTL Driver
- P/N DS0812 SP2T SWITCH

DAICO INDUSTRIES, INC.
2139 East Del Amo Blvd. Compton, CA 90220
Telephone (213) 631-1143. FAX (213) 631-8078

GaAs FET SPST SWITCH

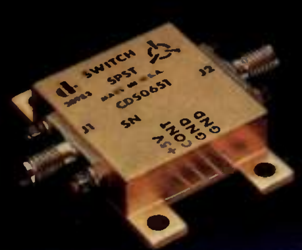

- Operating frequency: 10MHz-2GHz
- Transition time: 5ns
- Switching speed: 16ns
- Isolation: 57dB 10 - 1000MHz
  52dB 1000 - 2000MHz
- Power Requirements: 2mA at +5V
- Built-in 50ohm Terminations
- Built-in TTL Driver
- P/N CDS0651 SPST SWITCH

DAICO INDUSTRIES, INC.
2139 East Del Amo Blvd. Compton, CA 90220
Telephone (213) 631-1143. FAX (213) 631-8078

SURFACE MOUNT GaAs FET SWITCH

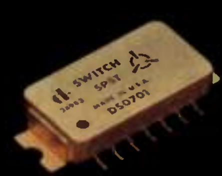

- Operating frequency: 10MHz-1GHz
- Transition time: 14ns
- Switching speed: 28ns
- Isolation: 70dB 10 - 200MHz
  62dB 200 - 500MHz
  52dB 500 - 1000MHz
- Power Requirements: 0.45mA at -15V
- Built-in 50ohm Terminations
- Built-in TTL Driver
- Pre-formed leads, low-stress design
- P/N DS0701 SPST SWITCH

DAICO INDUSTRIES, INC.
2139 East Del Amo Blvd. Compton, CA 90220
Telephone (213) 631-1143. FAX (213) 631-8078

GaAs FET SP2T SWITCH

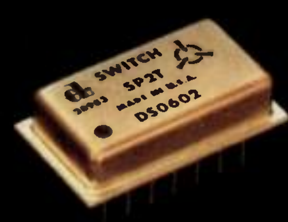

- Operating frequency: 5MHz-4GHz
- Transition time: 4ns
- Switching speed: 26ns
- Isolation: 45dB
- Power Requirements: 0.15mA at -5V
- Built-in 50ohm Terminations
- Built-in TTL Driver
- P/N DS0602 SP2T SWITCH

DAICO INDUSTRIES, INC.
2139 East Del Amo Blvd. Compton, CA 90220
Telephone (213) 631-1143. FAX (213) 631-8078

mp89503

INFO/CARD 3

rf design

April 1990

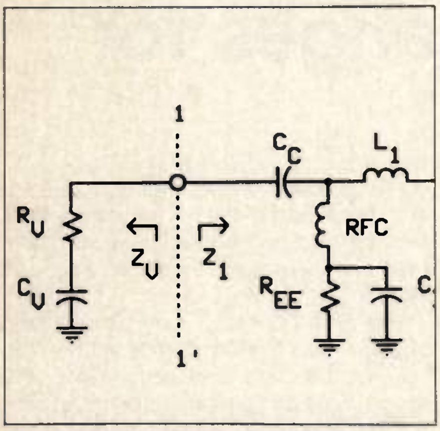

Page 29 — Nonlinear CAE Software

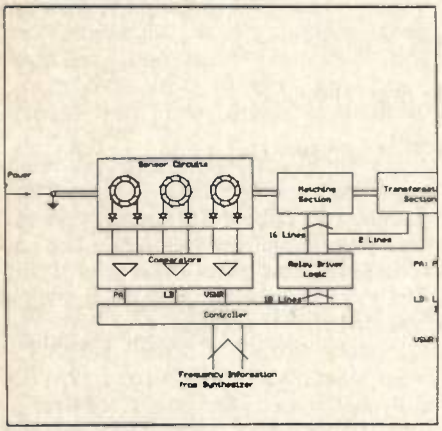

Page 32 — Antenna Matching

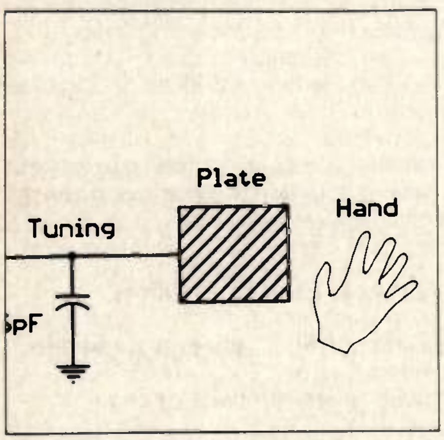

Page 52 — Human Antenna

R.F. DESIGN (ISSN: 0163-321X USPS: 453-490) is published monthly plus one extra issue in September. April 1990, Vol. 13, No. 4. Copyright 1990 by Cardiff Publishing Company, a subsidiary of Argus Press Holdings, Inc., 6300 S. Syracuse Way, Suite 650, Englewood, CO 80111 (303) 220-0600. Contents may not be reproduced in any form without written permission. Second-Class Postage paid at Englewood, CO and at additional mailing offices. Subscription office: 1 East First Street, Duluth, MN 55802, (218-723-9355). Domestic subscriptions are sent free to qualified individuals responsible for the design and development of communications equipment. Other subscriptions are: $33 per year in the United States; $43 per year in Canada and Mexico; $47 (surface mail) per year for foreign countries. Additional cost for first class mailing. Payment must be made in U.S. funds and accompany request. If available, single copies and back issues are $4.00 each (in the U.S.). This publication is available on microfilm/fiche from University Microfilms International, 300 N. Zeeb Road, Ann Arbor, MI 48106 USA (313) 761-4700.
POSTMASTER & SUBSCRIBERS: Please send address changes to: R.F. Design, P.O. Box 6317, Duluth, MN 55806.

rf editorial

Design Challenges for the '90s

By Gary Breed
Editor

Maybe you already have been assigned a task like this:

"Here's the specs for a new thromdimbulator. Marketing says we have 10,000 potential customers if we move quickly. Make sure it uses readily available and cheap components and can be at least 90 percent assembled by our new automated pick-and-place equipment. Try not to use a multi-layer board, either. They cost too much and they're hard to repair.

"Oh yeah, make it work without all those trimmers and pots that the last model had, because we have to cut down on setup and test time. Be sure to keep up with the project tracking file on the company network, too. Bruce in Purchasing, Jack in Production, Wilma in Test and Jim in Customer Service will all be giving you their comments. Have your preliminary design ready for a meeting next Thursday."

Right now, a lot of attention is given to high-level business competition, with Europe, the Far East, and other regions catching up or passing the U.S. In electronics as well as many other industries, American companies are looking for new ideas to successfully compete with these tougher adversaries, with increased efficiency a major part of the strategy. One essential part of increased efficiency is *design for manufacturability*, a process which has not been a significant part of the RF industry, where function and performance usually take precedence over assembly, testing, and service.

For an engineer, it may be a drastic change to do things differently. The "perfect" design is no longer one with the ultimate performance specifications, but is the one which meets basic standards at the lowest possible overall costs —including the cost of component parts, assembly labor, alignment, test, and shipping. Finally, the customer wants the cost of ownership to be minimal, including repair and calibration.

For some engineers, this isn't really new. Management may use new language to describe the process, but many of these ideas are already used by innovative industries. However, some RF products have put pure performance first. Military standards and the near-monopoly status of some companies have often discouraged economical design techniques. But this is changing, too. The biggest companies have seen the need for greater competitive strength, and are implementing new productivity and efficiency plans.

The challenge is clear — You still have to be the best technical engineer around...then you have to add a little economics, ergonomics, robotics, and politics. Global competition has found its way to your bench. Be a tough enough competitor to handle it!

Gary H Breed

Noise Com: Quality. Performance. Service.

From the leader in noise sources.

No one delivers noise performance like Noise Com. And no one delivers it on time, time after time, like Noise Com. We've built a solid reputation for quality, performance, and service that is unmatched in the industry.

Noise Com offers the industry's broadest spectrum of noise products — from diode chips to hermetically-sealed noise diodes to precision coaxial and waveguide noise sources, and manual, automated, and high-power noise generating instruments.

Noise Com also designs custom subassemblies that combine noise technology with passive and active components. We have constructed fast-switching frequency-hopping generators, extremely stable noise generating subsystems, frequency-agile jammers, and secure communications subsystems.

Quality products and the industry's most responsive service and support have made Noise Com the leader in noise technology.

Put our resources to work for you.

Call **Gary Simonyan** at Noise Com, (201) 261-8797.

For Noise Com's complete line of products see the Microwaves & RF Product Data Directory

Wideband noise-generating instruments for the bench

NC 6000 Series

DC to 18 GHz

- Rugged design
- Precision attenuator
- Crest factor 5:1
- Excellent flatness

The NC 6000 Series are rugged noise generating instruments designed for applications on the test bench, or in test stations in which an NC 6000 Series unit is incorporated with other equipment to provide a wide variety of functions.

Programmable broadband noise-generating instruments

NC 7000 Series

DC to 18 GHz

- Completely programmable—from front panel or IEEE-488 bus
- Non-volatile memory for measurement parameters
- Front panel display
- Fast-switching 127-dB attenuator
- +13 dBm or +30 dBm (1 W) white Gaussian noise output

The NC 7000 Series can be used alone to perform a programmed series of noise measurements, or they can be bus-controlled, for running a battery of tests automatically via any instrument controller.

High-power, broadband noise-generating instruments

NC 8000 Series

500 Hz to 500 MHz

- High power—up to 1 W (30 dBm)
- Uniform response— ±-2 dB
- Precision attenuator—100 dB in 10-dB steps (10 dB in 1-dB steps optional)
- Can be configured for custom requirements

The NC 8000 Series offers 1 W (+30 dBm) power output for applications such as EMC testing, broadband jamming, jamming simulators, in secure communications channels, and any other area requiring high-level noise.

NOISE/COM

Number One in Noise Sources.

E. 64 Midland Avenue, Paramus, New Jersey 07652
(201) 261-8797 • FAX: (201) 261-8339

INFO/CARD 5

rf design

a Cardiff publication Established 1978
Main Office:
6300 S. Syracuse Way, Suite 650
Englewood, CO 80111 • (303) 220-0600
Fax: (303) 773-9716

Publisher
Kathryn Walsh

Editor
Gary A. Breed

Assistant Editor
Liane Pomfret

Consulting Editor
Andy Przedpelski

Account Executive
Midwest/Southeast
Bill Pettit
Main Office

Account Executive
West Coast
Andrea Rogers
Main Office

Account Executive
Northeast
Kristine Rallis
Main Office

Market Research Director
Susan See

Editorial Review Board
Alex Burwasser, Ed Oxner
Doug DeMaw, Andy Przedpelski
Dave Krautheimer, Jeff Schoenwald
James W. Mize, Jr., Raymond Sicotte
Robert J. Zavrel, Jr.

Advertising Services
Cindy Wieland

Secretary
Theresa Maier

Assistant Circulation Manager
Cindy Zimmer

Convention Manager
Kristin Hohn

Registration Coordinator
Anne Stookesberry

Customer Service Representative
Leann Nowacki

Associate Production Managers
Matt Park, Maurice Lydick

Artists
Kim Austin, Paul Rivera
Joyce Fields, Shelley Moore
Brad Fuller, Sheri Ryder

Composition
Mike C. Moore, Marcie Tichenor

Published by
CARDIFF PUBLISHING COMPANY, INC
BPA

President
Robert A. Searle

Vice President — Production
Cherryl Greenman

Vice President — Convention Management
Kathy Kriner

Circulation Director
Patricia Shapiro

Controller
Jennifer Burger

Credit Manager
Patti McManness

Please address subscription inquiries to:
RF Design, Cardiff Publishing Company,
P.O. Box 6317, Duluth, MN 55806
Postmaster: send form 3579
to the above address.

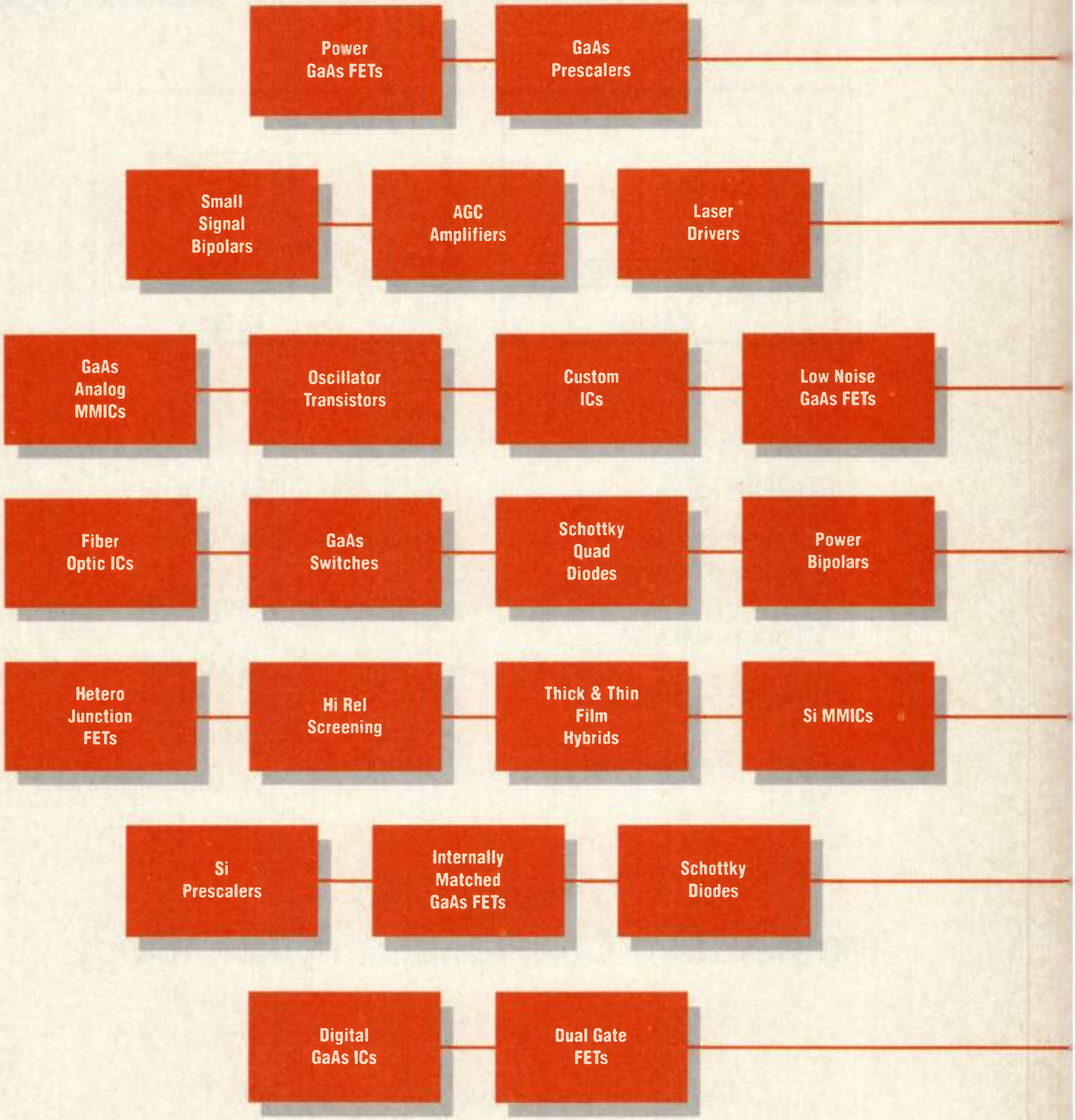
Power GaAs FETs
GaAs Prescalers
Small Signal Bipolars
AGC Amplifiers
Laser Drivers
GaAs Analog MMICs
Oscillator Transistors
Custom ICs
Low Noise GaAs FETs
Fiber Optic ICs
GaAs Switches
Schottky Quad Diodes
Power Bipolars
Hetero Junction FETs
Hi Rel Screening
Thick & Thin Film Hybrids
Si MMICs
Si Prescalers
Internally Matched GaAs FETs
Schottky Diodes
Digital GaAs ICs
Dual Gate FETs

rf letters

Letters should be addressed to: Editor, *RF Design*, 6300 S. Syracuse Way, Suite 650, Englewood, CO 80111.

Are RF Active Filters Noisy?

Editor:

I've noted a number of papers in *RF Design* in recent years regarding the use of analog operational amplifier techniques in RF circuitry. A case in point is the article "An RF Active Elliptic Filter," by Eric Kushnick, (February 1990 *RF Design*). One of the aspects seldom presented is the low noise performance of these types of filters in terms of some easily understood parameters such as the noise figure, minimum usable signal, or noise floor. To many of us old timers these methods are not suitable at or near the front-end of receivers, since relatively high noise levels are only suitable for video-type processing after the initial low level RF amplification and filtering.

The next time I see an article in *RF Design* regarding digital or operational amplifier methods, how about pointing out the practical low level noise limits? In terms of modern RF design methods some of us believe that true LC lowpass and bandpass methods perhaps with "noiseless feedback" using very low resistance inductors instead of resistors, are superior.

Ralph W. Burhans
Burhans Electronics
Athens, Ohio

LINC Transmitter Comments

Editor:

In regards to the article entitled "The LINC Transmitter," p. 41, February 1990. The author states that this method of generating an AM signal is perhaps the most efficient and indeed it is.

The author indicates that his reason for investigating methods of high-efficiency AM transmissions is to reduce the spectrum width now required by current FM systems. A laudable goal, on the surface. But FM communication is wide for a reason, namely it improves the signal-to-noise ratio for signals above a certain threshold value.

If the desired result is to achieve bandwidth reduction and improved efficiency, AM is certainly not the way to go about it. It has long been known that single-sideband systems give the highest utilization efficiency of the spectrum along with very good transmitter efficiencies when the carrier is reduced about 15 dB. For the system to function, this remaining "pilot carrier" is extracted and cleaned up in a PLL and then mixed with the recovered sideband for signal detection in the receiver.

A full analysis of nearly all SSB systems including those appropriate for land-mobile service can be found in the December 1956 issue of the *Proceedings of the IRE*, especially pp. 1834-1838.

Craig J. Brown
Corona, California

rf calendar

April 24, 1990
79th Semiannual IEEE Seminar: "International Telecommunications: Global Networking in the 1990s"
United Engineering Center, NY, NY
Information: Tel: (212) 825-1527 or (201) 467-9650

May 2-9, 1990
Electronics and Electrical Engineering '90
Hannover Fairgrounds, Hannover, West Germany
Information: Hannover Fairs USA, Inc., 103 Carnegie Center, Princeton, NJ 08540. Tel: (609) 987-1202

May 7-10, 1990
IEEE 1990 International Radar Conference
Arlington, VA
Information: Russell J. LeFevre, Technology Service Corp., 2950 31st Street, Santa Monica, CA 90405-3093

May 7-11, 1990
1990 IEEE MTT-S International Microwave Symposium
Dallas Convention Center, Dallas, TX
Information: LRW Associates, 1218 Balfour Drive, Arnold, MD 21012. Tel: (301) 647-1591

May 9-11, 1990
Electro 90
John B. Hynes Convention Center, Boston, MA
Information: Alexes Razevich, Director of Marketing, Electronic Conventions Management. Tel: (213) 772-2965

May 10-11, 1990
ARFTG 35th Conference
Dallas Convention Center, Dallas, TX
Information : ARFTG, P.O. Box 2182, Longmont, CO 80502-2182. Tel: (303) 776-4501

May 23-25, 1990
44th Annual Frequency Control Symposium
Stouffer Harborplace Hotel, Baltimore, MD
Information: Dr. R.L. Filler, U.S. Army Electronics Technology and Devices Laboratory, Attention: SLCET-EQ, Fort Monmouth, NJ 07703-5000. Tel: (201) 544-2467

June 5-7, 1990
AFCEA
Washington D.C. Convention Center, Washington, DC
Information: AFCEA, 4400 Fair Lakes Court, Fairfax, VA 22033. Tel: (800) 336-4583, ext. 6189; (703) 631-6189

Building Blocks

RNet™ Telemetry Radios from Motorola

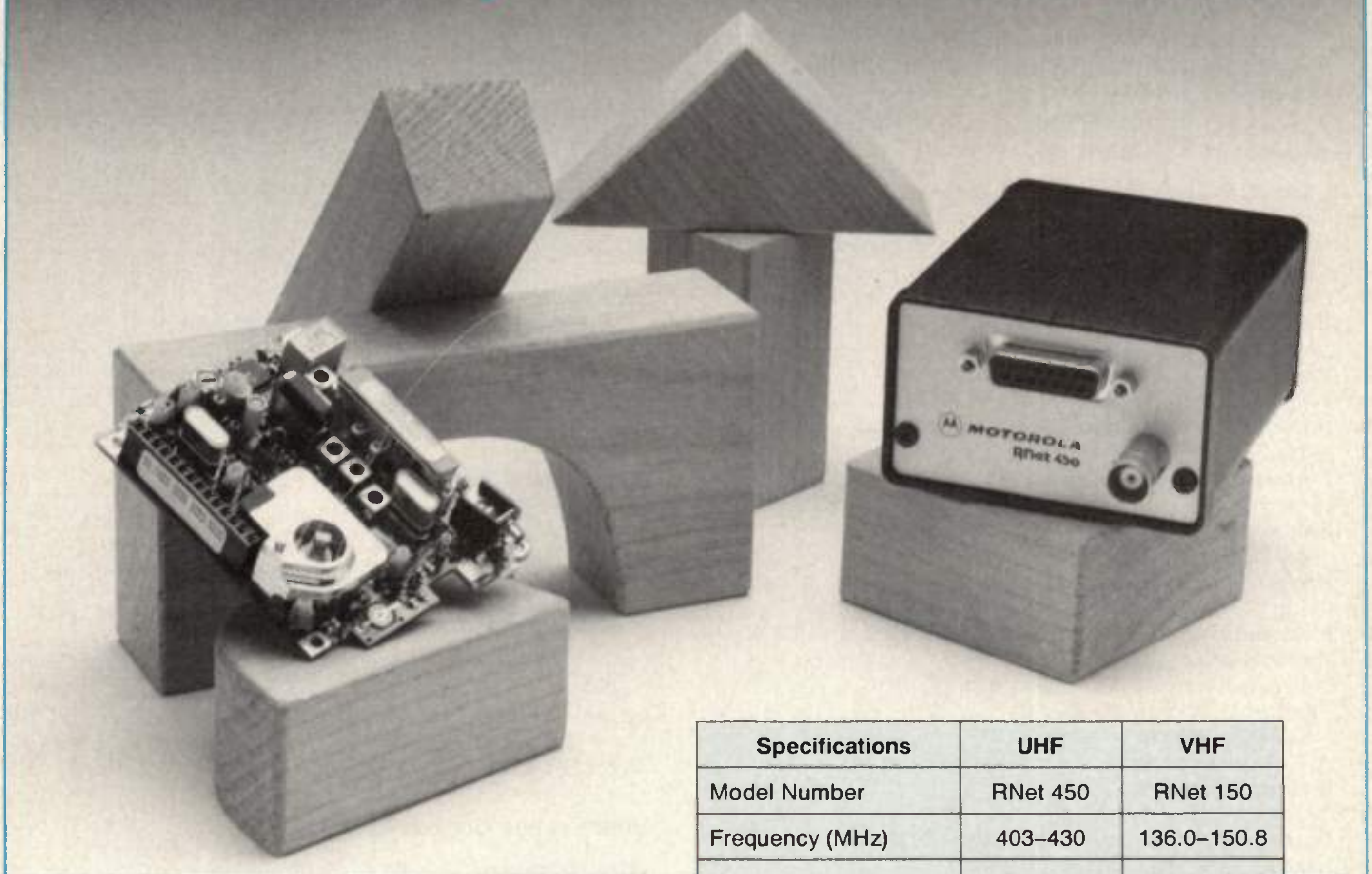

Specifications	UHF	VHF
Model Number	RNet 450	RNet 150
Frequency (MHz)	403–430	136.0–150.8
	450–470	150.8–162.0
		162.0–174.0
Nominal Power Supply	10 VDC to 17 VDC	
Current Drain		
Standby:	16mA	20mA
Receive:	16mA	20mA
Transmit:	800mA (2W)	800mA (2W)
	1400mA (4W)	1400mA (4W)
Dimensions	3.3″ x 2.7″ x 1.52″	
RF Output-TX	2W or 4W	2W or 5W

For years, design engineers seeking solutions have been turning to Motorola for product support. Now, as you envision new opportunities within the context of a wireless society, Motorola is there again with building block RF components that will enable you to move from design to production . . . the RNet™ Series of telemetry transceivers and OEM radio modules.

It doesn't matter if you are dealing with remote control, RF Data Collection, alarm reporting, status monitoring, metering or SCADA applications, Motorola's heritage of quality engineering and world class products provides you with voice and data capable telemetry radios that will fit your project.

- Competitively Priced
- Made in the U.S.A. for faster delivery
- Backed by 3 Year Limited Warranty*

Envisioning . . . that's your job.
Enabling . . . that's ours.

For more information and detailed specifications on RNet™ telemetry radios and OEM radio modules,

call 1/800-624-8999
Ext. 5992

Ⓜ, MOTOROLA, Radius and RNet are registered trademarks of Motorola, Inc.
F.C.C. type approval pending.
Specifications subject to change without notice.
*Telemetry radio models only.

MOTOROLA
Radius Division
1301 East Algonquin Road • Schaumburg, IL 60196

INFO/CARD 14

rf courses

Arizona State University

Fiber Optic Communications
June 11-13, 1990, Sunnyvale, CA

Information: Center for Professional Development, College of Engineering and Applied Sciences, Arizona State University, Tempe, AZ 85287-7506. Tel: (602) 965-1740

The George Washington University

Cable-Free Data Transmission Systems
April 16-18, 1990, Washington, DC
Modern Communications and Signal Processing
April 16-20, 1990, Washington, DC
Integrating Fiber Optics and Analog/RF Communications Systems
April 23-25, 1990, Washington, DC
Trends in Digital Signal Processing
April 30-May 4, 1990, Washington, DC
Introduction to Modern Radar Technology
May 2-4, 1990, Washington, DC
Frequency-Hopping Signals and Systems
May 7-9, 1990, Washington, DC
Electromagnetic Interference and Control
May 7-11, 1990, Washington, DC
Radar Systems and Technology
May 14-18, 1990, Washington, DC
Ionospheric Radio Propagation: Principles and Applications
May 29-June 1, 1990, Washington, DC
Electronic Countermeasures
June 4-8, 1990, Washington, DC
An Introduction to Numerical Techniques in Electromagnetics
June 5-8, 1990, Washington, DC
Spread-Spectrum Communications Systems
June 11-15, 1990, Colorado Springs, CO
New HF Communications Technology: Advanced Techniques
June 18-22, 1990, Washington, DC

Information: Merril Ferber, Continuing Engineering Education, George Washington University, Washington, DC 20052. Tel: (800) 424-9773; (202) 994-6106

Research Associates of Syracuse

ELINT/EW Applications of Digital Signal Processing
May 1-3, 1990, Syracuse, NY
ELINT Analysis
May 9-11, 1990, Syracuse, NY
Radar Vulnerability to Jamming
May 17-18, 1990, Syracuse, NY
Integrated EW
May 22-23, 1990, Syracuse, NY

Information: RAS, Inc., Hancock Army Complex, 510 Stewart Drive, N. Syracuse, NY 13212. Tel: (315) 455-7157. Fax: (315) 455-8037.

Design and Evaluation, Inc.

Worst Case Circuit Analysis
May 21-23, 1990, Washington, DC

Information: Design and Evaluation, Inc., 1451B Chews Landing Road, Laurel Springs, NJ 08021. Tel: (609) 228-3800

Fluke-Philips

Principles of Analog Oscilloscopes
May 15-16, 1990, Atlanta, GA
Principles of Digital Oscilloscopes
May 17-18, 1990, Atlanta, GA

Information: John Fluke Mfg. Co., Inc., PO Box 9090, Everett, WA 98206. Tel: 1-800-443-5853 ext. 73. In Canada: (416) 890-7600

TKC

Design for ESD and RFI
May 16, 1990, North Redington Beach Hilton, FL

Information: Ms. Jean Whitney, TKC, The Keenan Building, 8609 66th St, North, Pinellas Park, FL 34666. Tel: (813) 544-2594. Fax: (813) 544-2597

CEI-Europe/Elsevier

RF and Microwave Circuit Design I: Linear Circuits
June 18-22, 1990, Cambridge, UK
RF and Microwave Circuit Design II: Non-Linear Circuits
June 18-22, 1990, Cambridge, UK
SAW - Surface Acoustic Wave Devices for Signal Processing
June 18-22, 1990, Cambridge, UK

Information: Mrs. Tina Persson, CIE-Europe/Elsevier, Box 910, S-612 01 Finspong, Sweden. Tel: 46 (0) 122-17570. Fax: 46(0)122-14347

Interference Control Technologies, Inc.

Grounding and Shielding
April 17-20, 1990, Washington, DC
Practical EMI Fixes
May 7-11, 1990, Washington, DC
Introduction to EMI/RFI/EMC
May 22-24, 1990, San Francisco, CA

Information: Elizabeth Price, Interference Control Technologies, Inc., State Route 625, P.O. Box D, Gainesville, VA 22065. Tel: (703) 347-0030

EEsof, Inc.

Touchstone
May 22-24, 1990, Westlake Village, CA
OmniSys
May 30-June 1, 1990, Westlake Village, CA
Libra
June 5-7, 1990, Westlake Village, CA
mwSPICE
June 12-14, 1990, Westlake Village, CA
Academy (Schematic)
June 19-20, 1990, Westlake Village, CA
Academy (Layout)
June 21-22, 1990, Westlake Village, CA

Information: Sande Scoredos, Training Coordinator, EEsof, Inc., 5795 Lindero Canyon Road, Westlake Village, CA 91362. Tel: (818) 991-7530, ext. 197

IBM Scientists Demonstrate Fastest Transistor for New Circuits

IBM Scientists from the Thomas J. Watson Research Center showed an experimental 27 GHz PNP transistor at the 1989 International Electron Devices Meeting. Scientists have reported that digital circuits built with the new transistors switch on and off 25 billion times per second, more than three times as fast as previous generations of PNP circuits. The PNP devices run at speeds comparable to the historically higher operating speeds of the more commonly used NPN bipolar transistors. The high speeds of the NPN circuits are necessary for today's high-speed logic and memory applications in high-end computer systems. Until now, the slower PNP devices and the difficulties of combining both devices in one chip have hindered the development of faster generations of complementary bipolar circuits using both PNP and NPN devices.

Now, many researchers believe that complementary bipolar circuits using both devices will be able to outperform circuits based solely on NPN devices by allowing higher speed operation at lower levels of power consumption. Since the p and n dopant types are reversed in PNP and NPN devices, the voltage required for switching the device on and off is reversed and the direction of the current flow is reversed as well. IBM used existing double-poly technology to manufacture the high-performance PNP devices. Researchers also believe that the advent of complementary bipolar circuits may revolutionize this field in the same way that the combination of NMOS and PMOS devices in Complementary Metal Oxide Semiconductor (CMOS) circuits produced dramatic advances in MOS technology.

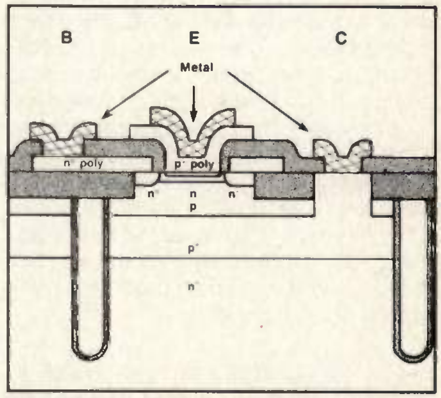

Schematic cross section of the PNP transistor.

INFO/CARD 15

The devices have 80 nm wide ion implanted bases, optimized emitter and collector dopant profiles, and are fabricated on a thin p-type epilayer in order to achieve high collector current driving capability. Devices with emitter sizes down to 0.5 microns were fabricated on an epitaxial layer over a heavily doped p subcollector. The n-substrate, polysilicon filled deep trench and a beakless shallow trench field oxide provided device isolation. The minimal thermal cycle of the shallow trench isolation process was essential in maintaining an accurate control of the epi-flat zone thickness. They have arsenic implanted bases and a collector profile designed to provide a thin base and to prevent base stretching at high current densities.

NAB Convention to be Held at World Congress Center in Georgia — The National Association of Broadcasters will hold its annual convention March 31 to April 3 with more than 700 exhibitors. The convention will attract people from all areas of the broadcasting industry — owners of radio and TV stations, users and buyers of broadcast equipment and many more. There will be more than 40 seminars offered this year on all aspects of the broadcast industry. Some of the engineering sessions will feature digital technology, AM systems engineering, radio production and audio processing. For television there will be sessions on advanced television and UHF transmission systems There will also be a series of special programs for foreign attendees with an emphasis on changes in the european market.

Scientific-Atlanta to Build NASA Antenna System — Scientific-Atlanta has announced the sale of an Automatic Precision Tracking Transportable Telemetry Antenna System to the NASA Goddard Space Flight Center, Wallops Island, Virginia. The sale is the second system sold to NASA in the past six months. These tracking systems will be used to track sounding rockets and low earth orbit satellites.

Foundation for Amateur Radio Announces Scholarships — The Foundation for Amateur Radio has announced that it plans to award thirty-three scholarships for the academic year 1990-91 to assist licensed Radio Amateurs. Licensed Radio Amateurs may compete for these awards if they plan to pursue a full-time course of studies beyond high-school and are enrolled in or have been accepted for enrollment at an accrecited university, college or technical school. For more information or an application form, write to: FAR Scholarships, 6903 Rhode Island Avenue, College Pa-k, MD 20740.

M-tron and AT&T Network Systems Sign Agreement for Marketing Oscillator — AT&T and M-tron have signed an agreement to private label MS Oscillators for worldwide distribution by M-tron. The MS Series Oscillator was conceived and developed at AT&T Bell Laboratories for use in AT&T voice and data communication applications.


BOONTON 8220 MODULATION METER
AF OUT
LINE
RF IN 50Ω

Alcatel and QUALCOMM Sign Joint Venture Agreement — Alcatel and QUALCOMM, Inc have announced the signing of a joint venture agreement to support multiple, continent-spanning operations of a satellite-based communications and position reporting systems for trucking fleets and other mobile users. The agreement covers marketing, manufacture, service and distribution of QUALCOMM's OmniTRACS[R] throughout Europe, North Africa and the Middle East. QUALCOMM has also recently implemented the QUALCOMM Automatic Satellite Position Reporting (QASPR[TM]) system into OmniTRACS. In the United States, Boyd Bros. Transportation Company recently signed a contract for over 300 OmniTRACS units to be installed in their fleet.

Hewlett-Packard Signs Joint Agreement with Aeritalia — HP has announced a joint agreement with Aeritalia's Systems and RPV Group to market electromagnetic-compatibility (EMC) measurement systems. HP will supply its EMC and general purpose test and measurement instrumentation as well as computers and peripherals. Aeritalia will design custom EMC systems and provide integration, installation, training, and hardware and software support.

Teradyne Test System Units Purchased by Texas Instruments and Micro Linear Corp — Teradyne has announced the sale of four A500 Family Systems to TI-Japan, TI-Nice, Motorola and Micro Linear. The A500 family system is a workstation-based test system offering a full complement of instrumentation modules for testing a wide range of standard linear devices.

Avantek Receives Subassembly Contract from Tridom — Avantek has announced that it has received a $12.5 million Ku-band subassembly order for transmitter RF assemblies for VSATs in the AT&T Skynet[R] Clearlink service. During the multi-year contract run, Avantek will supply several thousand assemblies to Tridom, an AT&T VSAT subsidiary.

AEL Wins $2.42 Million Contract from Dalmo Victor — AEL Industries has been awarded a contract to produce Compression Video Amplifier Detectors (CVAD) for the ALR-67 program. AEL's Microwave/Hybrid Division will act as a subcontractor to Dalmo Victor, who in turn will supply the ALR-67 system to the Naval Air Systems Command. The CVAD unit is located in the low-band receiver and quadrant receivers of the ALR-67 radar warning system.

Leader Instruments Corp. Establishes New Subsidiary — Leader Instruments Corporation has announced the establishment of a new European subsidiary, Leader Instruments Europe, Ltd. The new office, based in London, England opened in late January.

Aeroflex Laboratories Acquires Comstron Corporation — Comstron Corporation was completely integrated

INFO/CARD 18

into the Aeroflex facility during December, 1989 and the combined operation is functioning smoothly. Aeroflex is now able to offer Comstron's line of high speed frequency synthesizers, subsystems and frequency control products in addition to their standard product line.

Echelon Signs Agreements with Motorola and Toshiba — Motorola and Toshiba have entered into agreements with Echelon to launch a new communications and control network technology. Under the terms of the agreements, both Motorola's Semiconductor Products Sector and Toshiba's Semiconductor Group will manufacture and sell integrated circuits designed by Echelon. The ICs implement the Local Operating Network (LON[R]) System, which is a collection of intelligent, programmable nodes. Included in each node in the network are ICs capable of sensing, controlling, and reporting status to any node as well as responding to messages received from other nodes.

Rantec Microwave Moves — Rantec Microwave and Electronics, Inc., Anechoic/Shielding Division has announced their move to new facilities in Chatsworth, Calif. The company's new address is: Rantec Microwave & Electronics, Inc., Anechoic/Shielding Systems, 9401 Oso Avenue, Chatsworth, CA 91311. Tel: (818) 885-8223. Fax: (818) 772-2355.

Microdyne Signs Letter of Intent to Purchase Acurex Corporation's Telemetry Products Business Unit — Microdyne Corporation has announced that it has executed a formal letter of intent to purchase the telemetry products business unit of Acurex Corporation. The telemetry products line consists of wireless data couplers, RF equipment used to sense and transmit data over short distances from harsh environments and rotating equipment. The acquisition price will be between $4 and $5 million and completion of the acquisition will be subject to the company's finalization of an agreement.

Amoco Technology Acquires Meret Optical Communications — Amoco Technology Company (ATC) has announced its purchase of Meret Optical, a manufacturer of wideband analog fiber-optic transmission systems. Meret is the fifth company to join the photonics group of ATC.

Ion Implant Services Opens New Facility — Ion Implant Services (IIS) has opened a new facility to provide high-quality particle-free implants, installed in two certified class 10 clean rooms. IIS has teamed up with Sematech to provide its customers with the Genus 1500 high-energy implantation system at approximately one tenth the cost otherwise incurred for ion implantation.

rf q&a forum

Questions should be addressed to: Q&A Forum, *RF Design*, 6300 S. Syracuse Way, Suite 650, Englewood, CO 80111. Questions chosen for publication will not use the author's name.

AM Synchronous Detection

Q&A Forum:

I am working on the subject of AM synchronous detection in communication receivers, and have been unable to find much in my library research. Can you direct me to appropriate reference material? Any help would be greatly appreciated.

K.W.
Louisville, KY

[*Thanks to Dan Baker for providing this month's reply.*] Several textbooks on communications systems have good discussions of various AM detection/generation methods. Most combine discussions of DSB, SSB, and VSB, rather than offering a separate section on synchronous detection.

My first recommendation is *Introduction to Communication Systems* by Ferrel G. Stremler (Addison-Wesley, 1977). Chapter 5 is on AM theory, and my personal copy is full of highlighter marks and coffee rings. Section 5.6.1, pp. 240-242, deals with this topic, showing how the quadrature components of the narrowband noise cancel to gain a 3 dB S/N improvement.

Next is *Modern Digital and Analog Communication Systems*, by B.P. Lathi (Holt, Reinhart and Winston, 1989). Chapter 4 is the place to look (section 4.5). The Costas loop is described on page 256, a neat way of detecting DSB-SC signals where the frequency is known, but there is no pilot carrier.

Another good reference is *Phaselock Techniques*, by Floyd Gardner (Wiley & Sons, 1979), Section 9.2, pp. 167-172. If noise performance is of interest, this is a good reference for comparison to square-law or envelope detection.

Dan Baker
TV Engineering
Tektronix, Inc.

The Changing Face of Consumer Electronics

By Liane Pomfret, Assistant Editor and Mark Gomez, Technical Editor

Today's consumer electronics industry is undergoing a period of change caused by the evolving nature of the consumer market. Today's consumer wants a product that is faster, smaller and better. So, in order to compete, manufacturers have to keep up with current trends and be able to produce a marketable product or else they risk losing their share of the pie.

One of the latest trends has been the move towards surface-mount technology (SMT). While surface-mount construction has been around for several years, it's only been recently that manufacturers have started using it on a large scale. According to Marty Markson, vice president of sales and marketing for Sprague-Goodman Electronics, Inc., "In terms of new designs and applications we are seeing more interest in surface-mount than in plated through-hole type designs." Claude Profnier, RF communications strategic manager for Motorola's Linear IC Division, agrees "In the consumer industry, we have seen some statistics that indicate about 60 percent of the market is surface mount and 40 percent non surface-mount." Part of the reason behind increased SMT use is that the consumer wants smaller products and SMT makes it easier to achieve this goal. "People are looking for smaller size and surface-mount is a major factor," state Paul Liebman, marketing manager for Coilcraft. Steve Skiest, RF products manager at Toko America, Inc. agrees, "The trend is towards smaller devices, surface-mount is becoming very critical." In addition to the size consideration, pricing of components is also very important. Jon GrosJean, of Woodstock Engineering, design consultants, notes, "In many cases, they [surface-mount components] are now cheaper than the through-hole." In fact, many manufacturers are now offering a better product at the price of the old product or the old product at a reduced price because they use the less expensive surface-mount components in their designs. GrosJean continues "You now see surface-mount boards with parts on both sides." This is an added bonus when board space is at a premium and RF concerns are not of major importance. The versatility of SMT has made it attractive to manufacturers in all areas of consumer electronics, including cellular communications.

The cellular telephone and personal communications market has seen tremendous growth recently and this trend is expected to continue. Rich Potyka, manager of applications engineering at Motorola's Linear IC Division, confirms this "Personal communications, in general, is one of the large growth areas for the early 90s." Part of this is due to a change in the average consumer. "The nature of the consumer is changing. If you look at what defined a consumer product ten years ago versus today, a lot more has been added to the realm of consumer goods," says Peter Himes, product marketing manager for consumer linear at National Semiconductor. Essentially, consumers have become more sophisticated and as a result, now expect a more sophisticated market. Manufacturers of components are feeling the impact of the new consumer and must plan their market strategies accordingly. Jerry Kolbe, the product engineer for Murata-Erie North America says,"We sell a lot of components to the cellular telephone market and the pocket pager market." An indication, that even on the components level, the wants of the consumer are still felt.

While cellular communications products are the hot item for now, manufacturers are already looking down the road to the next big market trend. Many believe that the next wave to sweep the market will be in the area of home security and automation. Steve Ulett, sales manager for Penstock, Inc. comments, "Cellular radio and smart appliances like the sophistication of dishwashers and refrigerators is going to get higher and higher, to the point where you might have a remote control or home computer system for those appliances." These systems might use any number of transmission methods — wired links, infrared, or RF frequencies but will all accomplish the same task.

Systems for the home are not the only trends companies see for the future of consumer electronics. Steve Ulett believes that "Another area (of growth) is tagging and inventorying. ID cards are an area that is going to explode because you can't do bar coding on dirty surfaces." Another trend in the future might be the use of smart license plates on cars. These license plates would contain a chip and lithium battery in the renewal sticker and police or toll authorities could use them to collect information without having to stop the vehicle.

Despite all the talk about promising trends, there is concern among American manufacturers about off-shore producers. Neil Albaugh, the high speed product line manager at Burr-Brown Corporation observes, "The Korean market in the consumer electronics industry is definitely growing. It is probably growing faster than Japan these days." While many consider Korea to be the new star, the upcoming reorganization of Europe will also be a significant factor in how well the United States will do in worldwide competition.

Economically, the consumer electronics industry is growing at approximately three to five percent per year. "Overall the market is fairly flat, but there are identifiable markets within consumer electronics that have high activity." says Peter Himes. Gary La Belle, director of marketing for semiconductor products at Avantek, Inc. sees a more stable market overall, "I certainly see growth in the consumer market. The automobile applications, GPS, communications and the personal telephone market are growing." However, some manufacturers see some areas quite differently. "We see the automotive business as being rather stagnant," notes Skiest. Manufacturers are taking a closer look at their marketing strategies and directing their efforts towards areas where they feel they will do best.

The evolution of today's consumer electronics industry is moving faster than ever. Adaptability is the key word for manufacturers who want to survive in the world market. rf

A DESIGN ENGINEER DISCUSSES TRAK MICROWAVE'S BREAKTHROUGH NEW PRODUCT.

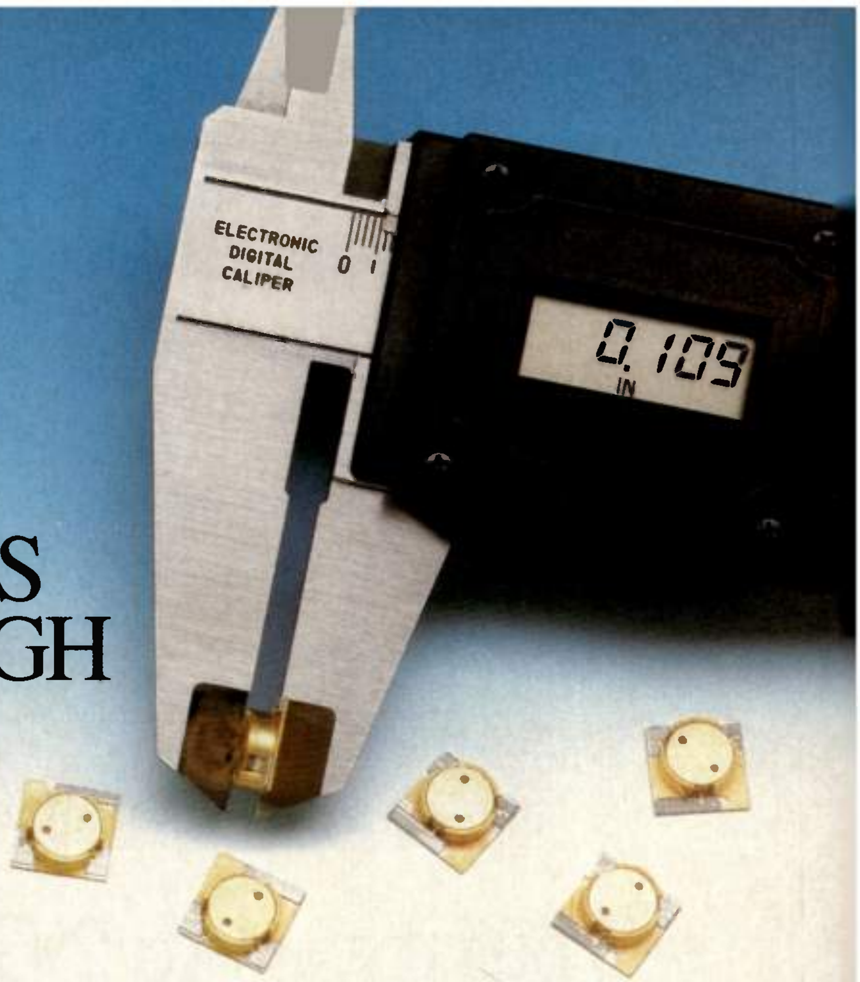

"It's really small. The component was designed to fit into a hermetic housing... because of cooling system requirements and the necessity to pack the modules into the X-Band element spacing of 0.7", we had a severe height requirement of 0.109". Meeting that was the most important aspect of the TRAK design."

"True surface mount... its height to RF circuitry is similar to other hybrid circuits; it butts right up to 25-mil alumina parts. And if RF lines are needed, they also line up well with the TRAK part."

"It has a flat base, so I can machine the housing with a flat floor — no cavity required. That not only keeps the price down but, most importantly, it assures a good joint between each subassembly and the housing floor."

"Because the part is built with 80/20 Au/Sn solder, I can mount the device

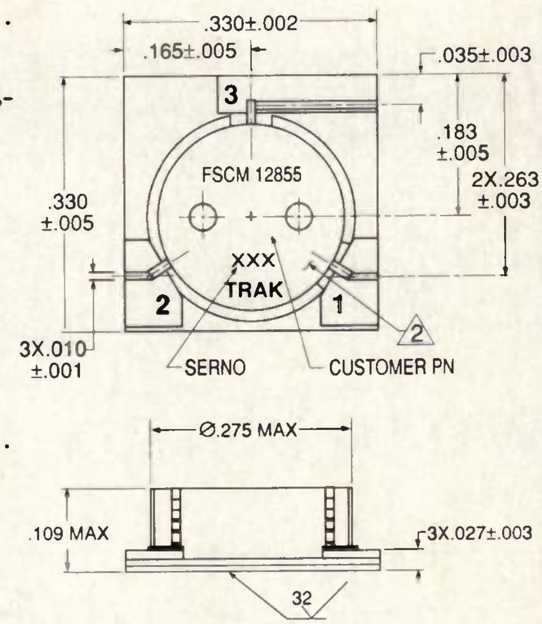

- ☐ Truly microstrip compatible
- ☐ Shielded
- ☐ Low loss, high isolation
- ☐ Temperature stable
- ☐ Low, 0.109" profile
- ☐ Fluxless assembly
- ☐ MIC technology
- ☐ Gold eutetic bonding
- ☐ Military grade
- ☐ Production item

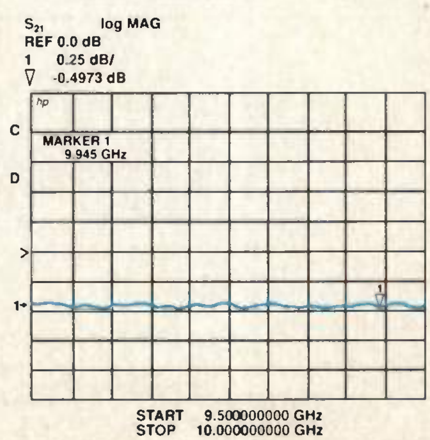

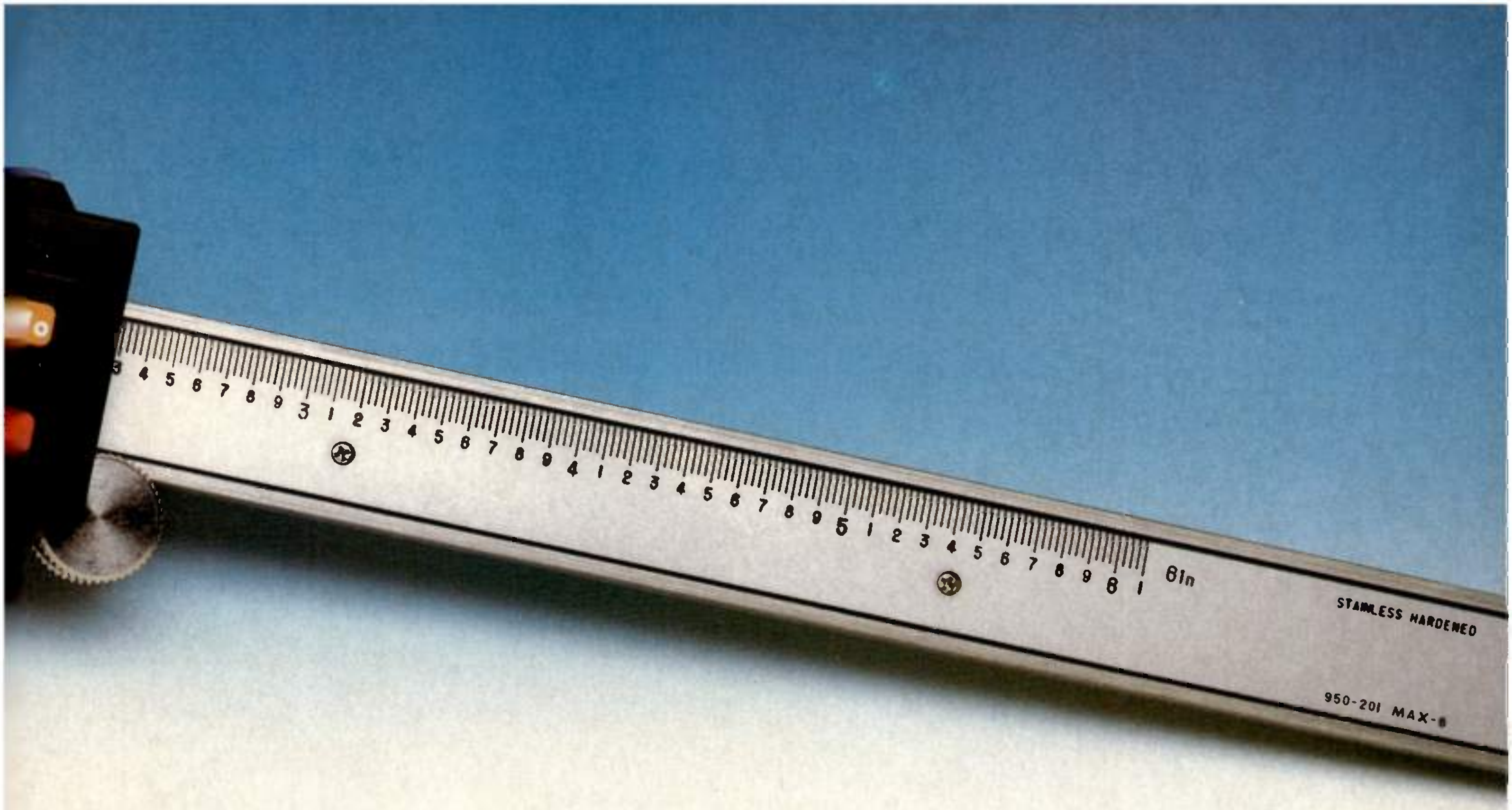

with 50/50 Pb/Sn solder... an ideal combination in reliability and manufacturability. And since both

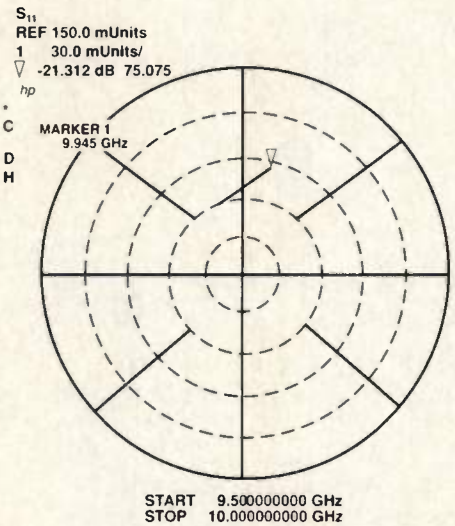

solders are fluxless, I avoid a chance of exposing active devices in the module to harmful contaminants... 'Better safe than sorry.'"

"The magnetic shielding of this part is extraordinary. For us, it was overkill. Its loss and isolation compare to something installed with bolts."

"It's built solid. The one-piece housing and screw-on lid probably have a lot to do with its ruggedness. I'm going airborne, accelerating it to 5,000 Gs... it holds together great. I believe the part is capable of 20,000 Gs, but we aren't required to meet that high level."

"Delivery was important; even though they were custom, I needed hundreds of these parts. TRAK produced them."

That's what he said. And that's what our labs can do. So look at our specs, and think how you could use a circulator or isolator like this.

Then, think TRAK.

Call or write for our Free Components Catalogs. See EEM or MPDD for other TRAK military products.

TRAK MICROWAVE CORPORATION
Microwave Sales
4726 Eisenhower Blvd.
Tampa, Florida 33634-6391
Phone: (813) 884-1411
TLX: 52-827
FAX: 813-886-2794

TRAK MICROWAVE LTD.
Microwave Sales
3/4 Lindsay Court
Dundee, Scotland DD21TY
Phone: (44) 382-561509
TLX: (851) 76266
FAX: (44) 382-562643

TRAK MICROWAVE CORPORATION

THINK TRAK

TRAK MICROWAVE CORP. 30 ANNIVERSARY

INFO/CARD 22

Nonlinear CAE Software Optimizes Oscillator Design

By Octavius Pitalis and Tom Reeder
EEsof, Inc.

The design of high-frequency oscillator circuits has become easier in the past few years thanks to the development of new CAE software tools for nonlinear circuit design and optimization. This article reviews the application of these tools, using a 2 GHz common-base transistor oscillator as a practical example. While the use of EEsof's Touchstone linear simulator and Microwave SPICE time-domain simulator have become increasingly popular in oscillator design, the application of EEsof's Libra harmonic-balance simulator is shown to have important advantages, especially for circuits that require nonlinear optimization to achieve prescribed goals for frequency, harmonic purity, and power output.

High-frequency oscillator design has traditionally been considered an arduous task. Designs operating above 100 MHz must carefully consider small circuit parasitics, and the simultaneous optimization of frequency, power output, and spectral purity requires a complex nonlinear analysis. However, the availability of new commercial CAE design tools makes the job much easier. We will show how EEsof's Touchstone[R], Microwave SPICE[R], and Libra[TM] simulators provide a complete tool kit for oscillator design, from the determination of start oscillation conditions through the analysis and optimization of oscillator power output and spectral purity. In particular, we shall highlight the capabilities of the Libra harmonic-balance simulator, which provides analysis and nonlinear optimization of oscillator steady-state operation.

Basic Oscillator Design

Consider the oscillator circuit shown in Figure 1. This common-base bipolar transistor topology is often used to build compact voltage-controlled-oscillator (VCO) circuits. The NE416 transistor and circuit values listed in Figure 1 are appropriate for an oscillator operating near 2 GHz; other transistors and circuit element values could be specified for frequencies in the 100 to 4000 MHz range. A varactor device, represented here by the series circuit R_V–C_V, provides a variable capacitance for oscillator tuning. The output circuit, here represented primarily by the simple parallel combination of resistor R_L and inductor L_3, is usually an interstage or output amplifier circuit designed to meet specified conditions for load matching and/or harmonic rejection. These more ambitious output circuits are not considered here but could be easily represented in later simulations.

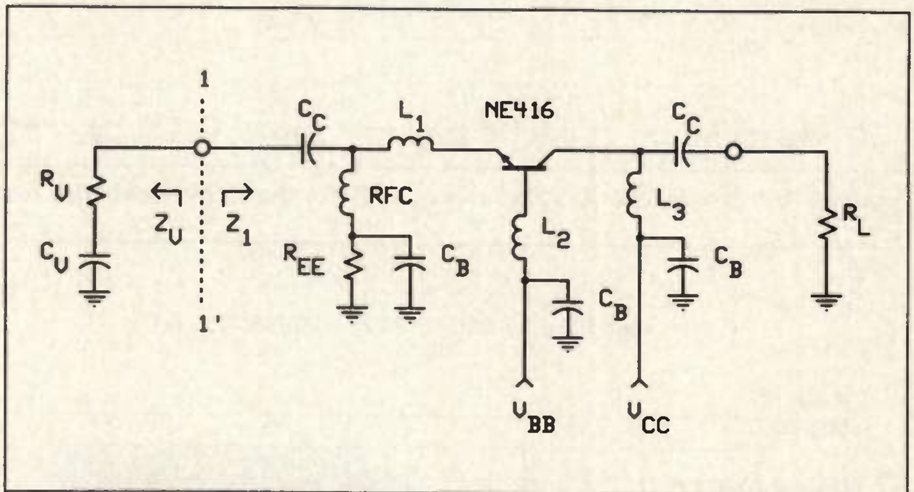

R_V = 6 ohms	L_1 = 3.0 nH	L_2 = 3.0 nH	L_3 = 3.0 nH
C_V = 0.66 pF	R_{EE} = 35 ohms	R_L = 100 ohms	C_C = 50 pF
V_{BB} = 1.7 volts	V_{CC} = 12 volts	RFC = 100 nH	C_B = 1000 pF

Figure 1. Circuit schematic for the 2 GHz bipolar transistor oscillator.

Oscillators using the circuit in Figure 1 fall into the "negative resistance" class. Conditions for oscillation are found by evaluating the impedance (or admittance) at circuit plane 1-1'. The element Z_1 refers to the series impedance looking into the transistor emitter loop; the impedance Z_V is the complex impedance presented by the varactor. The threshold for circuit oscillation occurs when the impedance sum at plane 1-1' is zero (1): $R_V + R_1 = 0$, $X_V + X_1 = 0$. Note that at this point of threshold oscillation, circuit conditions are linear, so a linear CAE simulator like Touchstone can be utilized. While the equations must be precisely satisfied at the exact threshold of oscillation, it is also clear that a linear circuit analysis that finds net negative resistance over the desired frequency range will assure that the circuit is capable of oscillating over that range. Figure 2 shows plots of R_1 and X_1 versus frequency for our assumed circuit example. The simulations show that a net negative resistance is observed as the transistor base circuit inductance L_2 is selected for operation at frequencies in the desired operating range. The use of Touchstone to define oscillation starting conditions in this way is well known and has been documented earlier (2).

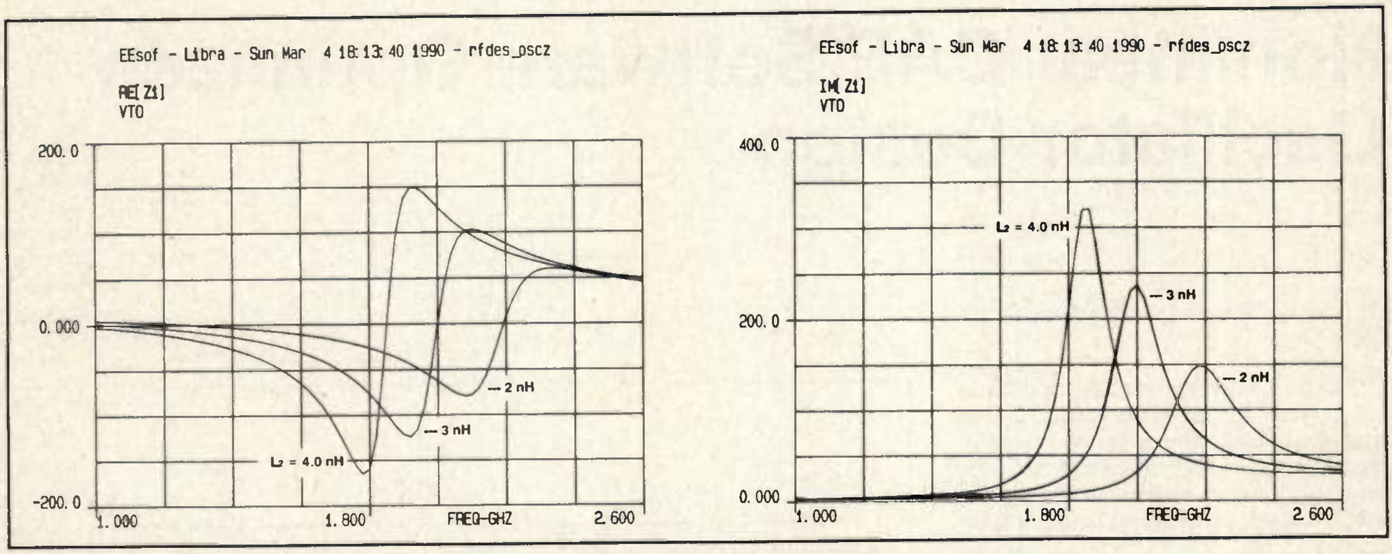

Figure 2. Plots of R_1 and X_1 versus frequency for the 2 GHz oscillator example.

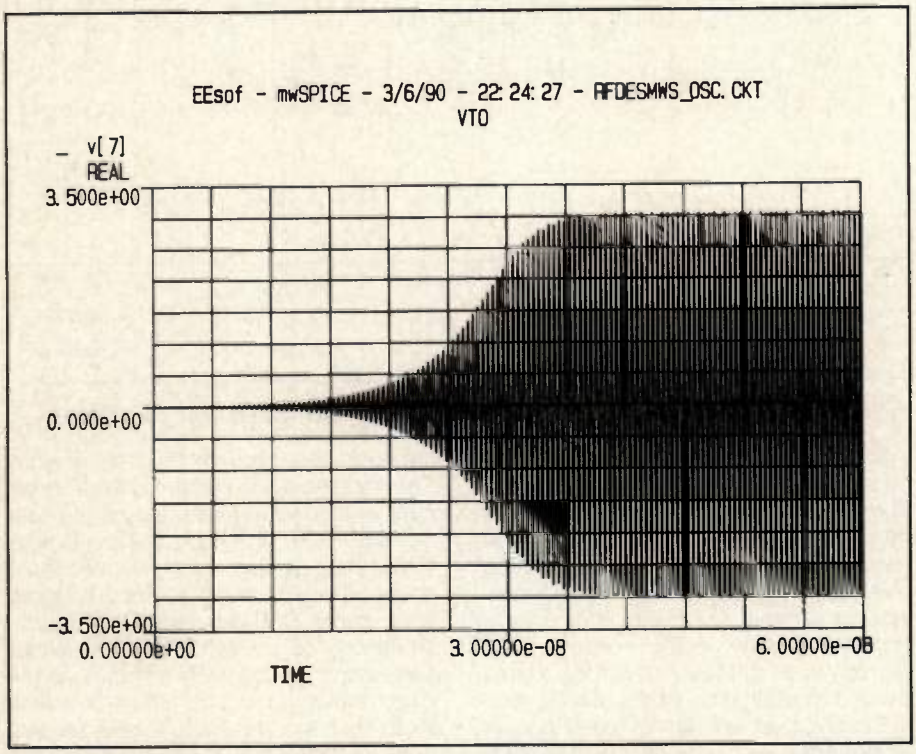

Figure 3. Start up condition voltage and current waveforms at transistor collector as simulated in Microwave SPICE.

Another software tool often used in oscillator design is the simulator SPICE, which was first developed in university research at Berkeley (3). A number of commercially based SPICE simulators have been introduced during the past five years. EEsof's Microwave SPICE builds upon and extends the algorithms introduced in Berkeley SPICE, and also provides excellent large signal transistor models, as well as a useful set of high frequency and microwave transmission line models. Microwave SPICE allows the designer to set up a simulation that evaluates the true start up conditions for oscillation. As shown by the simulation in Figure 3, the designer can watch the oscillation waveform grow from zero to a steady-state sinusoidal output. To achieve the simulation in Figure 3, a small impulse signal is introduced in the transistor emitter loop at t = 0. Microwave SPICE has the advantage that it accurately represents the circuit for both small signal and large signal operating conditions. However, for circuits controlled by medium to high-Q resonances, the computation time to simulate a complete oscillator start up can be excessive. This makes circuit optimization inefficient, as numerous simulation runs are usually necessary to achieve the desired circuit performance.

Harmonic-Balance: A New Software Technology for Oscillator Design

One of the exciting new software technologies to emerge recently is the harmonic-balance high frequency circuit simulator. Building on university research reported in the early '80s, EEsof introduced the first commercial harmonic-balance simulation product in 1987 (4, 5). Harmonic-balance combines frequency domain analysis of linear circuit elements with time domain analysis of nonlinear elements (e.g., transistors). The method is based on the assumption that for a given sinusoidal excitation, a steady-state solution exists that can be approximated with sufficient accuracy by a finite trigonometric series. Fast Fourier Transform techniques are used to relate the time domain analysis to the frequency-domain linear circuit solutions; thus, harmonic-balance provides both time-domain and frequency domain characteristics in its basic solutions.

Since its introduction, Libra has

proven itself a fast simulator for typical high frequency and microwave nonlinear circuits -- amplifiers, mixers, multipliers, etc. Simulation times for Libra are typically faster than for SPICE, because simulation frequency is known in advance and complex time-sampling algorithms are avoided. Even so, until recently it was not clear how to apply Libra to oscillators. Since known test signals are used in the harmonic-balance algorithm, it was not obvious how this approach could be utilized for an oscillator, where the exact operating frequency is a function of nonlinear variation, and therefore hard to predict.

EEsof has found an innovative way to analyze oscillators in Libra by defining a special test element called OSCTEST™. We have redrawn our 2 GHz oscillator circuit in Figure 4 to show how OSCTEST is inserted for oscillator analysis. OSCTEST is a special directional coupler, which has zero electrical length and is designed to be invisible at oscillator fundamental frequency fo. OSCTEST has the following properties:

1) Ports 1-4 and 3-2 provide broadband wave coupling at all frequencies including fo and its harmonics, and 2) transmission from port 1 to port 2 rejects signals at frequency fo but passes all of its harmonics. By injecting a test signal (f_o) at Port 3, the Port 2 oscillator terminal is stimulated and the resulting regenerative signals entering Port 1 can be sensed by the directional coupler output at Port 4.

Conditions for oscillation are found when the ratio of coupler voltages, V_4/V_3, has unity magnitude and zero phase. This condition can be forced by sensing V_4/V_3 while applying a test signal of variable amplitude and frequency at Port 3 of the OSCTEST coupler. In this way, oscillation conditions are found — under actual nonlinear operating conditions. With the current version of Libra (version 2.1), this procedure is carried out by iterative manual simulation. However, an automated oscillator software optimization routine has been added to the forthcoming Libra version 3.0.

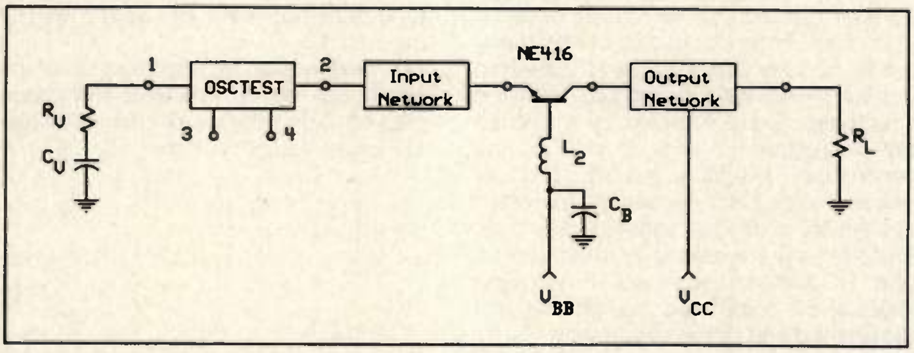

Figure 4. Oscillator schematic showing the use of the OSCTEST simulation element.

Figure 5 shows the result of a Libra OSCTEST simulation for our simple 2 GHz oscillator. Output at the load resistor R_L is shown, and both the waveform and power spectrum output are shown for operation at f_o=2.1 GHz. This result compares closely to the steady-state simulations found with Microwave SPICE. However, here we are able to carry out further nonlinear optimization, including interactive tuning, which is not possible with today's SPICE.

References

1. G. D. Vendelin, *Design of Amplifiers and Oscillators*, Wiley-Interscience, 1982, Chp 4.

2. R. A. Fratti, "Design of 7 GHz Negative Resistance Voltage Controlled Oscillator," *Proc. of EEsof User Group Meeting*, RF Expo West, October 1989, Paper 1.

3. L. W. Nagel, "SPICE2: A Computer Program to Simulate Semiconductor Circuits," Report No. ERL-M520, 1975, Univ. of Calif. at Berkeley.

4. C. Holmes, O. Pitzalis, and Y. Yuan, "Harmonic-Balance Software Simulates Nonlinear Circuits," *Microwaves & RF*, October 1987.

5. T. Reeder, "Harmonic-Balance Software Simplifies and Speeds Analysis of Nonlinear Microwave Circuits," *Microwave Journal*, May 1989.

About the Authors

Octavius Pitzalis is senior scientist and Dr. Tom Reeder is vice president of marketing at EEsof, Inc., 5795 Lindero Canyon Road, Westlake Village, CA 91362. They can be reached at (818) 991-7530.

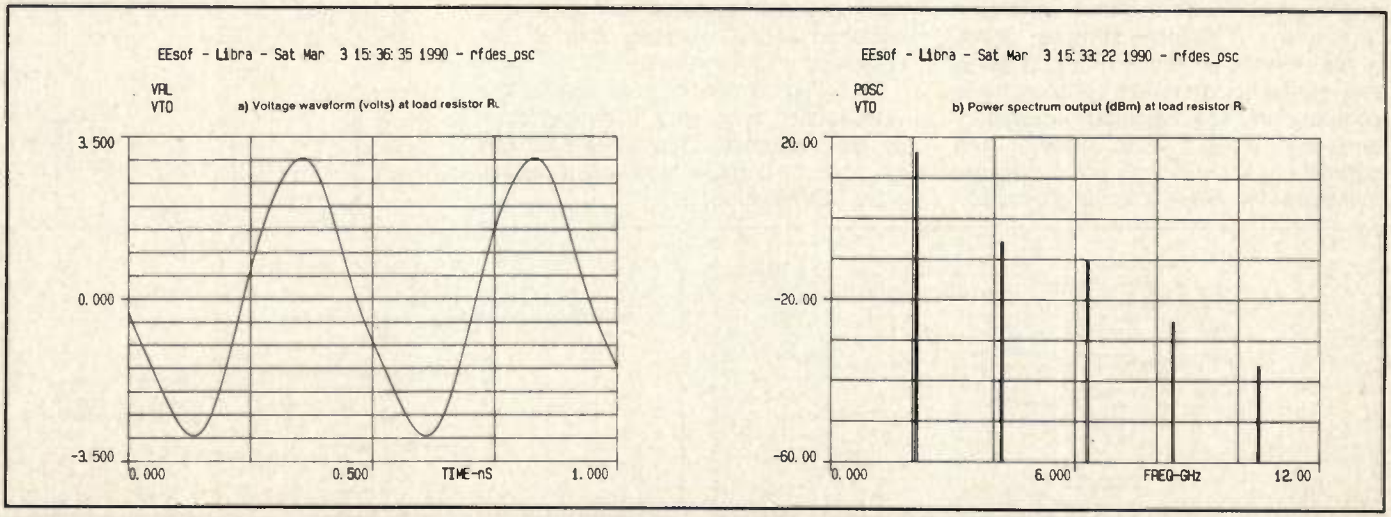

Figure 5. Oscillator output voltage and power spectrum simulated by Libra for oscillation at f = 2.1 GHz.

High-Speed Microprocessor Controlled Antenna Matching Unit

By Hakan Turkoz and Yilmaz Oktay
ASELSAN (Military Electronics Industry), Turkey

Antenna matching is a major problem for the designer who works with radio system design. However, this problem can be solved with the method described in this article. Operation of the matching unit described here is derived from the maximum power transformation theorem.

An AMU (Antenna Matching Unit) has been designed with an efficient algorithm to ensure proper matching (VSWR $\leqslant 1.5$) over the entire 30-88 MHz FM military VHF band. The unit is physically designed as a module with a microprocessor employed in the unit as a controller. It satisfies single frequency matching by means of frequency information coming from the synthesizer section and keeps the previous matching information in 100 KHz steps in its memory until the matching condition fails as a result of obstacles near the antenna or a change in the antenna type.

Description of the Block Diagram

The output of the RF power amplifier stage of the wireless is connected to the antenna through the sensors' matching and transformation sections as shown in Figure 1. The three sensors, phase angle, load discriminator and VSWR, are interfaced to the controller by three comparators. The matching section contains two banks, serial inductor and parallel capacitor, which are connected to the load by relays. The transformation section of Figure 1 contains two elements, L_p and L_s, connected to the load by relays for suitable transformation. The relays of the matching and transformation sections are driven by the controller through the relay driver logic. In addition, the controller also obtains the frequency and transmit/receive information of the wireless. The controller block contains a battery backup memory in which frequency versus matching information is stored.

Operation of the Sensors

A commonly used toroidal type VSWR bridge is used for the VSWR decision (1). The center conductor of the transmission line behaves as a one-turn primary and the forward and reflected components are sampled by a toroidal type transformer and coupled to the secondary resulting forward and reflected voltage components separately, at which point the voltages are peak rectified by the diodes and capacitors. So, DC voltages obtained at the terminals of the comparator are proportional to forward and reflected voltages.

For null adjustment, a variable capacitor (C_1) is used. To calibrate the circuit, the output is terminated with a 50 ohm reference load and a 0 volt reading is obtained at the inverting input of the comparator with the help of C_1.

An R_1 adjustment of 1.5 or less for this work is also necessary for proper comparator response. This adjustment can be done by using a load which causes a 1.5 VSWR value.

Phase Angle Sensor

In this circuit, a logic high level at the output of the comparator is obtained when the imaginary part of the load impedance is inductive (2,3). That means, the sampled line current on the toroidal type transformer lags the sampled line voltage. If, for a capacitive loading, the line current leads the line voltage resulting in a negative voltage at the comparator input terminals, then the output is logic low. Since the capacitor values are small compared to the operating frequency, the voltage sampling circuit (voltage divider capacitors) does not bring any phase shift to the circuit.

An expression for the operation of the circuit can be derived from the phase diagram using the law of cosines shown in Figures 4a, b, c and d.

$$|V_3| = \left[|V_1|^2 + \left|\frac{V_2}{2}\right|^2 - 2\,|V_1|\left|\frac{V_2}{2}\right|\cos\left(\frac{\pi}{2} + \theta\right) \right]^{1/2} \tag{1}$$

that means,

$$|V_3| = \left[|V_1|^2 + \left|\frac{V_2}{2}\right|^2 + |V_1|\,|V_2|\sin\theta \right]^{1/2} \tag{2}$$

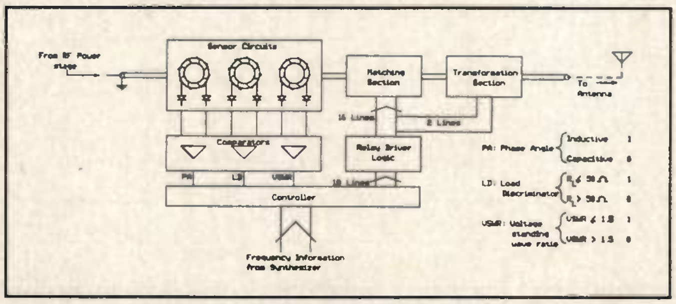

Figure 1. Block diagram of antenna matching unit.

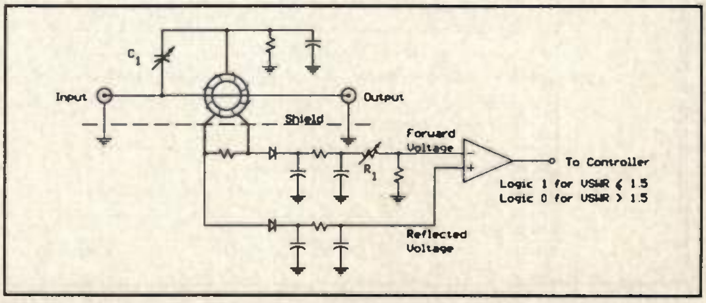

Figure 2. Schematic diagram of the VSWR sensor.

Amplifonix Quality Tips the Scales in Your Favor

You can depend on amplifiers and cascade design technology from Amplifonix ... your #1 second source company.

Amplifiers, limiting amplifiers, attenuators and limiters...plus switch attenuators, switches and mixers... in flat packs, surface-mount, TO, DIP packages and cascaded housings for a variety of voltage, current, gain, noise figure and medium power applications. **We will also *modify* our standard units to meet *your* performance specifications.**

For added convenience, just insert our CASCADE floppy disk in your desktop computer and it will display the amplifiers for the best-fit cascade based on the design parameters *you* enter.

Guaranteed performance; kHz-2 GHz; screening to the tables of MIL-STD-883.

Call or write today for information on our "Quick Delivery Program"...it could be worth a mint to you.

Amplifonix

2010 CABOT BLVD. WEST • LANGHORNE, PA 19047 • (215) 757-9600 • FAX: 215-757-0378

INFO/CARD 24

Higher performance EMI filtering for high speed data lines

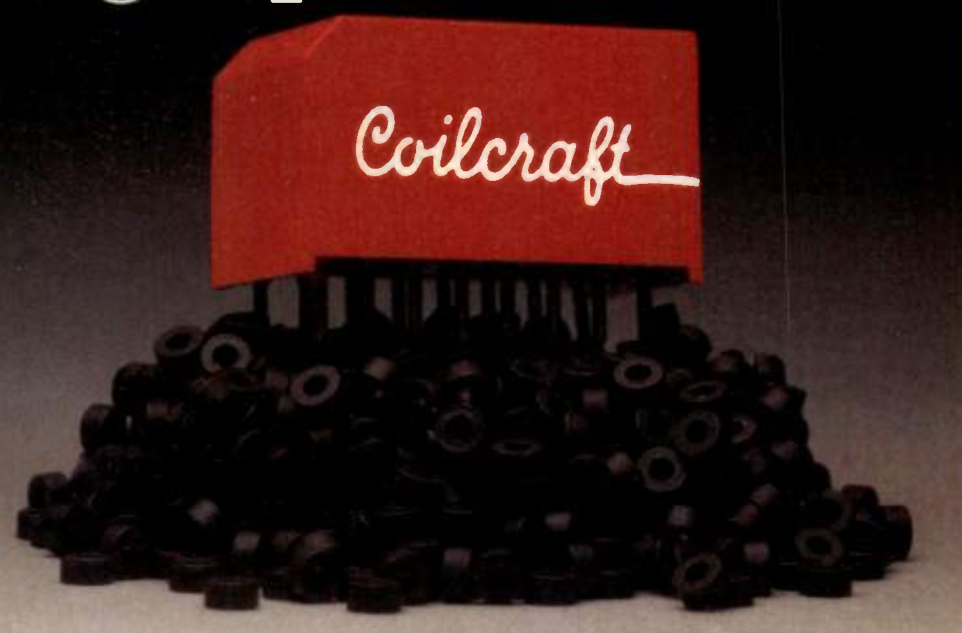

All these ferrite beads can't equal the EMI suppression of a single Coilcraft Data Line Filter.

Our new DLFs are the most effective, low-cost way to eliminate common mode EMI from digital signals, logic level power lines, and inter-equipment cables.

Available in 8, 4, 3 and 2-line versions, Coilcraft DLFs provide >15 dB attenuation from 30 to 300 MHz. Up to 40 dB simply by adding capacitors!

Because they use a single magnetic structure to filter multiple lines, you get differential *and* common mode noise suppression, something other filters can't do.

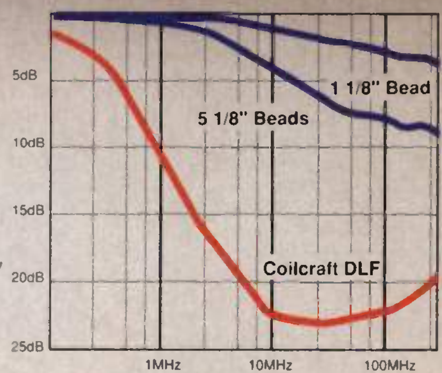

Attenuation
(50 Ohm System)

Coilcraft Data Line Filters are easier to install and usually take less board space than beads or baluns. And they're far less expensive than filtered connectors–around 2¢ per dB per line.

For details on our complete line of Data Line Filters, circle the reader service number. Or call **800/322-2645** (in IL 708/639-6400).

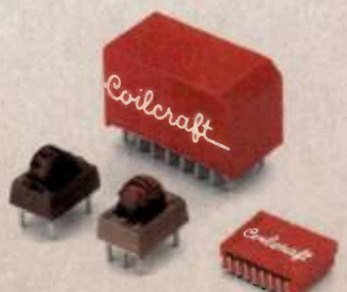

Designer's Kit D101 contains 2,3,4 and 8-line filters. $65.

Coilcraft

1102 Silver Lake Road, Cary IL 60013

INFO/CARD 32

Coilcraft Designer's Kits

These low cost kits put hundreds of coils, chokes and other magnetics at your fingertips

"Unicoil" 7/10 mm Tuneable Inductors
.0435 µH - 1.5 µH
49 shielded, 49 unshielded (2 of each)
Kit M102 $60

"Unicoil" 5 mm Tuneable Inductors
9 µH - 281 µH
19 shielded, 19 unshielded (2 of each)
Kit M105 $60

"Slot Ten" 10 mm Tuneable Inductors
0.7 µH - 1143 µH
18 shielded, 18 unshielded (3 of each)
Kit M100 $60

Surface Mount Inductors
4 nH - 33 µH
48 values (10 of each)
Kit C100 $125

Axial Lead Chokes
0.1 µH - 1000 µH
25 values (5 of each)
Kit F101 $50

Horizontal Mount Inductors
Tuneable and fixed
Inductance: 31.5 - 720nH
33 Values (3 of each)
Kit M104 $60

Common Mode Data Line Filters
Attenuation bandwidth: >15 dBm 1.5-30 mHz
DC current capacity: 100 mA
2, 3, 4 and 8 line styles (4 of each)
Kit D101 $65

Common Mode Line Chokes
Current: .25 - 9 amps RMS
Inductance: 508 µH - 10.5 mH
8 styles (2 of each)
Kit P202 $100

Current Sensors
Sensing range: 0.5-35 amps
Freq. resp.: 1 - 100 kHz, 50 - 400 Hz
Transformer and sensor-only versions
8 styles (15 total pieces)
Kit P203 $50

Base/Gate Driver Transformers
Inductance: 1.5 mH Min.
Frequency: 10 - 250 kHz
2 single, 2 double section (2 of each)
Kit P204 $50

Power Filter Chokes
Current: 3, 5, 10 amps
Inductance: 5 - 300 µH
18 styles (48 total pieces)
Kit P205 $75

Axial Lead Power Chokes
Current: .03-4.3 amps
Inductance: 3.9 µH - 100 mH
60 styles (2 of each)
Kit P209 $150

To order call 800/322 COIL

Coilcraft

1102 Silver Lake, Cary IL 60013

INFO/CARD 57

Linear Diode Low Level Envelope Detector

By Pete Lefferson
St. Petersburg, FL

Envelope detector designs began with the invention of radio. However, the imperfect diode with its square law region is a challenge in the design of envelope detectors. The traditional method to obtain the largest linear detector response has been to employ good impedance control and high RF voltage. Other design options have been invented in recent years such as the many forms of synchronous detection and ideal op amp ideal rectifier circuits. The design described here was an entry in the 1989 RF Design Awards Contest.

The following envelope detection circuit employs only five parts and does not require an active gain stage. It is the solution to the task of monitoring a low voltage IF module output level as a part of a module self testing system. The last IF gain stage is in a detector module.

A conventional "L" matching circuit (Figure 1) steps up the source impedance level to the diode high dynamic resistance that occurs at low forward current. The "L" match acts as a high impedance source passing current through the diode to charge the filter cap. This causes the DC output to become linear (Figure 2).

The limitation of this circuit is that it is indeed a series resonant shunt across the source when the RF level is low. There must be resistance in series with the coil (Figure 3) to limit this drop to a practical level. If the circuit is connected to a properly terminated line, the drop at low level RF can be calculated as:

$$20\log\left[2R_1/(Z_0 + 2R_1)\right]\ \text{dB}$$

An expression for the detector gain constant is simple if one neglects parasitic parameters and R_1:

$$\text{Output DC/Input RF(RMS)} = R_2(C_1/2L)^{1/2}\ \text{V/V}$$

To minimize the voltage drop when the detector is attached to a terminated line, one would use the appropriate large value of R_1 along with the largest practical L/C ratio. The DC response is linear only when the inductive reactance is large with respect to R_1.

The circuit values shown in Figure 1 give an example where R_1 is actually the coil internal series resistance at 10 MHz and C_1 is 5.4 pF. The voltage drop at low RF level when the detector is attached is only 0.4 dB. Using the smallest practical value for C_1 requires careful control of stray capacitance and this makes development of the complete detector gain constant a complex modeling problem. Fortunately, this is easily modeled on circuit analysis software.

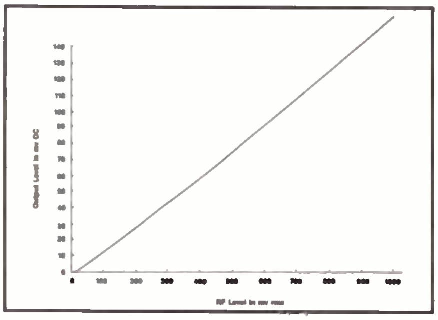

Figure 2. Envelope detector response for the circuit of Figure 1.

The component values in Figure 3 were selected for a lower L/C ratio to demonstrate the effect of R_1 on voltage drop and DC linearity. Standard 10 percent tolerance parts were used. As R_1 is increased from 0 to 180 ohms, the low RF level line voltage drop decreases from 8 dB to 0.8 dB (Figure 4). As R_1 is increased a diode threshold voltage becomes more visible in the DC response (Figure 5). For comparison, this figure also contains conventional envelope detector circuit response obtained by increasing C_1 to 0.1 uF.

There appears to be no perfect envelope detector. This circuit was an inexpensive solution to a level monitoring problem and offers another detector design alternative.

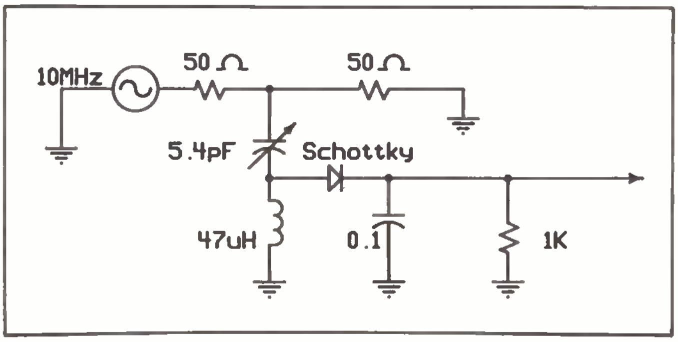

Figure 1. Low level envelope detector with high L/C ratio.

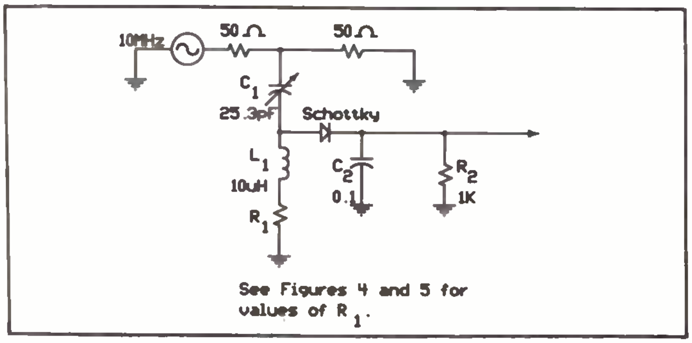

Figure 3. Low level envelope detector with lower L/C ratio to illustrate the effect of R.

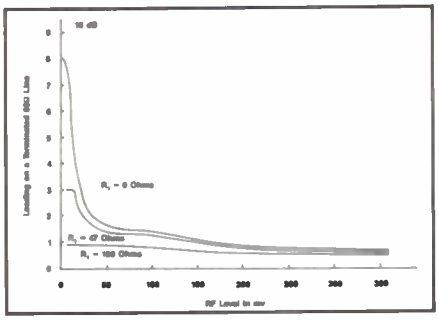

Figure 4. Terminated 50 Ohm line voltage drop for 3 values of R_1 vs. the RF level.

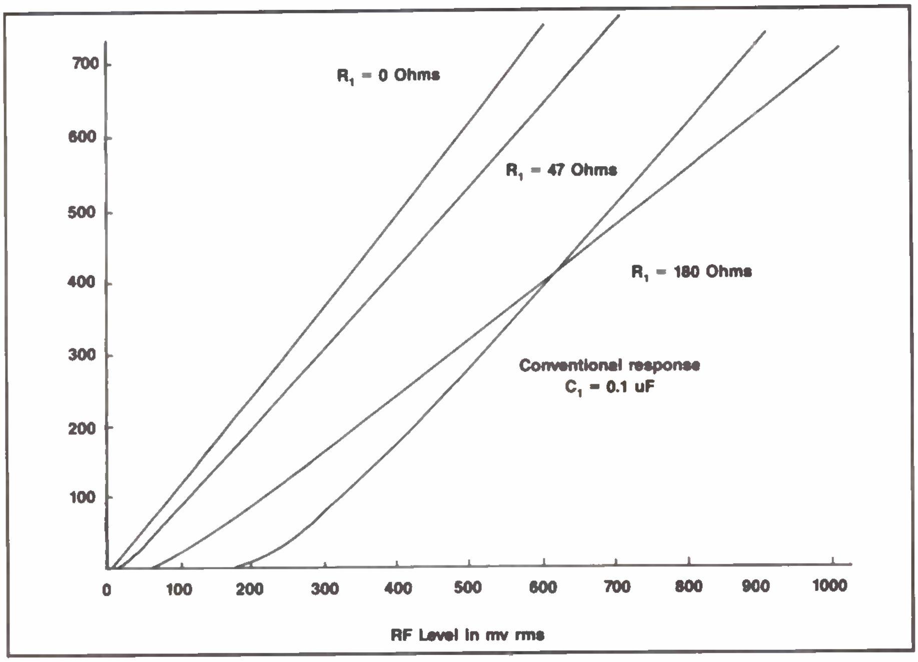

Figure 5. Envelope detector response for 3 values of R.

About the Author

Pete Lefferson, P.E., is an electronic design consultant at 6101 7th Ave. N., St. Petersburg, FL 33710.

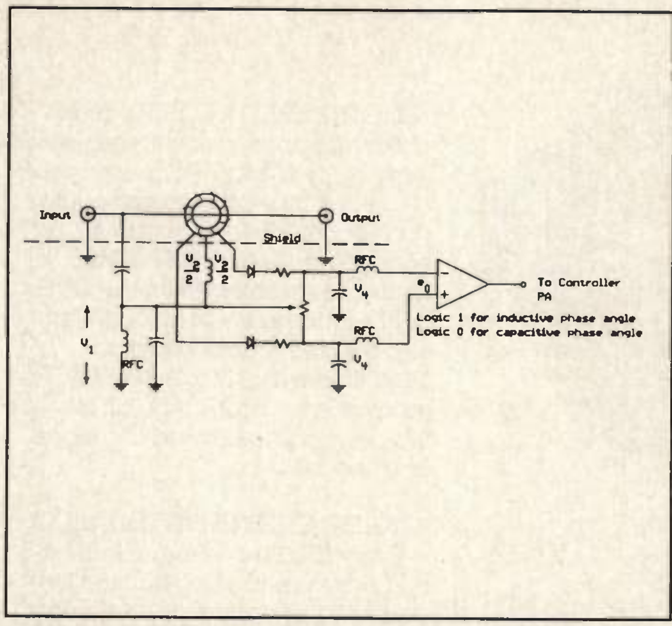

Figure 3. Schematic diagram of the phase angle sensor.

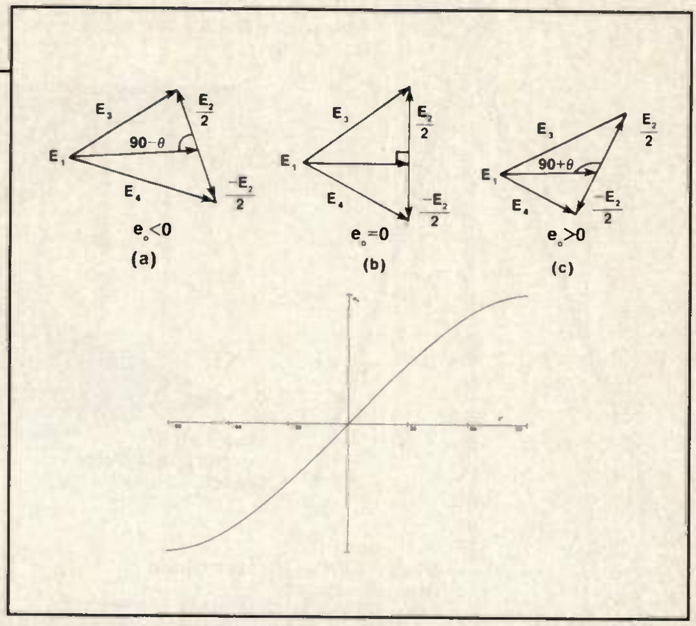

Figure 4. Voltage vector diagram a) $e_o < 0$; b) $e_o = 0$; c) $e_o > 0$; d) output voltage versus phase variation of phase angle sensor.

similarly,

$$|v_4| = \left[|v_1|^2 + \left|\frac{v_2}{2}\right|^2 - 2\,|v_1|\,|v_2|\,\sin\theta \right]^{1/2} \tag{3}$$

since $|v_1| \approx |v_2|$ for a small phase shift, then,

$e_o = |v_3| - |v_4|$

$$= v_1\left(\sqrt{1.25 + \sin\theta} - \sqrt{1.25 - \sin\theta}\right) \tag{4}$$

This circuit provides a DC output voltage to comparator which is a function of the real part of the terminating impedance regardless of the imaginary part (2,3). The DC output voltage is positive when the real part of the terminating impedance is greater than 50 ohms and negative if the termination impedance is less than 50 ohms.

The same type of toroidal transformer that is used in VSWR and phase angle sensors is also employed for this circuit.

To show the operation principle, the following derivation is used:

Suppose that the terminating impedance is $Z_l = R + jX$. Therefore an expression for line voltage v_l and sampled voltage v_1 can be written as,

$$v_1 = \alpha v_L \tag{5}$$

Since the current produces voltage V_2 as in Figure 5

$$v_2 = \beta I_L = \beta \frac{v_L}{R + jX} \tag{6}$$

where α and β are sampling and coupling coefficients respectively.

$$e_o = |v_1| - |v_1 - v_2| = |\alpha v_L|$$

$$- \left|\alpha v_L - \frac{\beta v_L}{R + jX}\right|$$

$$= v_L \left[\alpha - \left(\frac{(\alpha R - \beta)^2 + \alpha^2 X^2}{R^2 + X^2} \right)^{1/2} \right] \tag{7}$$

For a terminating impedance of 50 ohms

$$e_o = 0 \geqslant \left[\alpha - \left(\frac{(\alpha R - \beta)^2 + \alpha^2 X^2}{R^2 + X^2} \right)^{1/2} \right] \tag{8}$$

This equation can be written as;

$$2\alpha R - \beta = 0 \tag{9}$$

The result of this formula is interesting since the imaginary part of the terminating impedance has disappeared. The result is shown in Figure 6. From here it can be seen that, the output voltage is positive in the region $0 < R < \beta/2\alpha$, zero at $R = \beta/2\alpha$ and negative in the region $\beta/2\ \alpha < R$.

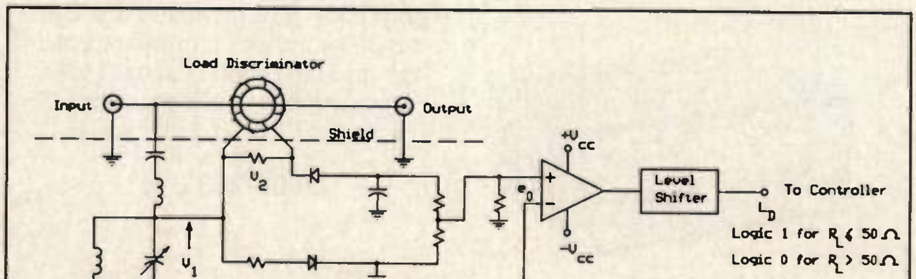

Figure 5. Schematic diagram of load discriminator.

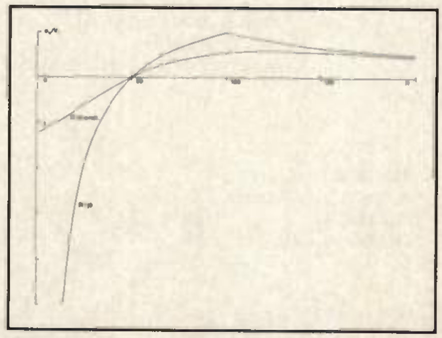

Figure 6. Output voltage versus resistance variation of load discriminator.

Model 3115 Double Ridge Guide
1–18 GHz
Model 3116 Double Ridge Guide
18–40 GHz

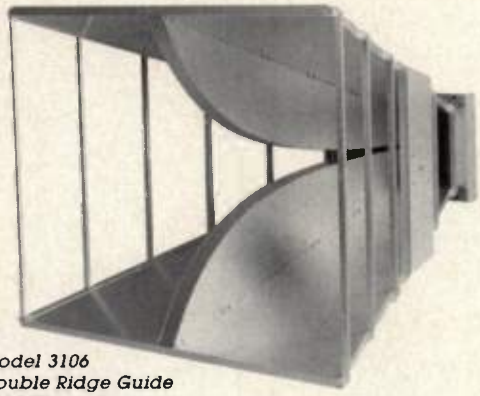

Model 3106
Double Ridge Guide
200 MHz–2 GHz

Model TR3 Non-Metallic Tripod
22.68 kg capacity
two other models available

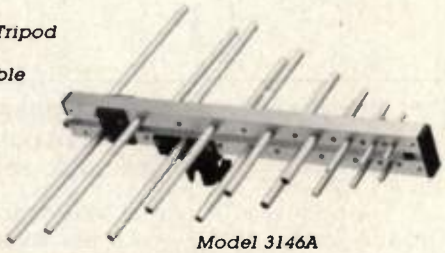

Model 3146A
Log Periodic
300 MHz–1 GHz
four other models available

Model 1060 Turntable
with controller and IEEE-488 bus option
1-7.6 meter diameter available
three other models available

Model 6502
Active Loop
10 kHz–30 MHz
four other models available

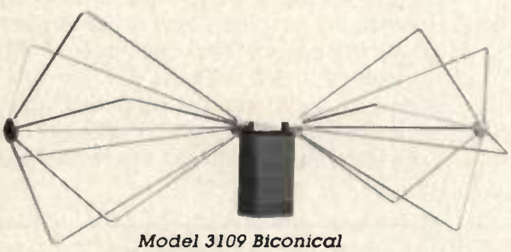

Model 3109 Biconical
20–300 MHz
three other models available

Model 3925 PLISN
5 kHz–1 GHz
five other models available

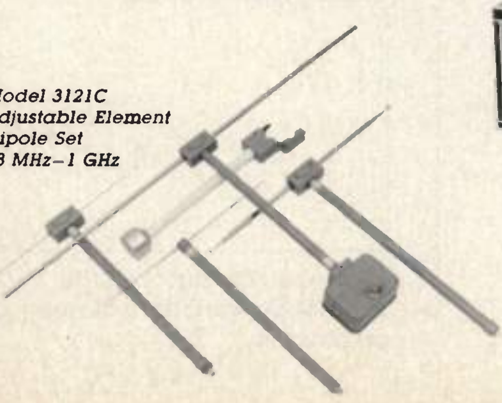

Model 3121C
Adjustable Element
Dipole Set
28 MHz–1 GHz

TEST WITH CONFIDENCE.

ENGINEERED TO PERFORM

If compliance testing is your primary responsibility, you need top-of-the-line products you can count on. Like EMCO antennas, designed for repeatable FCC/VDE testing. Manufactured for the stringent requirements of MIL-STD testing. With high sensitivity for TEMPEST testing. Most have VSWR ratios of less than 2:1. And all exhibit exceptional dynamic range and linearity.

CALIBRATED INDIVIDUALLY

Every EMCO antenna is individually calibrated using both C63.4 and ARP 958 standards, then shipped to you with a signed Certificate of Compliance—a claim no other manufacturer of test antennas can make.

MANUFACTURED WITH CARE

We choose only the best and most durable materials for EMCO products. Then we pay close attention to details—machined tolerances are often less than one one-thousandth of an inch. And while we've automated for efficiency, we still take the time to hand-assemble and inspect each one of our products.

TWO-YEAR WARRANTY, SERVICE WORLD-WIDE

Because we know how well every EMCO product is engineered and built, we can back each one with a two-year warranty—twice the industry standard. And EMCO has more than 30 representatives worldwide to help you—wherever you are. Call our 800 number for more information and the name of your EMCO representative. Ask for your free catalog of EMCO products, too!

1-800-253-3761

EMCO™

The Electro-Mechanics Company

Call toll-free between 7:30 AM and 4:30 PM Central Time
800-253-3761 in USA or 512-835-4684 in Texas
Telex 797627 Fax 512-835-4729
P.O. Box 1546 Austin, Texas 78767

08151/89161 Fax 08151/16610
Munchner Str. 2 D-8137 Berg 1 West Germany

Matching Algorithm

The matching section contains one parallel capacitor, one series inductor bank, and two transformation inductances. One transformation inductance is in parallel (L_p) and the other is in series (L_s) as shown in Figure 7.

The maximum value of the inductor and capacitor banks are calculated for the worst case situation (for this case 30 MHz) as the total inductance L_t and total capacitance C_t.

Then, individual capacitor and inductor values are calculated as shown below,

$$C_o = \frac{C_T}{2^8 - 1} \qquad C_i = 2C_{i-1} \qquad i = 1....7 \tag{10}$$

$$L_o = \frac{L_T}{2^8 - 1} \qquad L_i = 2L_{i-1} \qquad i = 1....7 \tag{11}$$

This type of approach is based on the binary increment concept. C_t and L_t should be chosen for optimum values so that fine tuning steps, C_0 and L_0, are sufficiently small and the covered matching region is enlarged.

Transformation inductances L_p and L_s should also be chosen with the worst case situation in mind to ensure the transformation of the load impedance to the region where the capacitor and inductor banks can match the load properly.

Initially the capacitor bank is open circuited while the inductor bank is kept short circuited. In the program this is shown as OOH (hex). The complex impedance plane is divided into three non-overlapping regions in the Smith Chart as shown in Figures 8, 9 and 10. In Figure 8, the load impedance is shown in the shaded region as point A.

First, the capacitor bank is incremented until the R=50 Ohm circle is crossed in the capacitive region (this process is

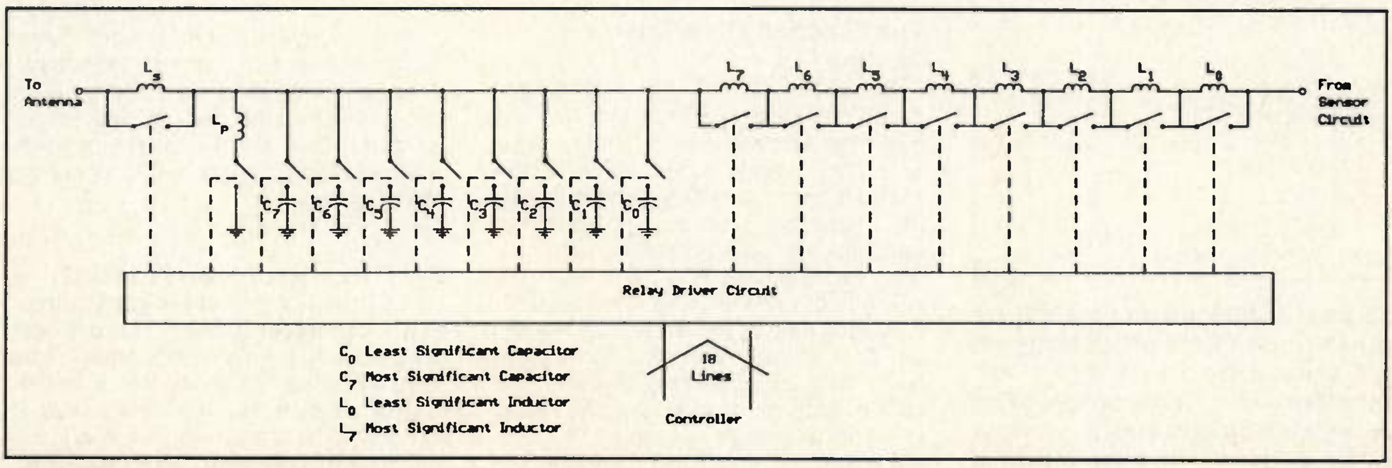

Figure 7. The matching network.

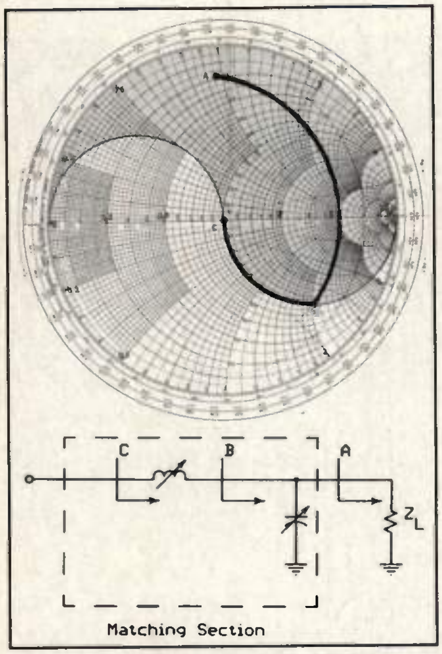

Figure 8. Shaded region will be matched by the network configuration. Example of matching path in that region. Note: Realize that the transformation network is not employed for this region.

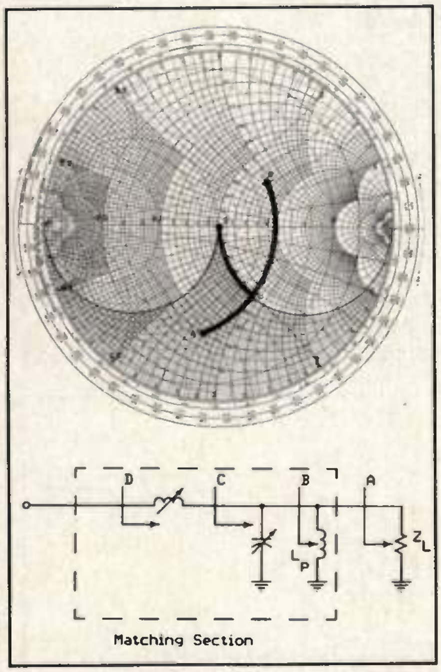

Figure 10. Shaded region will be transformed to the shaded region of Figure 8 by using L_p(0.1 uH) transformation inductance. The above matching network configuration is used. An example of a matching path in that region.

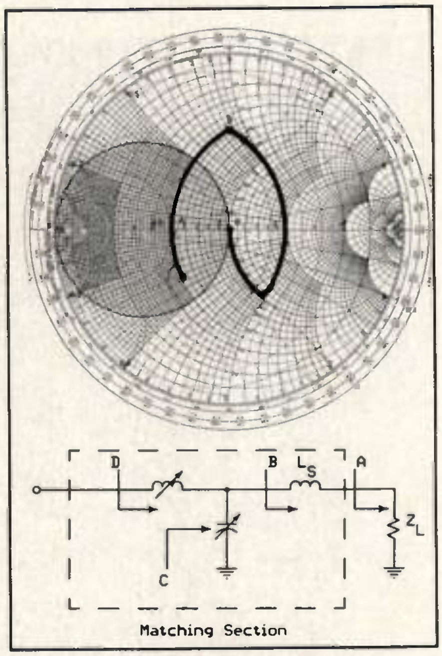

Figure 9. Shaded area will be transformed to the shaded region of Figure 8 by using L_s (0.3uH) transformation inductance. The network configuration is used. Example of a matching path in that region. B to D path as shown in Figure 8.

the capacitive region (this process is shown as path A to B). Then, the inductor bank is incremented to a sufficient VSWR (VSWR ≤1.5). In Figures 9 and 10, the same philosophy is applied after transforming the load impedance to the shaded region of Figure 8 by L_s or L_p respectively.

The program is composed of two main sections. One is the main program and the other is the interrupt routine (4).

The Function of the Interrupt Routine

Since the unit is not capable of matching without RF power, all the matching action is done when the radio is in the transmit mode. If the mode changes from transmit to receive during the matching process, the program automatically enters the interrupt routine. The Matching Flag (MF), indicates whether or not matching is completed. If it is completed, MF will be 0, if not MF will be 1. If the matching is incomplete when the mode changes to receive, the current settings of all relays are stored in a special part of the memory. Then, the recent settings in the preset memory corresponding to the operating fre-

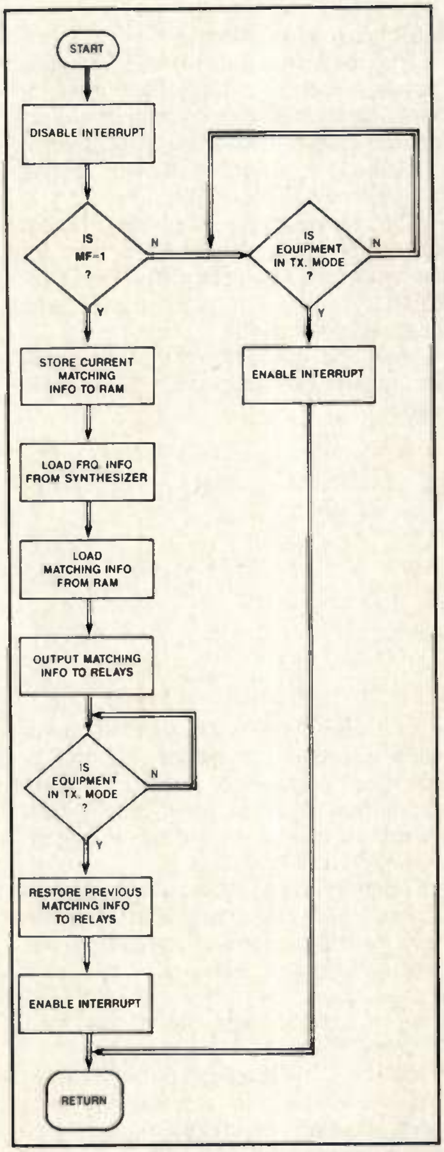

Figure 11. Interrupt routine flow chart.

quency are used until it reenters transmit mode. After that, incomplete settings stored in the memory are reloaded and the process continues in the main program. This ability makes the unit faster and more reliable for the receiving case (Figure 11).

The Function of Main Program

The matching process is started from label A of the flow diagram. This process can be traced from the diagram with the help of Figures 1, 2 and 3. Briefly, three regions are detected by the sensors and the proper transformations and adjustments are employed until sufficient matching is obtained.

Conclusion

Although this unit is designed for a specific frequency range, with careful modification, the unit can be adopted to any desirable frequency range by changing the matching section and sensor circuits.

This unit has the disadvantage that matching can not be performed while the radio is in receiving mode. Fortunately, this problem is solved to some extent with the preset memory.

The lowest operating input RF power of the unit is 1W. If it is desired to decrease this minimum power level, it is possible to do so by properly biasing the diodes in the sensors.

The output power range of the power amplifier in this work is 2W to 4.5W. During the matching process, VSWR may sometimes reach very high values which can possibly damage the RF power amplifier. However, in this work, the RF transistors can tolerate an infinite VSWR. If these types of transistors are not selected for the RF power amplifier, an attenuator should be inserted in the system to avoid possible damage during the matching process.

It is observed that within this range (30-88 MHz and 2W−4.5W) for an arbitrary load, value matching is successful. However, for higher power ranges, a careful inspection of component values should be made. For higher frequencies, the contact impedances of the relays and the stray capacitances of the lumped components (ceramic capacitors, molded inductors, etc.) become very important. Therefore, suitable components and relays should be used.

Acknowledgement

The authors wish to express their deep appreciation to Professor Canan Toker, staff member of Middle East Technical University and Mr. Ismail Kurtoglu, engineer at ASELSAN for their kind help and guidance.

References

1. Doug DeMaw, *Practical RF Design Manual*, Prentice-Hall Inc., 1982.

2. Fuat Akcayoz, A M.S.E.E. thesis at METU (Middle East Technical University - Ankara), August 1979.

3. V. Manassewitsch, *Frequency Synthesizers Theory and Design*, Wiley, 1976.

4. *Intel Embedded Controller Handbook*, Volume I, 8-Bit.

About the Authors

Hakan Turkoz and Yilmaz Oktay work for ASELSAN Military Electronics Industry as chief engineers. Both have B.S.E.E. and M.S.E.E. degrees from Middle East Technical University, Ankara, Turkey, 1983 and 1986 respectively.

Optimum Lossy Broadband Matching Networks for Resonant Antennas

By F.J. Witt
AT&T Bell Laboratories

Common examples of practical resonant antennas are the quarter-wave monopole, n/2-wavelength dipoles, where n is an odd positive integer, and the full-wave loop. Another example is a short non-resonant antenna which has been made resonant by the addition of a reactive element. The resonant antenna has inherent broadband radiating properties, but its match bandwidth falls short of meeting requirements in many applications. This paper addresses the problem of optimizing the design of a fixed matching network located between the transmission line and the resonant antenna.

The matching network contains a transformer and a resonator. The analysis differs from previous results (1,2,3) in that it yields explicit formulas which provide maximum match bandwidth and that account for the incidental losses which are inherent in most practical matching networks. The goal of the optimization presented here is to maximize the match bandwidth for a given maximum standing wave ratio (SWR) over the operating band.

In his classic work, Fano (1) addressed the same problem in a very general sense, but treated only the lossless case. Fano's generality included a wide class of load impedances and high order matching networks. He and others (2,4,5) have observed that large match bandwidth improvements are possible with very simple matching networks. This paper treats such a case. A recent examination of the same single resonator matching network structure was reported by Hansen (3). He recognized the importance of accounting for matching network loss, but did not include it explicitly in his evaluation. The value of the results described here is that concise design formulas which account for the losses in the matching network are provided.

Antenna Impedance

The analysis which follows applies to antennas whose impedance near resonance may be approximated by a series RLC circuit as shown in Figure 1. The use of this approximation makes the analysis tractable, and, as will be seen later, is accurate enough to provide useful design information. The results apply to the dual case as well, however this case will not be covered here.

It will be assumed that the real part of the antenna impedance $R_A(f)$, does not vary much over the operating band. It is set equal to the value of the real part of antenna impedance at resonance, R_o. The antenna driving point impedance is thus established by three parameters: the resonant frequency, F_o, the real part of the antenna impedance at resonance, R_o, and the Q of the antenna at resonance Q_o.

$$Q_O = \left(\frac{F_O}{2R_O}\right)\frac{dX_A(f)}{df}\bigg|_{f=F_O} = \frac{2\pi F_O L_A}{R_O} \qquad (1)$$

where L_A=antenna inductance

Transformer Matching

Before treating the transformer/resonator matching case, it is helpful to consider the simplest form of a matching network which consists of a transformer whose bandwidth is large compared with the bandwidth of the resonant antenna. The topology, which assumes that the transformer losses are negligible, is shown in Figure 2(a). Maximum bandwidth is not achieved when a perfect match (SWR = 1:1) exists at resonance. In Figure 3, the intentional mismatch at resonance is seen. That mismatch is achieved by driving the antenna with a generator whose impedance is greater than R_o, causing the SWR to equal S_L at resonance. A generator impedance lower than R_o will not yield optimum matching.

The analysis is facilitated by transforming the bandpass network of Figure 2(a) to the lowpass network of Figure 2(b). The SWR versus frequency characteris-

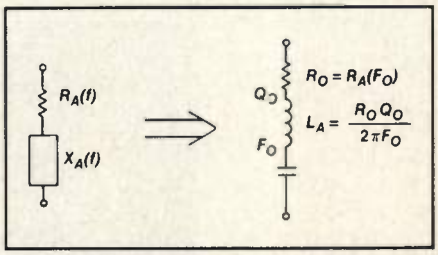

Figure 1. Dipole approximate equivalent circuit used in the analysis. R_A(f) includes both the radiation resistance and antenna losses.

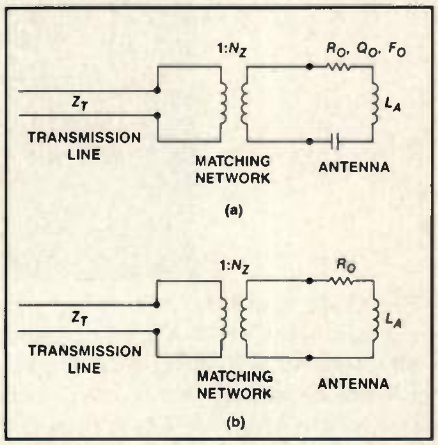

Figure 2. Transformer matching (a) equivalent circuit; (b) after bandpass to lowpass transformation.

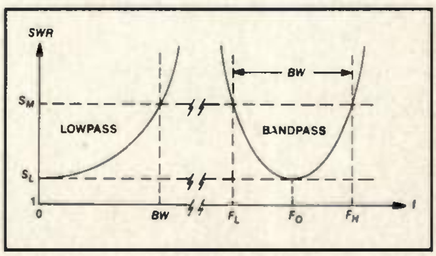

Figure 3. SWR versus frequency for optimum transformer matching.

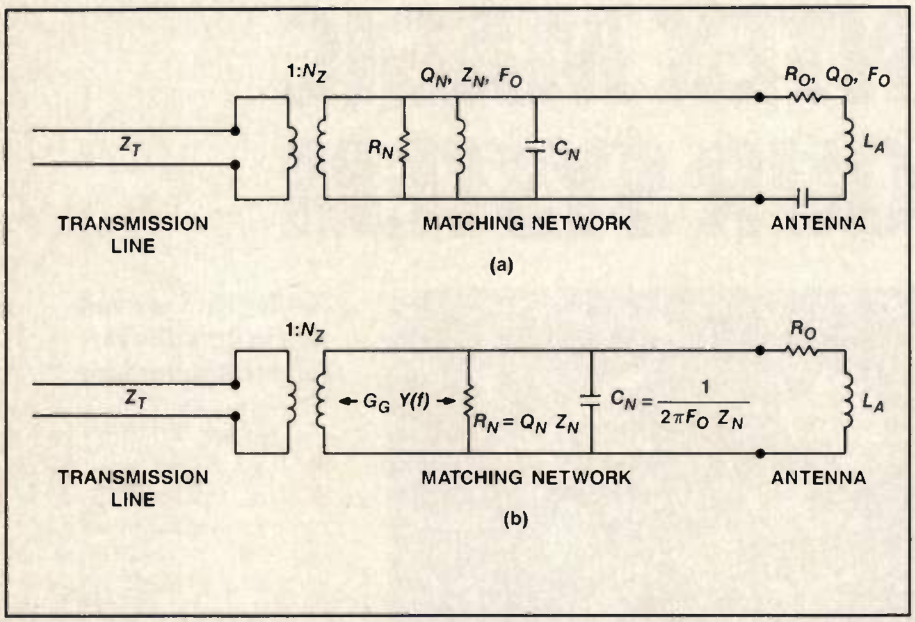

Figure 4. Transformer/resonator matching (a) equivalent circuit; (b) after bandpass to lowpass transformation.

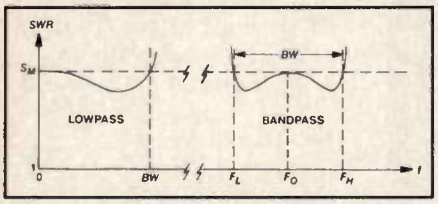

Figure 5. SWR versus frequency for optimum transformer/resonator matching.

tic of Figure 3 shows the relationship between the bandpass and lowpass SWR characteristics. The midband frequency, F_o, is the geometric mean of the band edge frequencies, F_L and F_H. Of interest is the bandwidth, BW, at a particular SWR, S_M. The reflection coefficient looking from the line into the matching network is given by:

$$\varrho(f) = \frac{R_O + j2\pi f L_A - Z_T N_Z}{R_O + j2\pi f L_A + Z_T N_Z} \tag{2}$$

$$= \frac{(1 - S_L) + j(f/F_O)Q_O}{(1 + S_L) + j(f/F_O)Q_O}$$

where Z_T=transmission line characteristic impedance (ohms), N_Z=transformer impedance ratio

Substituting f=BW in equation 2 and using

$$|\varrho(BW)| = \frac{S_M - 1}{S_M + 1} \tag{3}$$

yields

$$BW = \frac{F_O}{Q_O}\left[\left(S_M + \frac{1}{S_M}\right)S_L - S_L^2 - 1\right]^{1/2} \tag{4}$$

It is useful to define the normalized bandwidth, B_N, to be the product of the fractional bandwidth and the antenna Q:

$$B_N = \frac{BW}{F_O} Q_O \tag{5}$$

Also, the normalized reference bandwidth, BN_{ref}, is defined to be the normalized bandwidth for the case when the antenna is perfectly matched at resonance. Using equation 4 for S_L=1 yields:

$$B_{Nref} = \frac{S_M - 1}{\sqrt{S_M}} \tag{6}$$

By setting $dB_n(S_L)/dS_L$=0, the value of S_L, SL_{opt}, which gives the maximum bandwidth, may be determined:

$$S_{Lopt} = \frac{1}{2}\left(S_M + \frac{1}{S_M}\right) \tag{7}$$

Substitution yields the maximum normalized bandwidth, B_{Nmax}.

$$B_{Nmax} = \frac{1}{2}\left(S_M - \frac{1}{S_M}\right) \tag{8}$$

The required transformer impedance ratio is:

$$N_Z = \frac{R_O}{2Z_T}\left(S_M + \frac{1}{S_M}\right) \tag{9}$$

The improvement in match bandwidth with transformer matching is modest. If S_M=2:1, for example, by deliberately mismatching at resonance so that $S_L=S_{Lopt}$=1.25:1, the 2:1 SWR bandwidth is improved by only about 6 percent.

Transformer/Resonator Matching

In dramatic contrast to transformer matching, a matching network using a transformer in combination with a resonant circuit yields a significant improvement in match bandwidth. It is important, however, to properly account for losses in the matching network since these losses will influence the values of the design parameters in most practical applications. Fortunately, though somewhat tedious to derive, the results may be expressed as explicit formulas.

The antenna system for this case is shown in Figure 4(a). In the matching network, the transformer is used to deliberately raise the generator impedance seen by the antenna at midband to a high but acceptable level. The resonant circuit, which has the same resonant frequency as the antenna, is used to partially compensate for the reactance of the antenna for frequencies away from resonance. All of the losses in the matching network are represented by the Q of the matching network resonator Q_N. In addition to the transmission line and antenna parameters, Q_N is assumed to be known.

The same analysis approach used in the transformer matching case is used here. Refer to Figure 5. The parameters of the matching network are chosen so that the SWR at midband and at the band edges equals S_M. The optimization process involves determining the transformer impedance ratio, N_Z, and the matching resonator impedance level, Z_N, so that maximum bandwidth is achieved. Z_N is the impedance of the resonator inductor or capacitor at the antenna resonant frequency.

Referring to the lowpass equivalent circuit of Figure 4(b), at dc:

$$N_Z = \frac{S_M Q_N Z_N R_O}{Z_T(Q_N Z_N + R_O)} \tag{10}$$

Implicit in this equation is the assumption that the optimum condition occurs when the SWR is equal to S_M at the center of the band as well as at the band edges. The author has been able to prove this for the lossless case and has been unable to disprove it for the lossy

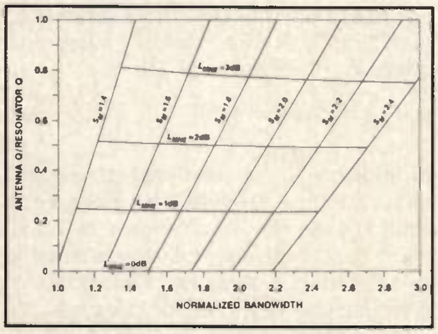

Figure 6. Tradeoff among bandwidth, match quality and matching network loss.

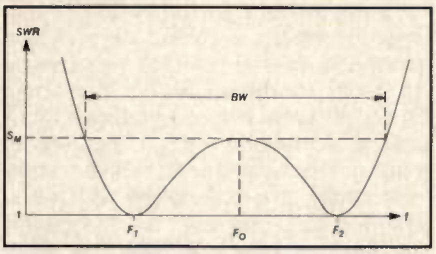

Figure 7. Perfect match at two frequencies.

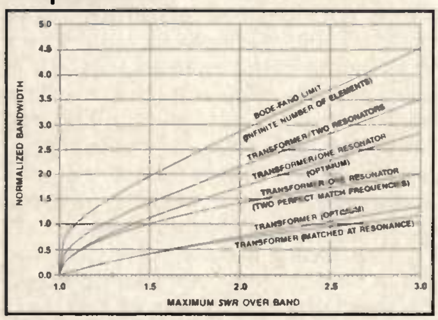

Figure 8. Normalized bandwidth versus maximum SWR over the band for the lossless matching network case.

case.

The matching network loss, L_{MN}, is defined as the ratio, expressed in decibels, of the total power delivered by the transmission line to the power delivered to the antenna load. It is given by:

$$L_{MN} = 10\log\frac{G_A + [1/(Q_N Z_N)]}{G_A} \qquad (11)$$

where G_A is the antenna conductance, which is given by

$$G_A = \frac{1}{R_O\{1 + [(f/F_O)Q_O]^2\}} \qquad (12)$$

Thus,

$$L_{MN} = 10\log\left(1 + \frac{R_O}{Q_N Z_N}\{1 + [(f/F_O)Q_O]^2\}\right) \qquad (13)$$

In the bandpass domain, at midband:

$$L_{MNO} = 10\log\left(1 + \frac{R_O}{Q_N Z_N}\right) \qquad (14)$$

and at the band edges:

$$L_{MNE} = 10\log\left[1 + \frac{R_O}{Q_N Z_N}(1 + B_N^2)\right] \qquad (15)$$

For any application, the matching network loss is highest at the edges of the band, so L_{MNE} will usually be the most important loss parameter.

The expressions for transformer impedance ratio and matching network loss pertain to the topology of Figure 4(a) and are very general. They apply for any matching network impedance level and normalized bandwidth. Some expressions for impedance level, normalized bandwidth and band edge loss for cases of particular interest are presented next.

Maximum Bandwidth

It is possible to write an explicit expression which relates Z_N and B_N. This is done by first determining the generator conductance, G_G, necessary to achieve SWR=S_M at resonance.

$$G_G = \frac{R_O + Q_N Z_N}{S_M R_O Q_N Z_N} \qquad (16)$$

The admittances, Y(f), facing the generator is given by: (17)

$$Y(f) = \frac{1}{Q_N Z_N} + j\frac{f}{F_O Z_N} + \frac{1}{R_O[1 + j(f/F_O)Q_O]}$$

The magnitude of the reflection coefficient is then:

$$|\varrho(f)| = \frac{|Y(f) - G_G|}{|Y(f) + G_G|} = \frac{SWR - 1}{SWR + 1} \qquad (18)$$

At the band edges, f=BW and SWR=S_M. With these substitutions, the general expressions for B_N and Z_N may be derived:

$$B_N = \left[2(S_M + \Delta)\frac{Z_N Q_O}{R_O S_M} - \left(\frac{Z_N Q_O}{R_O S_M}\right)^2 - 1\right]^{1/2} \qquad (19)$$

and

$$Z_N = \frac{R_O S_M}{Q_O}\left\{S_M + \Delta \pm [(S_M + \Delta)^2 - 1 - B_N^2]^{1/2}\right\} \qquad (20)$$

where

$$\Delta = \frac{Q_O}{2Q_N}\left(S_M - \frac{1}{S_M}\right) \qquad (21)$$

Note that for the lossless matching network case, $\delta=0$. The optimum impedance level, Z_{Nopt}, which yields for the maximum bandwidth is determined by setting $dB_n(Z_N)/dZ_N=0$ and solving for Z_N.

$$Z_{Nopt} = \frac{R_O S_M}{Q_O}(S_M + \Delta) \qquad (22)$$

The maximum normalized bandwidth, B_{Nmax}, is:

$$B_{Nmax} = [(S_M + \Delta)^2 - 1]^{1/2} \qquad (23)$$

The large bandwidth enhancement obtained by using the transformer/resonator matching network is seen from the following example: for the lossless case and S_M=2:1, B_{Nref}=1/2 and B_{Nmax}=3. Hence the bandwidth is increased by a factor of 2.45 over the case of a dipole matched at resonance. It is clear from equation 23 that the bandwidth is increased even further when a lossy matching network is used.

The matching network loss at the band edges, L_{MNE}, is given by:

$$L_{MNE} = 10\log\left\{1 + \frac{Q_O}{Q_N}\left[\frac{Q_O}{2Q_N}\left(1 - \frac{1}{S_M^2}\right) + 1\right]\right\} \qquad (24)$$

Notice the weak dependence on S_M. For cases when the matching network resonator Q is at least an order of magnitude greater than the antenna Q, the band edge loss simplifies to:

$$L_{MNE} \approx 10\log\left(1 + \frac{Q_O}{Q_N}\right) \qquad (25)$$

The above analysis provides the basis for a graphical representation of the relationship between normalized band-

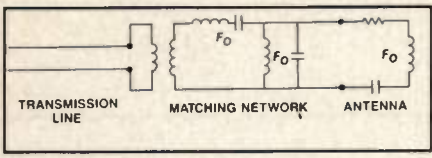

Figure 9. Transformer/two-resonator matching.

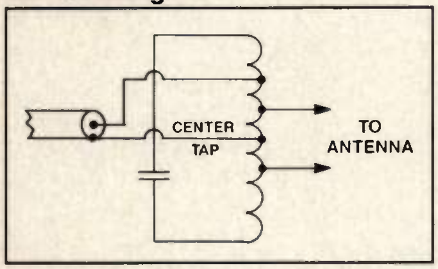

Figure 10. LC matching network.

width, matching network loss, Q_O/Q_N and S_M (Figure 6). For a particular application, where antenna Q and matching network resonator Q are given, this figure is very useful for quickly determining the tradeoff among match quality, bandwidth and matching network loss.

In most practical situations, the operating band over which matching is desired is given. In those cases, one wishes to know the best match achievable, S_{Mmin}, for a given normalized bandwidth B_N. Solving equation 23 for S_M yields:

$$S_{Mmin} = \left((B_N^2+1)^{1/2} + \left(B_N^2 + 1 + (2Q_O/Q_N)\cdot(1+Q_O/2Q_N)\right)\right)^{1/2} \Big/ 2(1+Q_O/2Q_N) \tag{26}$$

Minimizing Matching Network Loss

For situations where either the maximum possible bandwidth or minimum possible SWR is not required, equation 20 may be used to determine the necessary value of Z_N. Notice that for values of normalized bandwidth less than B_{Nmax}, there are two values of Z_N. The larger one is usually selected in order to minimize the matching network loss. An example later will show the potentially large impact of making the proper selection.

Perfect Matching at Two Frequencies

It is possible to find a value of Z_N which provides a perfect match at two frequencies, as seen in Figure 7 (6). For this case,

$$Z_N = \frac{R_O}{Q_O}\left[S_M + \frac{Q_O}{Q_N}(S_M - 1)\right] \tag{27}$$

and

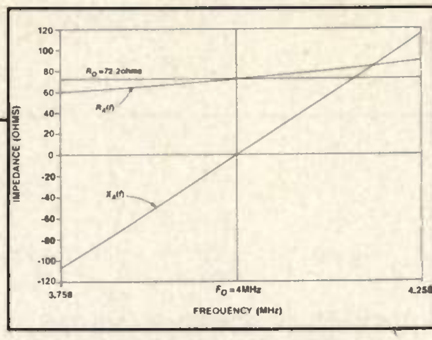

Figure 11. Impedance versus frequency for a 4 MHz half-wave dipole in free space.

$$B_N = (S_M - 1)^{1/2}\left\{2 + \frac{Q_O}{Q_N}\left[2 + \left(1 + \frac{Q_O}{Q_N}\right)\left(1 - \frac{1}{S_M}\right)\right]\right\}^{1/2} \tag{28}$$

This case may satisfy a special need, but it yields a smaller bandwidth and more loss than the case presented in the previous section. For the case when S_M=2:1, the achievable bandwidth is about 18 percent smaller than the maximum attainable with the same topology. This result is analogous to the transformer matching case, where obtaining perfect match at a frequency within the band does not yield maximum bandwidth.

The perfect match frequencies are given by:

$$F_1 = (F_O^2 + F_M^2)^{1/2} - F_M \quad \text{and} \qquad F_2 = \frac{F_O^2}{F_1} \tag{29}$$

where

$$F_M = \frac{F_O}{2Q_O}\left[\left(1 + \frac{Q_O}{Q_N}\right)(S_M - 1)\right]^{1/2} \tag{30}$$

Comparison with Earlier Results

Much has been reported regarding the design of optimum matching networks when the load is complex. In these analyses, the assumption has usually been that the matching network is made up of lossless elements. In order to compare the results of this investigation with the earlier results, it is necessary to set δ=0. The comparison may be made by showing the relationship between the normalized bandwidth and S_M, the maximum SWR over the operating band (Figure 8); equations 6 and 8 provide the required formulas for the dipole matched at resonance and optimum transformer matching, respectively. For the case of transformer/resonator optimum bandwidth matching, from equation 23,

$$B_{Nmax}\big|_{\delta=0} = (S_M^2 - 1)^{1/2} \tag{31}$$

For the case of transformer/resonator matching with two perfect match frequencies, from equation 28:

$$B_N\big|_{\delta=0} = [2(S_M - 1)]^{1/2} \tag{32}$$

In addition to the relationships derived above, Figure 8 gives the Bode-Fano limiting case (1), which shows the maximum bandwidth theoretically attainable with an infinite number of elements in the matching network. For this case,

$$B_{Nmax} = \frac{\pi}{\ln[(S_M + 1)/(S_M - 1)]} \tag{33}$$

The cases of transformer and transformer/resonator matching for maximum bandwidth exactly coincide with Fano's (1) results for the equivalent situations; his results were achieved using a more general technique, which involved a graphical solution for the final result. Incidentally, the terminology of Fano is different than that used in this paper, but the necessary translations were made to prepare Figure 8.

For comparison, the case which shows how much additional bandwidth could be obtained if one more resonator were added to the matching network is also given in Figure 8. this result is derived from Fano (1) and Levy (2); the two-resonator topology is shown in Figure 9. It has been shown that the analytically derived matching network optimization is not always optimum (7, 8). Thus for the two resonator case, the curve shown may not be optimum. However, for the lossless matching network cases presented in this paper, it may be shown that the true optimum has indeed been found.

Practical Matching Networks

Two types of matching networks are presented: an LC network and a transmission line resonator. Each is based on the transformer/single resonator topology of Figure 4a. The lumped LC resonator/transformer exhibits low matching network loss and has the potential for providing the balun function, i.e., allowing an unbalanced feedline to drive a balanced antenna without radiation from the feedline. The transmission line resonator may lead to more loss, but has the advantage that it may be integrated with the radiator.

In order to illustrate some of the important practical points associated with the design of a matching network, a specific example will be considered. The antenna to be matched is a half-

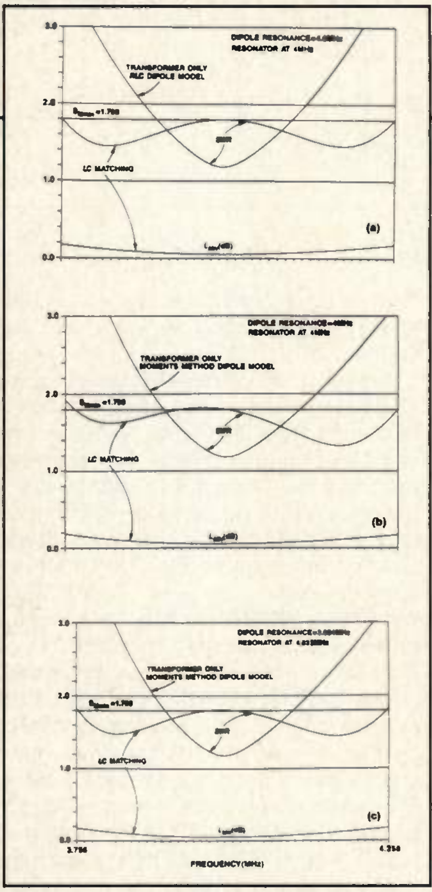

Figure 12. SWR and matching network loss for LC matching network example (a) calculated matching network parameters, RLC dipole model; (b) calculated matching network parameters, moments method dipole model; (c) perturbed dipole and matching network resonances, moments method dipole model.

wave dipole in free space resonant at 4 MHz. The desired operating bandwidth is 500 kHz. The method of moments using the program MININEC (9) was used to compute the driving point impedance of an uncompensated version of the antenna to be matched. The effect of the simplifying assumptions made through the use of the antenna model of Figure 1 may thus be seen. In practice, one may estimate R_O and Q_O, or better still, build the uncompensated version of the antenna and measure its feedpoint impedance prior to a final design of the matching network.

In the examples which follow, unless otherwise noted, the designs achieve the minimum SWR over the operating band. Other assumptions are:

F_L=3.758, MHz F_H=4.258 MHz, Z_T=50 ohms

LC Matching Network

A practical LC matching network is

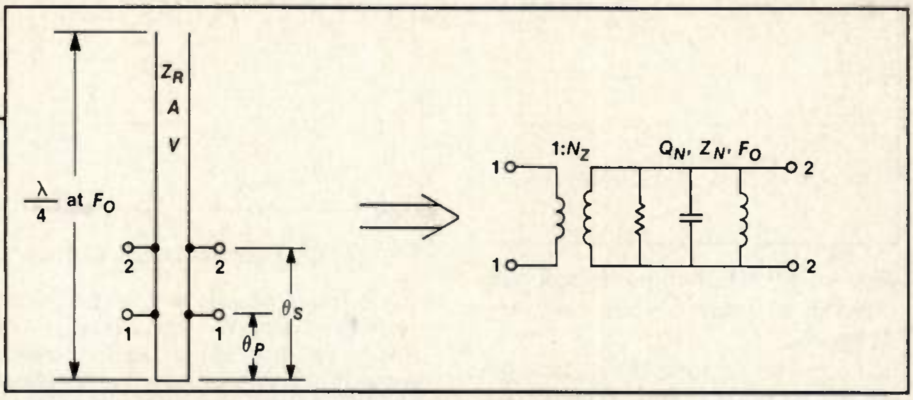

Figure 13. The quarter-wave resonator/transformer.

shown in Figure 10 (6). The function of a transformer is realized by providing primary and secondary taps on the coil. For the case when a coaxial transmission line is used and the resonant antenna load is balanced, such as a symmetrically-situated center-fed half-wave dipole, the network also serves as a balun. This is accomplished by connecting the shield of the coaxial cable to the center tap of the coil. By connecting the capacitor as shown in the figure, an optimum selection of matching network component may be made. In effect, the inductor is an autotransformer with three functional windings: a primary, a secondary and a capacitor winding.

Figure 11 shows the computed impedance of the 4 MHz half-wave dipole for the case when it is made of 14AWG wire (diameter 0.064 inch). Forty segments were used in the computer analysis. From these data, the antenna Q and radiation resistance at resonance are determined:

Q_O=12.2, R_O=72.2 ohms, Dipole length= 120.1 feet

By assuming Q_N=300, which is a readily attainable value in most practical situations, the following results are obtained:

F_O=4 MHz, S_{Mmin}= 1.798:1, Z_{Nopt}=19.41 ohms, N_Z=2.58:1, L_{MNE}=0.176 dB

After selecting the capacitor, the tapped inductor of Figure 10 may be designed. This procedure will not be covered here. It is important to realize that the components chosen must be capable of withstanding the large electrical stresses encountered when high transmitted power is involved. In the author's experience, high radio frequency currents which flow in the capacitor in this kind of service place particularly high demands on that component.

In Figure 12(a) is shown the SWR and matching network loss versus frequency characteristic for this example when the idealized RLC dipole model is assumed. Also shown for comparison is the SWR of a dipole when the actual dipole impedance frequency dependence is accounted for, the differences in SWR and loss are small. Note also from Figure 12(c) that the SWR characteristic may be made symmetrical by a slight perturbation of the dipole resonant frequency (−0.15 percent), and an increase of the resonator natural frequency (+0.6 percent).

Transmission Line Resonator Matching Network

Another way to realize a transformer/resonator is to use a resonant length of transmission line (10,11). The simplest form is a transmission line one-quarter wavelength long terminated with a short circuit at one end and an open circuit at the other end. In what follows, this form of resonator will be used, although there are applications where longer transmission line resonators could be used. In these latter cases, the power handling capacity of the matching network would be larger, but the resonatortor Q would be unchanged from the quarter-wave case.

Figure 13 shows a quarter-wave resonator/transformer. By driving and loading the resonator at different points,the function of a transformer is realized. The resonator has a Q which is related to the loss of the transmission line at the resonant frequency.

$$Q_N \approx \frac{2.774F_O}{AV} \tag{34}$$

where A=transmission line attenuation at $f=F_O$ (dB/100 feet), V=velocity factor

It is worth noting that since $A \propto \sqrt{f}$ for many transmission lines, $Q_N \propto \sqrt{F_o}$ (approximately). Hence, using the same cable type, higher Q's are obtained at higher frequencies. First order approximations to the equivalent circuit parameters are:

$$Z_N \approx \frac{4Z_R}{\pi}\sin^2\theta_s, \qquad N_Z \approx \frac{\sin^2\theta_S}{\sin^2\theta_P} \tag{35}$$

Where Z_R=characteristic impedance of the resonator transmission line (ohms)

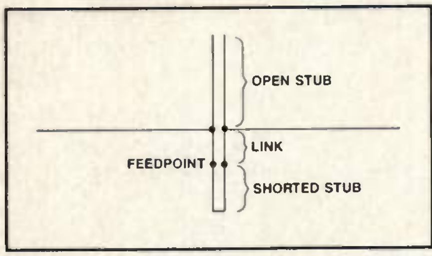

Figure 14. Half-wave dipole employing a quarter-wave matching network.

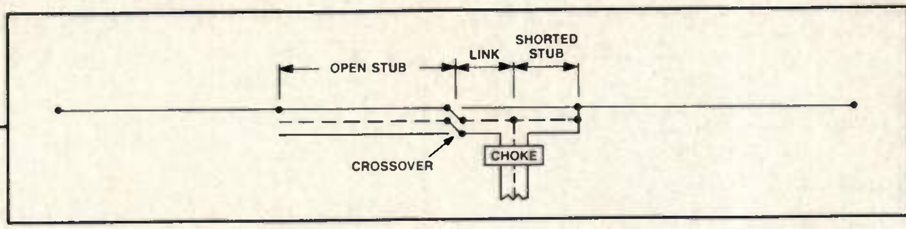

Figure 15. The coaxial resonator match.

and θ_s and θ_p are the electrical angles of the secondary and primary taps, respectively, measured from the shorted end of the resonator.

These approximations are useful only if other significant resonances are well separated from the band of interest. For example, the anti-resonance of the open stub occurs above the operating band and as the secondary tap approaches the short, that frequency approaches the operating band of the antenna system. In most practical cases, however, the equivalent circuit shown provides a sufficiently accurate initial set of matching network parameter values.

The application of the quarter-wave resonator/transformer as a matching network is shown in Figure 14. First the electrical angles (in radians), θ_s and θ_p, are determined:

$$\theta_S = \sin^{-1}\left(\frac{\pi Z_N}{4Z_R}\right)^{1/2}$$
$$\theta_P = \sin^{-1}\left(\frac{\pi Z_N}{4Z_R N_Z}\right)^{1/2} \qquad (36)$$

These results are used to determine the lengths (in feet) of the transmission line segments as defined in Figure 14

$$\text{Shorted stub:}\quad L_S = \frac{492V\theta_P}{\pi F_O} \qquad (37)$$

$$\text{Link:}\quad L_L = \frac{492V\theta_S}{\pi F_O} - L_S \qquad (38)$$

$$\text{Open stub:}\quad L_O = \frac{246V}{F_O} - L_S - L_L \qquad (39)$$

Incidentally, it may be shown that the L_S is independent of R_O, a fact which may be used to an advantage in a situation when R_O is not known accurately.

The Coaxial Resonator Match

By recognizing that the fields and currents in a resonator made from coaxial cable are mostly confined to be within the cable, one can, in effect, integrate the resonator within the antenna radiator. This has been called the coaxial resonator match and is shown in Figure 15 for the case of a half-wave dipole (10,11). Note that the elements of the matching network in Figure 14 are contained within the structure. Currents flowing on the outside of the resonator shield are associated with the resonator; currents flowing on the outside of the shield are the usual dipole radiator currents. Radiation from the feedline, which is connected off-center for the above design equations to apply, is avoided by the use of a longitudinal choke as seen in the figure. A minor modification of the design procedure would permit the feedline to be connected to the physical center of the antenna but this would not eliminate the desirability of a longitudinal choke when an arbitrary length of feedline is used.

In Figure 15, the extensions necessary to build out the antenna length to one-half wavelength are made from wire. These lengths could be made from the same coaxial cable material as the resonator; the results are similar. Assuming that the entire dipole is made from RG213U coaxial cable (shield diameter = 0.3 inch), the following design input parameters were derived using MININEC:

Q_O=10.2, R_O=72.1 ohms, Dipole length=119.5 feet

For RG213U cable,

Z_R=50 ohms, A=0.4 dB/100 feet at 4 MHz, V=0.66

Hence, QN=42.0, leading to the following results

F_O=4 MHz, S_{Mmin}=1.516:1, Z_{Nopt}=17.36 ohms, N_Z=1.99:1, L_{MNE}=1.00 dB, L_S=9.8 feet, L_L=4.4 feet, L_O=26.4 feet

Shown in Figure 16(a) are the SWR and matching network loss for the case when the RLC dipole model and lumped matching network approximation are used. In Figure 16(b) a simulation program which uses the MININEC-derived dipole model and an accurate representation of the transmission line segments was used to determine the SWR and matching network loss. One observes that the simulation yields results which closely match those predicted from the approximate analysis. An interesting observation is that a degree of serendipitous self-compensation takes place when a moments method dipole model and transmission line matching network are used. This is made clear when Figure 12(b) (where self-compensation is not present) and Figure 16(b) are compared.

A matter of practical interest is the electrical stress on the coaxial cable in this application. At 4 MHz, the loss in the cable is primarily ohmic. To accurately calculate the current and voltage distribution within the resonator, it is necessary to use the complex value of characteristic impedance, Z_F. The segment lengths associated with Figure 16(b) were used. When the total power into the antenna plus matching network is one kilowatt, the maximum equivalent power stress (occurring at the low end of the operating band) is 12.5 kilowatts. It is the current in the center conductor which places the highest stress on the cable. The peak voltage at the open circuit occurs at the high end of the operating band. When the total power into the antenna plus matching network is one kilowatt, this voltage is 826 volts.

Minimizing Matching Network Loss

In many applications, the allowable SWR over the operating band is larger than the minimum achievable SWR, S_{Mmin}. By designing for this larger SWR, lower matching network loss may be obtained. The matching network loss may be improved by using equation 20 to find Z_N. An example will illustrate this point.

In the previous example, the SWR over the 500 kHz operating band was 1.516:1. It will be assumed that the application allows, instead, SWR <2:1. Using equations 10, 15, and 20, the following results are obtained:

Z_N=51.5 ohms, N_Z=2.79:1, L_{MNE}= 0.36 dB (compared to 1.00 dB for the "Optimum" case)

Note that in the use of equation 20 the "+" root was chosen in order to minimize the loss. This case is shown in Figure 17(a) when the approximate dipole and matching network models were used to obtain the results of Figure 17(b). By perturbing the dipole resonant frequency and segment lengths, an SWR shape similar to that of Figure 17(a) is obtained, as shown in Figure 17(c).

The electrical stress of the resonator coaxial cable is reduced when match

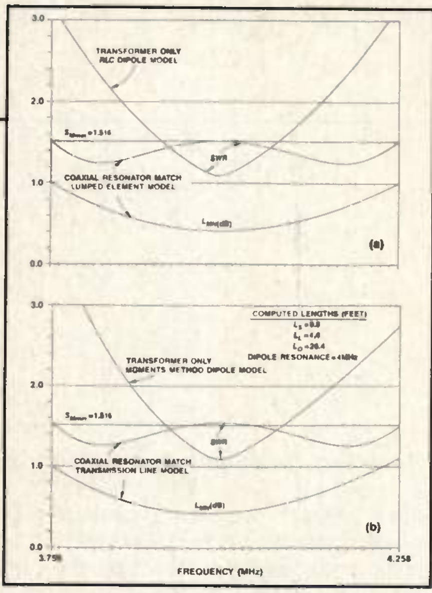

Figure 16. SWR and matching loss for coaxial resonator match example. (a) RLC dipole and lumped element matching, (b) moments method dipole and transmission line matching model.

quality is traded for improved matching network loss. For the case of Figure 17(c), when the total power into the antenna plus matching network is one kilowatt, the maximum equivalent power stress is 6.2 kilowatts and the peak voltage at the open is 507 volts (compared to 12.5 kilowatts and 826 volts, respectively, for the "optimum" case of Figure 16(b)).

If the "–" root has been chosen, the following parameters would have been obtained:

Z_N=10.2 ohms, N_Z=2.47:1, L_{MNE}=1.59 dB

Compare this result, shown in Figure 18, with Figure 17(a); the matching network loss is higher by a factor of 4.4. In general, the solution which yields the highest value of Z_N will have the lowest loss.

Conclusion

An important matching network for resonant antennas has been analyzed in detail. The importance stems from the large match improvements which a simple transformer/resonator matching network provides. The degree of improvement relative to simple transformer matching on one end and higher order matching on the other has been provided. Design equations, which account for the losses in the matching network, have been derived and applied to specific examples.

The author gratefully acknowledges the value of the stimulating discussions with J.J. Kenny and R.E. Fisher which influenced the work reported in this paper.

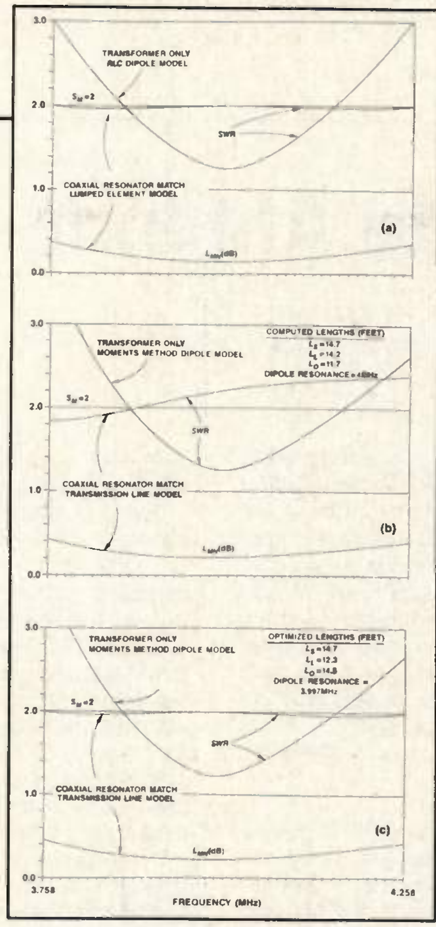

Figure 17. SWR and matching network loss characteristic when match quality is traded for reduced loss (a) RLC dipole model and lumped element matching network; (b) moments method dipole model and calculated segment lengths; (c) same as (b) except dipole resonance and segment lengths have been perturbed to restore SWR characteristic of (a).

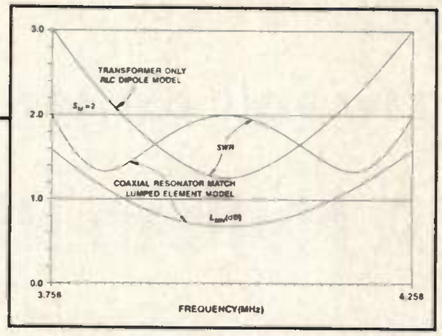

Figure 18. SWR and matching network loss for the "–" root of equation 20.

References

1. R.M. Fano, "Theoretical Limitations on the Broadband Matching of Arbitrary Impedances," J. Franklin Institute., vol. 249, pp. 57-83, Jan. 1950, pp. 139-154, Feb. 1950.
2. R. Levy, "Explicit Formulas for Chebyshev Impedance Matching Networks, Filters and Interstages," *Proc. Institute of Electrical Engineering.*, vol. 111, pp. 1099-1106, June 1964.
3. R.C. Hansen, "Evaluation of the Snyder Dipole," *IEEE Trans. Antennas Propagation*, vol. AP-35, pp. 207-210, Feb. 1987.
4. R.D. Snyder, "The Snyder Antenna," *RF Design*, Sept/Oct 1984, pp. 49-51.
5. J.D. Kraus, *Antennas*, New York: McGraw-Hill, 2nd ed., 1988, pp. 736-741.
6. F.J. Witt, "Broadband Dipoles —Some New Insights," *QST*, vol. 70, pp. 27-37, Oct. 1986.
7. H.J. Carlin and P. Amstutz, "On Optimum Broadband Matching," *IEEE Trans. Circuits Systems*, vol. CAS-28, pp. 401-405, May 1981.
8. J. Pandel and A. Fettweis, "Numerical Solution to Broadband Matching Based on Parametric Representations," *AEU*, vol. 41, pp. 202-209, April 1987.
9. J.C. Logan and J.W. Rockway, "The New MININEC (Version 3): Initial Concept of Employment," Naval Ocean Systems Center Technical Document 938, Sept. 1986.
10. F.J. Witt, "The Coaxial Resonator Match and the Broadband Dipole," *QST*, vol 73, pp. 22-27, April 1989.
11. F.J. Witt, "The Coaxial Resonator Match," *The ARRL Antenna Compendium, Newington*, CT, The American Radio Relay League, vol. 2, p. 110-118, 1989.

About the Author

F.J. Witt is the Department Head of the Digital Terminals and Microwave Technology Department at AT&T Bell Laboratories. He may be reached at (508) 960-6502.

A Human Plate Antenna

M. David Sullivan
Los Altos, Calif.

Occasionally the need arises for propagation of a radio wave using the human body as a radiating element. An application will be described wherein the movements of a PC Mouse are radio-linked to the host computer by a micro-plate antenna having dimensions λ/146 x λ/100 instead of being passed along a conventional wire cable or "tail." The RF "tail-less" Mouse affords a greater degree of freedom and convenience because the unwieldy tail is not present to tangle or to snag on articles on the work surface. Three AAA cells provide operating power and, to prolong life, are switched into the circuit only on demand; i.e., when Mouse movement is sensed. Such duty-cycle supply switching provides many months of battery life.

The 49.83 MHz narrowband FM cordless telephone band was chosen for its lax licensing requirements and the availability of inexpensive components. At this frequency, however, the wavelength is about 20 feet and any form of conventional antenna would be far too large and cumbersome to realize an advantage over the tail. Noting that the hand must rest upon the Mouse body to propel it and also operate function switches, it was decided to use the operator's hand and body for capacitive coupling of RF energy for the environment, thereby setting up a surface wave propagation mode. To that end, part of the inner surface of the Mouse enclosure's plastic top is equipped with a 1.60 in. x 2.35 in. rectangle of sticky-backed metal foil engaged by a short length of springy piano wire electrically connected to a transmitter residing on the same circuit board that houses the Mouse electronics. The plastic top serves as a dielectric between foil and hand, see Figure 1. The size of the foil rectangle was dictated solely by available flat surface in the plastic top.

Board space and component cost constraints require an unbuffered frequency modulated crystal oscillator to directly drive the antenna. Consequently, tank loading must be reduced which would otherwise excessively pull crystal frequency or even kill the oscillator as the hand approaches and grips the Mouse. The addition of a 3.3 pf coupler serves to isolate the tank from these effects, see Figure 1. This sort of scheme has traditionally been used although only a tiny fraction of available RF power is actually launched in an electromagnetic wave.

The problem of inefficient power coupling is overcome by adding a center-tapped loop comprised of a single turn of 0.03 in. width etched copper trace around the circuit board perimeter on both surfaces, see Figure 2. In effect, an inductive loop of 2 turns is formed having rectangular dimensions of 2.15 in. x 3.00 in. with turns spaced at the board's 0.06 in. thickness and with the plane of the loop parallel to the plate but about 1/2 inch below it. Such a loop generates very little radiated power but does cause the plate and hand to resonate with the 3.3 pf coupling capacitor which results in a radiated power boost over the plate and hand alone. Why the loop is used rather than a small tapped inductor, aside from cost advantage, will be discussed later.

In the circuit of Figure 2, the plate has been relocated to the loop's center-tap for impedance step up. Otherwise, the low plate/hand resistive component imposes too great a load on the oscillator at resonance. The 3.6 pf capacitor along with plate and hand capacitance are transformed by the loop to appear as a smaller value across the loop inductance but with a somewhat higher reactance such that:

$$\frac{X_C X_L}{X_C + X_L} = X_T = X_{3.3} \tag{1}$$

where X_C = sum of plate, hand and 3.6 pf reactance times n^{-2}, X_L = loop reactance, $X_{3.3}$ = reactance of 3.3 pf, X_T = net inductive reactance

It's important to note that X_T is always inductive; that is, X_C is always greater than X_L but decreases as the hand approaches the plate; reaching its smallest value with the hand fully gripping the Mouse. Plate radiation resistance is quite small relative to lossy and coupling resistances and the latter dominate to restrict Q to about 8.4.

The equivalent lumped resistance and Q are derived from Figure 3. R_T is attributed only to the plate and hand branches (the antenna) because of the 3.3 pf and 3.6 pf capacitors and the loop are of high Q. Radiation resistances of loop, plate and

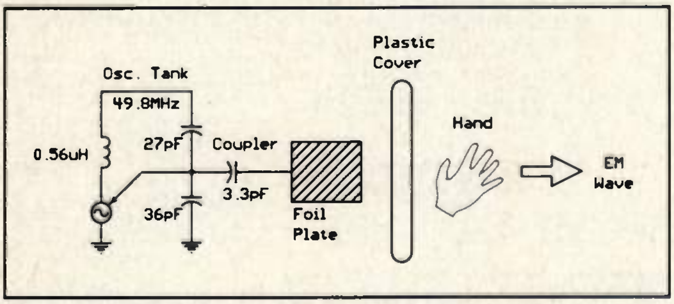

Figure 1. Conventional hand coupled plate.

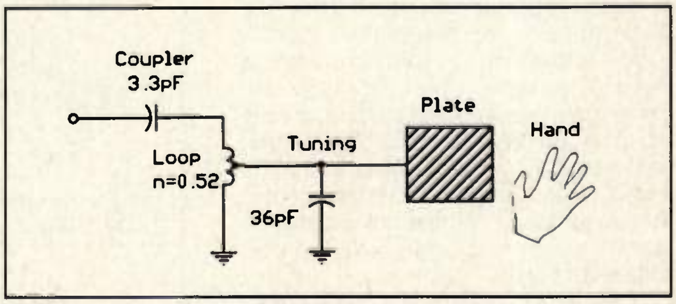

Figure 2. Plate antenna with loop.

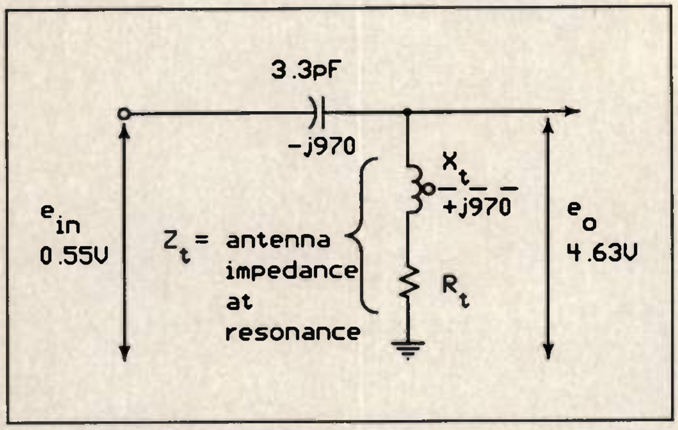

Figure 3. Impedance of loop and plate.

hand (body) and losses are accounted for in R_T which also contains "coupling" resistance representing RF energy transfer to the environment as will be explained later. Ground returns of plate and hand are provided by distributed impedances which are included in Z_T. From Figure 3 at resonance,

$$e_O = \frac{e_{in}}{R_T}\sqrt{R_T^2 + X_T^2} = e_{in}\sqrt{1 + \frac{X_T^2}{R_T^2}} = e_{in}\sqrt{1 + Q^2} \qquad (2)$$

thus,

$$Q = \sqrt{70.9 - 1} = 8.36 \qquad (3)$$

and

$$R_T = \frac{970}{8.36} = 116\Omega \qquad (4)$$

Experimental Measurements

The transmitter operates into a Motorola MC3362 FM receiver chip equipped with a standard stubby whip spiral-wound antenna. However, the receiver design was not ready for use at the time of transmitter testing. Instead, a single-turn 12 inch diameter loop connected to an RF voltmeter was laid flat on a lab bench about three feet from the Mouse for comparisons of tuned and untuned performance, see Figures 4, 5, 6 and 7.

A small plate antenna does not couple significant energy to a spatial wave since its radiation resistance is very small but, rather, it couples capacitively to people, walls, buildings, etc. via distributed impedance of the dimensions R−jX. Herein, therefore, coupling of RF energy is ascribed to "coupling" resistance analogous to the familiar radiation resistance concept. Relative values of plate and hand "coupling" resistances can be found from a consideration of Figure 4.

From Figure 4a,

$$X_p = \left(\frac{0.74v}{1.31 - 0.74v}\right)X_{3.3} = 1.27K\Omega \qquad (5)$$

$$P_{P1} = i_p^2 R_{cp} = \left(\frac{0.74}{1.27}\right)^2 R_{cp} = 0.340R_{cp} \qquad (6)$$

where R_{cp} = plate coupling resistance (Ω), X_p = plate reactance (KΩ), i_p = plate current (ma), p_{pl} = power in R_{cp} (μwatts)

From Figure 4b,

$$i_h = \frac{(1.31 - 0.53)v}{X_{3.3}} - \left(i_{p2} = \frac{0.53\ v}{1.27K}\right) \qquad (7)$$

$$X_h = \frac{0.53}{i_h} = 1.37K\Omega \qquad (8)$$

$$P_T = P_{P2} + P_h = i_p^2 R_{cp} + i_h^2 R_{ch} = \left(\frac{0.53}{1.27}\right)^2 R_{cp} + \left(\frac{0.53}{1.37}\right)^2 R_{ch} = 0.174R_{cp} + 0.148R_{ch} \qquad (9)$$

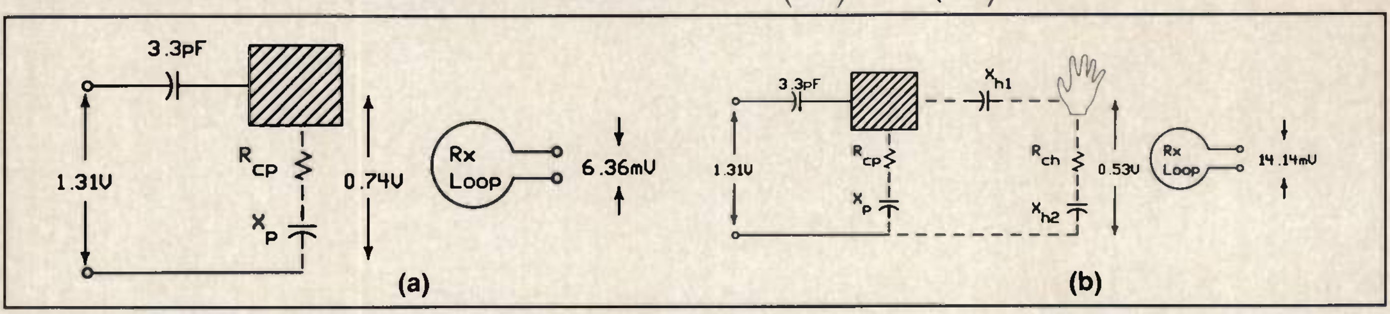

Figure 4. Receiver voltage with (a)conventional plate; (b) plate and hand.

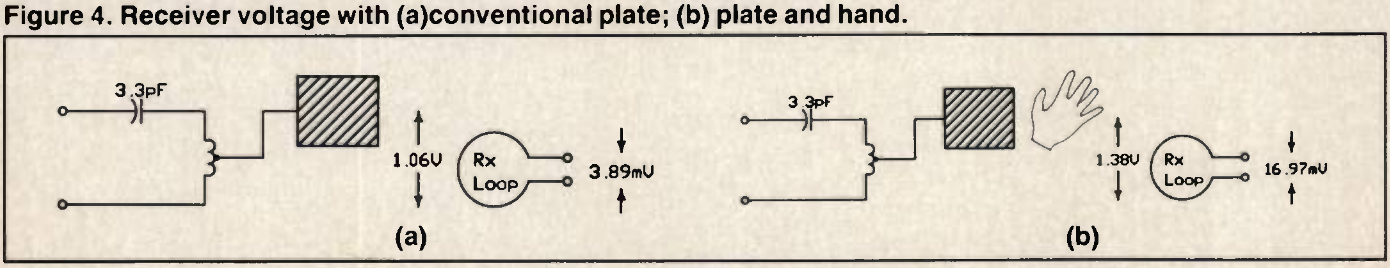

Figure 5. Receiver voltage with (a) plate and loop; (b) loop, plate and hand.

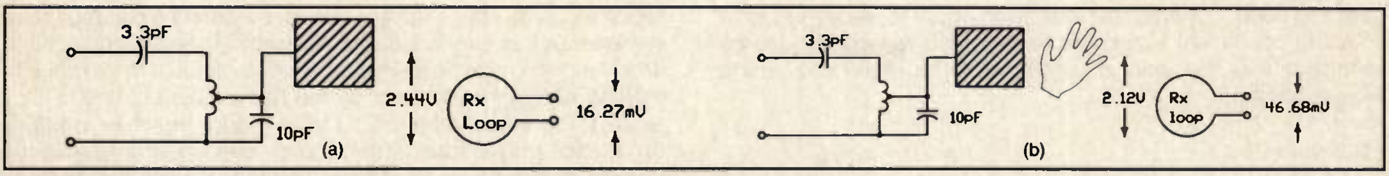

Figure 6. Receiver voltage with (a) tuned loop and plate; (b) tuned loop, plate and hand.

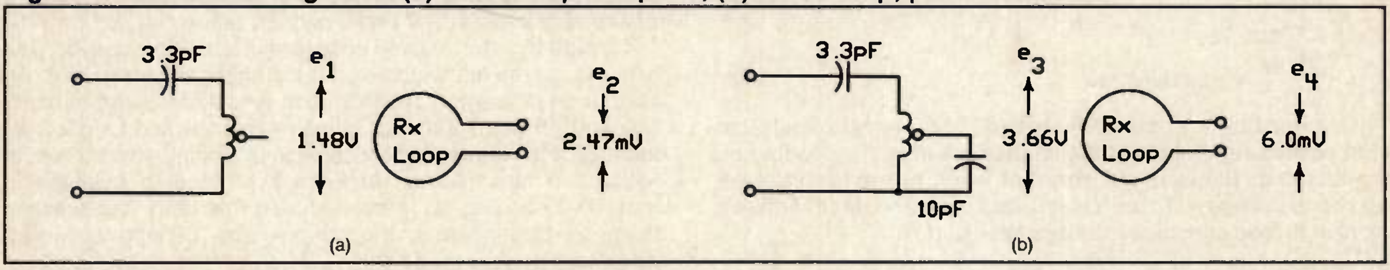

Figure 7. Receiver voltage with (a) loop; (b) tuned loop.

Notes:

1) R_{cp} */=X_p;R_{ch}*/=X_h 2) X_p and X_{h2} are distributed reactances terminating in transmitter common 3) X_{h1} is reactance between hand and plate

where R_{ch} = hand coupling resistance (Ω) X_{ch} = hand reactance (KΩ) i_h = hand current (ma), P_h = power in Rch (μwatts), P_T = total power in R_{ch} and R_{cp}

Because the square of voltage received in the 12 inch loop is proportional to radiated power,

$$\frac{P_T}{P_{P1}} = \left(\frac{14.14\text{mv}}{6.36\text{mv}}\right)^2 = \frac{0.174R_{cp} + 0.148R_{ch}}{0.340R_{cp}} \tag{10}$$

from Figures 4a and 4b

Then,

$$R_{ch} = \left[\left(\frac{14.14}{6.36}\right)^2 (0.340R_{cp} - 0.174R_{cp})\right] \frac{1}{0.148} \tag{11}$$

and

$$R_{ch} = 10.17R_{cp} \tag{12}$$

This result demonstrates the efficacy of the body as a coupler of RF power vis a vis the plate, having a "coupling efficiency" of 10.17 times that of the plate. These relative values of R_{cp} and R_{ch} can be used to predict received voltage ratios in other hand/plate configurations such as those depicted in Figures 5 and 6.

From Figure 5a,

$$P_P = i_p^2 R_{ch} = \left(\frac{1.06}{1.27}\right)^2 R_{cp} = 0.697R_{cp}(\mu w) \tag{13}$$

From Figure 5b,

$$P_T = \left(\frac{1.38}{1.27}\right)^2 + 10.17 \left(\frac{1.38}{1.37}\right)^2 R_{cp} = 11.50R_{cp}(\mu w) \tag{14}$$

The predicted receiver voltage ratio is P_t/P_p = 11.50/0.697 = 4.06. The measured ratio is 16.97/3.89 = 4.36 which agrees with the prediction within +7 percent. Again, using Figure 6 where 10 pf is added to the loop.

From Figure 6a,

$$P_p = \frac{2.44}{1.27}^2 R_{cp} = 3.691R_{cp}(\mu w) \tag{15}$$

From Figure 6b

$$P_T = \left(\frac{2.12}{1.27}\right)^2 + 10.17 \left(\frac{1.12}{1.37}\right)^2 R_{cp} = 27.132R_{cp}(\mu w) \tag{16}$$

Here, the predicted ratio 27.132/3.691 = 2.71. The actual ratio 46.68/16.27 = 2.87 which is within +6 percent of prediction.

Thus, from analysis of Figures 5 and 6, we see that relative coupling resistances are essentially constant and independent of both impressed voltage and shunt capacitance on the loop.

Finally, the transmission property of the loop itself, with and without the 10 pf loading, is examined using Figure 7. Because its radiation resistance is also negligible, coupling to the test loop is magnetic; that is, through transformer action.

Due to the transformer effect, receiver voltages should be in direct proportion to transmitter voltages, that is,

$$\frac{e_3}{e_1} = \frac{3.66}{1.48} = 2.47 \tag{17}$$

while

$$\frac{e_4}{e_2} = \frac{6.00}{2.47} = 2.43 \tag{18}$$

and agreement is within two percent. Now, if one were to describe loop voltage transfer from loop to receiver as a coupling coefficient k, defined as received voltage divided by voltage across the loop, its units would be mv/V. Examining Figure 7 again,

For Figure 7a

$$k = \frac{2.47\text{mv}}{1.48\text{v}} = 1.67\text{mv/V} \qquad (19)$$

and for Figure 7b

$$k = \frac{6.00\text{mv}}{3.66\text{v}} = 1.64\text{mv/V} \qquad (20)$$

As expected, k is the same within measurement limits for both circuits regardless of the change in capacitive loading of the loop tap. But, k is not constant when derived from plate and hand voltage transfer. Table 1 lists plate and hand k values alongside loop conditions to illustrate this point.

Antenna Coupling Coefficient

Clearly, from Table 1, as the loop is capacitively loaded, performance approaches the ideal 26.68 mv/V obtained when the loop is absent. Although the loop's own effect upon received voltage is very small (1.6 mv/V) and constant, its effect on plate/hand antenna performance is pronounced. From Table 1, the action of a field between loop and plate can be determined, which, as loop and plate currents diverge in relative magnitude, develops an attenuating or subtractive effect on the plate's ability to couple energy and/or on the energy passed to the hand. As relative current divergence lessens (as capacitance increases towards resonance and beyond), this attenuating or subtractive effect on antenna k tends to zero. The +7 percent and +6 percent discrepancies in measured vs. predicted k revealed by Figures 5 and 6, while small enough to invite dismissal, are the result of the capacitive loading change introduced by the hand. This change, 2.3 pf, tends to be masked by the 10 pf of Figure 6b while in Figure 5b, it adds only a small current to an already small capacitive current in the plate so the net change in loop/plate current difference is small in both circuits. But it is large enough to measurably boost k by 7 and 6 percent respectively.

Considering the above, observed k changes can only be linked to corresponding capacitance changes (which alter the magnitude difference between loop and plate currents) since Figures 5, 6 and 7 show coupling resistance and loop k to be constant and independent of capacitive loading and impressed voltage. In other words, antenna k is seen to increase as capacitive loading is increased and the only concurrently changing parameter is the relative size of loop and plate currents.

Now, the loop generates a magnetic field which, in the null plane, appears as a rectangular torus seen face on. The plate is a small distance above the torus and in a plane parallel to it. Consequently, induced current loops are created which may act in partial opposition to plate current. The net effect would be power lost to dissipation in some plate regions with less power available for coupling to electromagnetic waves.

Originally, when a small (1.4 in. diameter), center-tapped inductor was used to tune the plate, antenna performance was very sensitive to plate position relative to the oscillator circuitry and only improved as the plate was separated from it using a short umbilical wire. A similar sensitivity was obtained with no coil at all, with signal strength falling off and unacceptable

Loop Status	Figure	RX mv	Plate V	k(mv/V)
Untuned	5b	16.97	1.38	12.30
Tuned to fr, 3.6 pf	2,3	45.70	2.97	15.39
Tuned<fr, 10 pf	6b	46.68	2.12	22.02
Absent	4b	14.14	0.53	26.68

Table 1.

frequency pulling as the plate was positioned above the circuitry, improving when the plate was laid adjacent to it attached by a short wire lead. Indeed, the signals received in Figure 4 were not obtainable with the plate positioned directly above the circuit board as required for ultimate use. The loop therefore serves to reduce interaction between plate and oscillator circuitry while also reducing the coupling coefficient. If the plate must be physically isolated from the transmitter assembly, neither interaction nor k-losses would occur, but this is not an option in the present application.

From the foregoing, the loop must remain; but k can be increased by increasing plate current relative to loop current. After normalizing plate k and combined plate/hand k (by allowing the plate to take on $R_{cp} = R_{ch}$), it was possible to study k in relation to current ratios of several antenna configurations which resulted in the formula:

$$k_n = (14.34I_r)^2 \tag{21}$$

where k_n = normalized k, I_r = weighted antenna current to loop current ratio

The weighted current ratio is:

$$I_r = \frac{i_p + 0.12i_h}{i_L} \tag{22}$$

where i_p = plate current, i_h = hand current, i_L = loop current

Note that only a portion of hand current enters into this expression with the exact percentage worked out empirically. The ultimate direction taken by all infinitesimal elements of hand current is normal to the plane of plate eddy currents and so might seem to be unaffected by them. However, all such current elements originate in the plate and must therefore traverse some average path length through eddy disturbances before emerging from it. The 12 percent factor apparently accounts for this mechanism.

Conversion of normalized k_n to plate and composite k values is provided by:

$$k_p = \frac{k_n}{3.19} = \frac{(14.34I_r)^2}{3.19} \tag{23}$$

for the plate alone, and

$$k = \frac{k_n}{1.4} = \frac{(14.34I_r)^2}{1.4} \tag{24}$$

for the composite.

A comparison of measured and predicted k using Equations 22, 23, and 24 is presented in Table 2. As can be seen, prediction errors are reasonably small considering the simple first-order model used for current disturbance.

Coupled RF Power

Total power delivered to plate and hand is expressed by

$$P_T = i_h^2R_{ch} + i_p^2R_{cp}\ \mu w \tag{25}$$

FIG.	Measured k	k_n	I_r	Predicted k	% Error
5a	3.67	11.71	.239	3.68	+0.3
6a	6.67	21.28	.324	6.77	+1.5
5b	12.30	17.22	.283	11.76	−4.6
6b(1)	15.39	21.55	.323	15.32	−0.5
6b	22.02	30.83	.393	22.69	+3.0

(1) 10 pf replaced with 3.6 pf for series resonance with 3.3 pf coupler (Figure 3).

Table 2.

where

$$i_p = \frac{e_p}{X_p} = 0.787e_p \tag{26}$$

and

$$i_h = \frac{e_p}{X_h} = 0.730e_p \tag{27}$$

thus,

$$P_T = e_p^2(0.620R_{cp} + 0.533R_{ch}) \tag{28}$$

Substituting $R_{ch} = 10.17R_{cp}$ from equation 12

$$P_T = (0.620 + 5.421)e_p^2R_{cp} = 6.04e_p^2R_{cp} \tag{29}$$

From Figure 3, power may also be expressed by:

$$P_T = \frac{e_O^2R_T}{R_T^2 + X_T^2} = 2.61\ mw \tag{30}$$

where from Figure 3, e_o=4.63v, R_T= 0.116 K, and x_T= 0.970 K at resonance, which, combined with Equation 29 produces:

$$6.04e_p^2R_{cp} = 2.61mw \tag{31}$$

so,

$$R_{cp} = 48.9\Omega \tag{32}$$

and from equation 12

$$R_{ch} = 10.17R_{ch} = 497\Omega \tag{33}$$

where e_p = 2.97 v from Table 1.

But a component of R_{cp} may be viewed as k-factor loss resistance, R_k, to account for losses from $k*k_0$ with the balance, R_c, representing any conventional losses and coupling to the electromagnetic wave such that:

$$R_c = \frac{k}{k_o} R_{cp} \tag{34}$$

and

$$R_k = \left(1 - \frac{k}{k_o}\right) R_{cp} \tag{35}$$

Substituting R_c for R_{cp} in Equation 9 gives theoretical coupled power as:

$$P_c = 6.04e_p^2\left(\frac{k}{k_o}\right)R_{cp} = 0.30e_p^2\left(\frac{k}{k_o}\right) \quad (36)$$

Again it is assumed all power but k-loss appears as coupled energy. For the circuit of Figure 3, Table 1 gives k = 15.39, so

$$P_c = 2.61\left(\frac{15.39}{26.68}\right) = 1.51\text{mw} \quad (37)$$

In contrast to values calculated for R_{cp} and R_{ch}, plate and loop radiation resistances R_{rp} and R_{rl} are found by:

$$R_{rp} = 80\pi^2\left(\frac{L}{\lambda}\right)^2 = 0.076\Omega \quad (38)$$

where L = longest plate dimension of 5.97 cm, λ = 610 cm wavelength

and

$$R_{rl} = \frac{31{,}200N^2A^2}{\lambda^4} = 0.0016\Omega \quad (39)$$

where N = 2 turns, A = 41.6 cm^2 loop area.

Clearly, loop and plate radiation resistances contribute virtually nothing to total RF power output as comparison of their values with R_{cp} and R_{ch} reveals. While a value for human body radiation resistance is not available, it is assumed to be small. In any event, no inconsistencies arise since R_{ch} accounts for all power emanating from the body without regard to the mechanism of its development.

Optimized Antenna

Equations 21, 23 and 24 suggest that k can be made any desired value by selecting an appropriate current ratio I_r. However, it is actually k which limits I_r since $k_{max} = k_0 = 26.68$ mv/V. This upper limit of usefulness is given by:

$$\overline{I_r} = \frac{\sqrt{1.4k_o}}{14.34} = 0.426 \quad (40)$$

Increasing I_r beyond the useful limit will ultimately cause antenna performance to suffer from feedback if the plate is located near board circuitry. The relationship between I_r, plate distance and feedback deterioration has not been fully explored but feedback was not a problem at the current ratios studied.

To achieve a 0.426 current ratio, capacitive loading of the tap must be increased, thereby raising plate voltage relative to loop voltage. In turn, this will increase X_t, which will require a change in coupling capacitor value in order for resonance to occur. After some experimentation, 2.2 pf was added across 10 pf at the tap and 1.5 pf replaced the 3.3 pf coupler. A resonant peak was observed just before full hand grip; that is, with the hand resting lightly on the Mouse which was deemed appropriate to actual usage.

Plate voltage was measured at 3.1 v. No doubt, this would be much higher but for the soft oscillator output. Receiver loop voltage was measured at 81.2 mv corresponding to k = 26.20; a not disappointing result. RF coupled output power is calculated from Equation 36 at:

$$P_c = 0.30e_p^2\left(\frac{k}{k_o}\right) = 0.30(3.1)^2\left(\frac{26.20}{26.68}\right) = 2.83\text{mw} \quad (41)$$

Comparative Performance

Equation 41 gives an optimistic value of coupled RF output and almost certainly overstates it since there probably exist other loss mechanisms besides the k factor. However, to be conservative, the output of the optimized antenna given by Equation 41 is now assumed to radiate from a hypothetical lossless point source which would generate an electric field intensity at 3 feet given by:

$$E = \sqrt{\frac{P_T Z_O}{4\pi r^2}} = \sqrt{\frac{.00283(120\pi)}{4\pi(0.91)^2}} = 0.32\text{V/m} \quad (42)$$

where P_T = 2.83 mw, Z_o = 120π ohms free space impedance, r= 0.91m (3 feet)

Any antenna's received voltage is expressed by:

$$e_r = El_{eff} \quad (43)$$

The test setup used in a 12 in. diameter loop of effective length:

$$l_{eff} = \frac{2\pi AN}{\lambda} = \frac{2\pi(0.073)1}{6.1\text{m}} = 0.0752\text{m} \quad (44)$$

where A = loop area in m^2, N = number of turns, λ = wavelength

Combining Equations 42 and 44 with Equation 43 yields receiver voltage produced by the isotropic radiator:

$$e_r = 0.32\text{V/m}(0.0752\text{m}) = 24.08\text{mv} \quad (45)$$

The plate antenna produced 81.20 mv at the receiver or 3.37 times that produced by the hypothetical point source. Admittedly, the point source scenario assumes free space operation without benefit of surface reflections whereas Mouse measurements include indoor multipath linkages.

Conclusion

The comparison is quite favorable for a micro-antenna measuring only λ/100 x λ/146. A rectangular loop antenna's magnetic field was used to isolate a small plate antenna from its driving circuit while simultaneously boosting receiver voltage from the 14.14 mV produced by the conventional circuit of Figures 1 and 4(b) for a power gain of 15.2 dB.

About the Author

David Sullivan is a freelance consultant in California. He has worked on products from the DC to VHF range. He may be reached at (408) 737-9661. His mailing address is: 103, 2250 Homestead Court, Los Altos, CA 94024.

Cablewave Offers Field-Assembled Grid Parabolic Antennas

Twenty eight standard models of grid parabolic antennas are now available broken down into small packages, for ease of storage and transportation. Cablewave Systems offers models for 300 to 2700 MHz operation, with power ratings of 100 watts, feedpoint impedance of 50 ohms, and typical VSWR of 1.20:1. The feeds are unpressurized.

These antennas can be mounted for horizontal or vertical polarization, and include elevation and azimuth adjustment hardware and universal tower mounting clamps. Custom tower mounts are available. Reflectors are constructed of aluminum, tower mounts are hot dip galvanized steel, and hardware is stainless steel. **Cablewave Systems, Division of Radio Frequency Systems, Inc., North Haven, CT. Please circle Info/Card #200.**

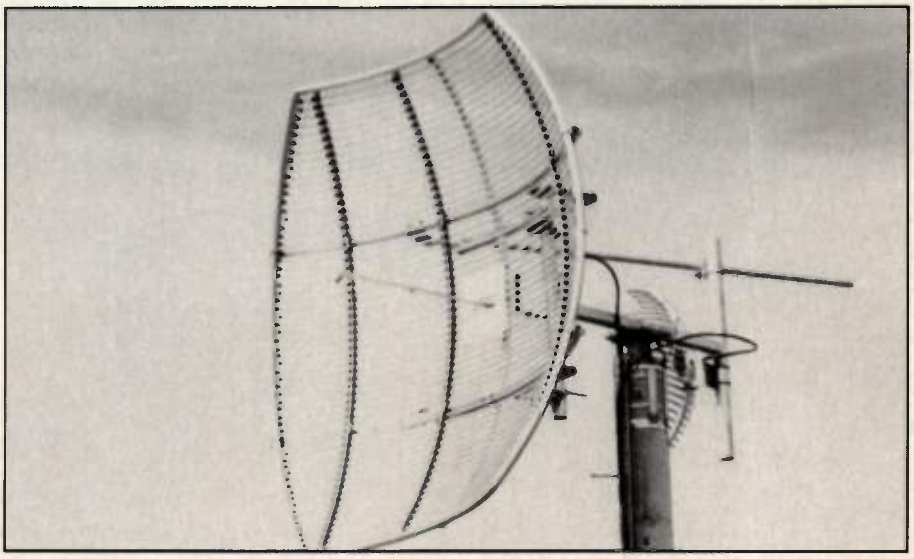

Eaton Introduces New Signal Generator

The Model 5225A Synthesized Signal Generator, covering 10 KHz to 2560 MHz, has been announced by Eaton Corp. The unit features switching speed of less than one microsecond and low spurious levels, greater than −90 dBc. Phase noise (specified at 640 MHz, 10 kHz offset from carrier) is −130 dBc. FSK, BPSK, pulse, and AM are the modulation types provided. The unit utilizes high speed direct digital synthesis with low noise, wideband PLL circuitry. Microprocessor control and a from panel display screen offer operational flexibility through menu-driven software. **Eaton Corporation, Electronic Instrumentation Division, Los Angeles, CA. Circle Info/Card #199.**

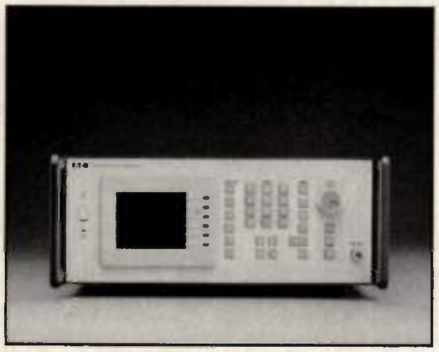

Non-Magnetic Differential Glass Trimmer

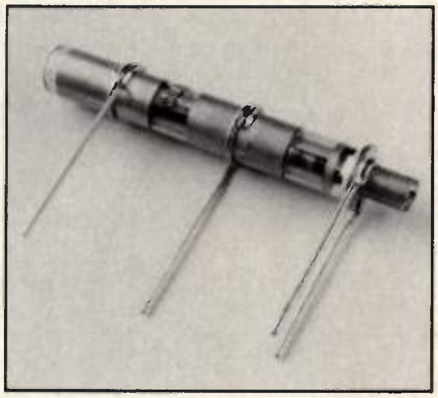

Voltronics Corporation has developed a completely non-magnetic differential trimmer capacitor for use in NMR/MRI probes. One capacitor rises in value as the other decreases. Each capacitor has a maximum value of 30 pF. Voltage rating is 1500 VDC, 1000 V RF peak pulse. Temperature coefficient is ± 50 ppm/C, and the Q is over 500 at 20 MHz. Different values can be made, typically 3, 8, 12, or 16 pF per capacitor. A split stator version, with both capacitors tuning the same direction, can be obtained. **Voltronics Corp., East Hanover, NJ. Info/Card #198.**

Armored Flexible Coaxial Cable Assemblies

UTiFLEX 161 cable assemblies from Rosenberger/Micro-Coax have a choice of armorings to protect them from mechanical stress. Electrical performance is optimal, with minimum attenuation DC−26.5 GHz. UTiFLEX 161−1 armor consists of a stainless steel spring covered by a polyurethane jacket. 161−2 armor is a stainless steel interlocked hose, to protect against harsh environments where pinching, crushing, or climatic changes may occur. Both armors have a crush resistance of 450 lbs./sq. in. and withstand a pull of 1200 lbs. A variety of connector options are available. **Rosenberger/Micro-Coax, Collegeville, PA. Info/Card #197.**

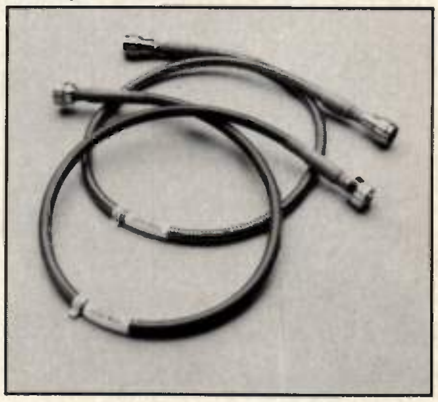

SMT Oscillators Introduced

The VF 315 series of SMT oscillators from Valpey-Fisher are available in frequencies from 1.5 to 55 MHz, and feature packages only 0.550 in. long by 0.340 in. wide. Four J-lead terminations with 0.200 by 0.300 in. spacing ensure compatibility with high-speed pick and place equipment. Options include enable/disable function, and packing in tape and reel or plastic tubes. Pricing is $3.69 in 10,000 quantities. **Valpey Fisher Corp., Hopkinton, MA. Please circle Info/Card #196.**

Heated Grid Antennas

For moderate to harsh winter climates, heated grid parabolic antennas are available from Mark Antennas Div. of Radiation Systems. A wide range of sizes and frequencies is available, from 4 to 15 feet diameter and from 335-2700 MHz. Heating elements are attached to the back of the grid elements and, depending on the frequency and size, the feed is heated by heater strap on the feed body or by a heat lamp mounted on the reflector. **Radiation Systems, Inc., Mark Antennas Div., Des Plaines, IL. Info/Card #195.**

New Couplers and Dividers

TRM, Inc. announces new products for the first quarter of 1990. Included are the DC210 100-2000 MHz, 20 dB directional coupler with 0.4 dB flatness and 1.0 dB maximum insertion loss; the DL360 3-way divider for 1-600 MHz, with 28 dB minimum isolation, 0.2 dB amplitude balance and 2 degree phase balance; and the DMS285 2-way divider, operating from 500 MHz to 20 GHz, with 0.4 dB amplitude balance, 4 degree phase balance, and 10 watts CW power handling capability. **TRM, Inc., Manchester, NH. Info/Card #194.**

Digitally Controlled Bandpass Filters

These extremely narrow, high selectivity filters allow transmitter/receiver installations to operate with minimum channel separation. Each filter is microprocessor controlled using a DC motor/absolute encoder arrangement in a closed-loop feedback system. Features include: 225-400 MHz or 100-163 MHz range, 600 kHz 3 dB bandwidth, 10 second typical tuning speed, and 2 dB insertion loss. **K&L Microwave, Inc., Salisbury, MD. Info/Card #193.**

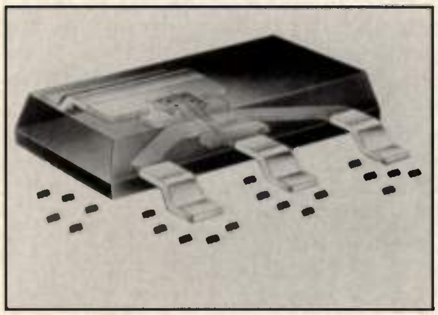

RF Transistors Offered in SOT223 One-Watt Package

Philips Components offers a family of wideband RF transistors in SOT223 packages capable of dissipating up to one watt. Types BFG97 and BFG35 are 6 GHz F_T devices, and BFG135 and BFG198 have F_T of 7.5 GHz. Pricing ranges from $.66 to $1.65 in 1000s. **Philips Components, Riviera Beach, FL. Info/Card #192.**

Precision Baseband Vector Network Analyzer

The HP 3577B network analyzer offers lower cost and more features than its predecessor HP 3577A. Covering 5-200 Mhz, the new model offers a discrete sweep mode to speed testing by only using highest resolution where it is desired. Control programs can be written directly by the unit with a keystroke capture feature. Accuracy is 0.02 dB and 0.2 degree, with resolution up to 0.001 dB, 0.001 degree, and 0.001 Hz. Price is $18,950, with options extra, including high stability time base, third channel, and additional memory. **Hewlett-Packard Company, Lake Stevens Division. Info/Card #191.**

Tunnel Diode Detectors

Midisco offers tunnel (back) diode detectors for stripline/microstrip assemblies from 0.01 to 18 GHz. They provide excellent sensitivity and flat response. Square law performance is essentially unaffected by changes in signals at levels of less than −23 dBm. **Midisco, Commack, NY. Please circle Info/Card #190.**

SMT Ferrite Chips

Ferrite chips for spurious oscillation elimination in amplifiers and other applications in the MHz to 100s of MHz range, are available from Murata Erie. BLM21, BLM31, and BLM41 can be mounted on 2.5 mm pitch p.c.b. lands for space savings. **Murata Erie North America, Smyrna, GA. Please circle Info/Card #189.**

Broadband Power Amplifier

Trontech introduces a 5-watt amplifier for applications in the 400-1400 Mhz range. The P1400M−37 offers 25 dB gain and ± 1 dB flatness over the band, requiring 2.4 A maximum from a

+24 V supply. Other high power class A amplifiers in this family are available in power outputs of 1 to 20 watts, or 100 watts class C. **Trontech, Inc., Neptune, NJ. Info/Card #188.**

Phase-Locked VHF Crystal Oscillators

Series PXS from Communication Techniques, Inc. contains a single crystal oscillator that can be locked to an external reference. The oscillator can be any frequency to 200 MHz, and can be phase locked to any reference frequency to 20 MHz. The output to input ratio may be an integer or non-integer ratio. Typical phase noise for a 101.1234 MHz output frequency is 136 dBc/Hz at 1 kHz offset, 152 dBc/Hz at 10 kHz. Various optional configurations are offered. **Communication Techniques, Inc., Whippany, NJ. Info/Card #187.**

Coaxial Connector Kits

AMP Incorporated has three coaxial connector kits with crimp, snap-in contacts, and multipurpose hand crimping tool. BNC kits for RG-58 and RG-59 cables contain 20 BNC plugs and the matching SUPER CHAMP hand tool. A UHF kit has 25 plugs and SUPER CHAMP tool. **AMP, Inc., Harrisburg, PA. Info/Card #186.**

VHF Synthesizers

Syntek announces the Series Q and Series R lines of frequency synthesizers for fine resolution in the VHF range. Tuning range, step size, and reference frequency may be specified by application, rather than selecting from a limited set of standard models. Series Q are available for up to 500 Mhz with good phase noise and spurious performance. Series R offers optimum phase noise up to 120 Mhz (typically 135 dBc/Hz at 1 kHz offset). **Syntek Corporation, Bohemia, NY. Info/Card #185.**

Digital FDM Demultiplexer

Watkins-Johnson introduces the WJ-9548, combining analog and digital signal processing in a digital FDM demultiplexer. Modular design allows configuration in 6, 12, 18, or 24 channels. A variety of analog and digital voice-grade channel output formats are available as field installed options. **Watkins-Johnson Co., Gaithersburg, MD. Info/Card #184.**

Power Amplifier Modules

Motorola offers two new series of power amplifiers for portable radios. All offer 7 watts output for 1 milliwatt input, with a 7.5 VDC supply. The MHW607–1 operates in the 136-154 MHz band, the MHW607–2 covers 146-174 MHz, model MHW707–1 operates over 403-440 MHz, and the MHW707–2 covers 440-470 MHz. The units feature greater than 40 percent efficiency. Prices (100s) are $39.00 for the MHW607 series, and $40.30 for the MHW707. **Motorola, Inc., Phoenix, AZ. Info/Card #183.**

Narrowband SAW Filter

The FB30–.2 SAW bandpass filter

achieves 70 dB rejection in a single device. Centered at 30.4 MHz, with a Gaussian-like passband shape, the −1 dB bandwidth is 150 kHz, min., and the −3 dB bandwidth is 250 kHz, nominal. Insertion loss is 25 dB This design is feasible for filters up to 500 MHz center frequency. **Phonon Corp., Simsbury, CT. Info/Card #182.**

High Power Resistive Components

Component General has expanded their line of resistors, attenuators and terminations, including units rated at 10 to 800 watts, based on 100 C case temperature. Frequency range is DC up to 4 GHz, depending on the size and configuration. Special configurations are welcome, with prototypes available in 1-3 weeks. **Component General, Inc., Odessa, FL. Info/Card #181.**

High Power UHF Pulsed Sources

AccSys Technology introduces a line of high peak power pulsed sources for RF-driven accelerators and other applications requiring wide bandwidth amplitude and phase modulation. Customer requirements can be met for pulse widths to 1 ms, duty factors to 2.5 percent, and operating frequency of 200-850 MHz with greater than 20 MHz output stage bandwidth. Low pulse droop (0.1 percent) and dynamic amplitude and phase control (± 0.5 percent, ± 0.5 degree, respectively), are standard features. **AccSys Technology, Inc., Pleasanton, CA. Info/Card #180.**

Step Attenuators

Kay Elemetrics announces a new line of step attenuators, with 3 watts power rating and up to 3 GHz frequency range. An example is the model 1/839, offering 0–21.1 dB attenuation (50 ohms) with 0.1 dB minimum step size, 1.1:1 VSWR and 0.2 dB insertions loss over 0-250 MHz, 1.3:1 VSWR and 0.5 dB loss up to 1000 MHz. **Kay Elemetrics Corp., Pine Brook, NJ. Info/Card #179.**

Digital Radio Test System

The HP 11758T digital radio test system consists of many discrete test functions integrated into one portable system. Included are an 18 GHz power meter, 22 GHz spectrum analyzer, a banded RF source, and a flatness analyzer. Also included are a three-tone IF source, a multipath fading simulator, a 300 kHz to 3 GHz IF tracking generator, and an event counter. System price is $58,000. **Hewlett-Packard Company.**

Please circle Info/Card #178.

SP9T PIN Diode Switch

The model PS601C offers 30 dB isolation, 2 dB insertion loss, and 60 us. switching speed over a 10-1000 MHz bandwidth. SMA connectors are provided, and either CMOS or TTL interface is available. **Phoenix Microwave Corp., Telford, PA. Info/Card #177.**

rf software

Touchstone/AutoCAD Interface
TS2ACAD is a program that integrates EEsof's Touchstone[R] simulator with AutoCAD[R]. It converts each microstrip or stripline element in the Touchstone circuit file into its AutoCAD graphic equivalent. Elements are connected together graphically by node numbers. Without this package, a user has to enter each coordinate of each element into AutoCAD manually. The program runs on PC-compatible computers and does not require either Touchstone or AutoCAD to operate. It is priced at $495. **ASM Software, Inc., Santa Cruz, CA. INFO/CARD #210.**

Spice Macromodels
Linear Technology has released Spice macromodels for over 40 of their IC operational amplifiers. The models are based fundamentally on the Boyle model, but feature many enhancements to make them mirror the real op amps. A macromodel is a simplification using a few transistors, diodes, and controlled current and voltage sources to mimic the behavior of the op amp. **Linear Technology Corp., Milpitas, CA. Please circle INFO/CARD #209.**

Signal Processing Software
The latest version of Comdisco Systems' digital signal processing design and simulation software, the Signal Processing WorkSystem™, includes the Block Oriented Systems Simulator™ functionality and runs on two new workstations — the Sun-4™/SPARCstation™ and the DECstation™. Release 2.6 allows the designer to graphically and interactively capture, simulate, test and implement their designs at the system level. **Comdisco Systems, Inc., Foster City, CA. INFO/CARD #208.**

CAD Software
Aptos Systems offers p.c.b., IC, and schematic software for MS-DOS computers. RF, analog, and hybrid/IC layouts are supported, as well as odd-shaped or curved boards. **Aptos Systems Corp., Aptos, CA. Please circle INFO/CARD #207.**

rf literature

EMI/RFI Filter Catalog
Schaffner EMC's 1990 EMI/RFI filter catalog includes electrical specifications, mechanical dimensions and insertion loss curves. It also contains information on safety standards, EMI/RFI measurement techniques, and EMI/RFI test limits for FCC and VDE compliance. **Schaffner EMC, Inc., Union, NJ. INFO/CARD #230.**

Transfer Switches Brochure
Failsafe and latching miniature transfer switches that operate from DC to 18 GHz are presented in this brochure. Application notes describe uses for transfer type microwave switches with schematics of optional circuit enhancements like TTL drivers and indicator circuits. DC-12 GHz high power latching and failsafe transfer switches suited for 50 ohm transmission lines are also included. **Teledyne Microwave, Mountain View, CA. INFO/CARD #229.**

Catalog Describes SMA Connectors
A catalog that helps designers and specifiers in the selection of SMA microwave connectors and cable assemblies is available from Lemo rF. It contains specifications for SMA connectors, interface mating dimensions, part number guidelines and a connector finder for various SMA connector applications. Dimensions, photographs and drawings are included. **Lemo rF, Huntingdon Valley, PA. Please circle INFO/CARD #225.**

rf literature *Continued*

Brochure on Transient Generators

This brochure describes R&B's line of transient generators. Information on a gasket test system, a low cost RS05 system and new generators to meet the requirements of RTCA D0160B and SAE-AE4L is provided. A section on generators designed to meet the EMP requirements of MIL-STD 461C/462 Notice 5 and Notice 6 is featured. **R & B Enterprises, West Conshohocken, PA. INFO/CARD #222.**

Test and Measurement Catalog

The 1990 Fluke and Philips Test & Measurement catalog features 20 new products, a rack mount selection guide, a glossary of terms, and an abbreviations and symbols section to assist users. Descriptions, photos, product selection guides and ordering information for over 650 products, accessories and software programs are included. **John Fluke Mfg. Co., Inc., Everett, WA. INFO/CARD #221.**

Newsletter on Simulating Crystal-Controlled Oscillators and Diodes

Intusoft's latest newsletter focuses on in-depth simulation tips for modeling crystal-controlled oscillators and varactor diodes. It covers IsSpice approaches using AC analysis techniques to predict circuit performance of oscillators. A short article on modeling varactor diodes includes model listings for a VCXO circuit. **Intusoft, San Pedro, CA. INFO/CARD #220.**

Recruitment

Advertising Index

SILICON POWER MMICS

1 WATT
Broadband Amplifiers

SGS-Thomson Microelectronics introduces the AMP 3020, a +30 dBm, 50 ohm cascadable gain block in the popular 200 mil hermetic, ceramic package.

This unique MMIC amplifier brings a new dimension in power to our silicon MMIC family, a series of broadband amplifiers designed to provide the circuit and system designer with reliable, cost-effective gain-blocks for broadband and narrowband, commercial and military IF and RF applications.

The "AMP" series cascadable, 50 ohm MMIC amplifiers are manufactured with a proprietary, space-qualified refractory-gold metallization and operate at low junction temperatures for maximum reliability.

A variety of hermetic, surface mount, ceramic package styles are offered to suit individual requirements with chips available for applications demanding the ultimate in miniaturization.

If you are looking for low-cost, reliable solutions to your amplifier needs, come to the Power Source.

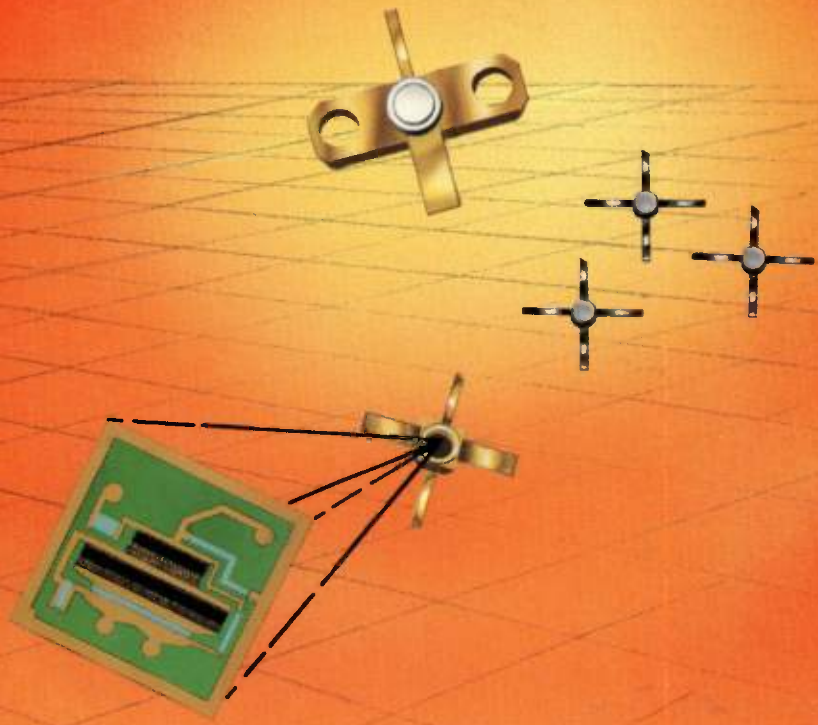

"AMP" SERIES SILICON MMIC AMPLIFIERS

Model #	Freq. GHz	Gain (dB)	Gain* (dB)	Pout (dBm)	N.F. (dB)	Vd/Id (v/ma)
AMP3020	0.5	8.0	8.5	29.5	8.0	17/300
	0.2	8.2	8.5	31.0	7.0	17/300
AMP0135	1.0	19.0	20.0	3.0	4.5	5/17
AMP0235	1.0	12.5	13.0	5.0	5.5	5/25
AMP0335	1.0	11.5	12.5	10.0	6.0	5/35
AMP0435	1.0	8.5	9.1	11.2	6.0	5.3/50
AMP0420	1.0	10.0	11.5	14.0	6.5	6.3/90
AMP0520	1.0	9.7	9.2	23.0	6.5	12/165
AMP0635	1.0	19.0	20.0	4.5	3.0	3.5/16
AMP0735	1.0	13.0	13.7	5.5	4.5	4/22
AMP0835	1.0	19.0	31.0	14.0	3.0	7.8/36
AMP0910	1.0	8.7	8.0	11.3	5.5	7.8/35
AMP1025♦	1.0	6.3	7.6	27.0	9.0	15/325
AMP1120	1.0	11.5	12.2	17.5	3.5	5.5/60

*Gain @ 0.1 GHz ♦Measured in a 50Ω System

SGS-THOMSON
MICROELECTRONICS

INFO/CARD 55

SGS-THOMSON Microelectronics
211 Commerce Drive
Montgomeryville, PA 18936-1002
(215) 362-8500 • FAX: (215) 362-1293